NASA CR-120917

TOPICAL REPORT

GLASS FIBER REINFORCED METAL PRESSURE VESSEL DESIGN GUIDE

by

R. E. Landes

STRUCTURAL COMPOSITES INDUSTRIES, INC.
Azusa, California

In Collaboration With

THE BOEING COMPANY
Seattle, Washington

Prepared for

NATIONAL AERONAUTICS AND SPACE ADMINISTRATION

NASA-Lewis Research Center

Contract NAS 3-14380

James R. Faddoul, Project Manager

1. Report No. NASA CR-120917	2. Government Accession No.	3. Recipient's Catalog No.
4. Title and Subtitle GLASS FIBER REINFORCED METAL PRESSURE VESSEL DESIGN GUIDE		5. Report Date July 1972 6. Performing Organization Code
7. Author(s) R. E. Landes		8. Performing Organization Report No. 10. Work Unit No.
9. Performing Organization Name and Address Structural Composites Industries 6344 N. Irwindale Ave. Azusa, California 91702		11. Contract or Grant No. NAS 3-14380 13. Type of Report and Period Covered Contractor Report
12. Sponsoring Agency Name and Address National Aeronautics and Space Administration Lewis Research Center 21000 Brookpark Rd. Cleveland, Ohio 44135		14. Sponsoring Agency Code

15. Supplementary Notes
Project Manager, James R. Faddoul
Materials and Structures Division
NASA Lewis Research Center Cleveland, Ohio 44135

16. Abstract

This Engineering Guide presents curves and general equations for safelife design of lightweight glass fiber reinforced (GFR) metal pressure vessels operating under anticipated Space Shuttle service conditions. The high composite vessel weight efficiency is shown to be relatively insensitive to shape, providing increased flexibility to designers establishing spacecraft configurations. Spheres, oblate spheroids, and cylinders constructed of GFR Inconel X-750, 2219-T62 aluminum, and cryoformed 301 stainless steel are covered; design parameters and performance efficiencies for each configuration are compared at ambient and cryogenic temperature for an operating pressure range of 690 to 2760 N/cm^2 (1000 to 4000 psi). Design variables are presented as a function of metal shell operating to sizing (proof) stress ratios for use with fracture mechanics data generated under a separate task of this program. Application of the fracture mechanics information to the data of this Guide provides a basis for appropriate selection of vessel proof test levels and safelife design configurations for Space Shuttle composite tanks with load sharing liners.

17. Key Words (Suggested by Author(s))	18. Distribution Statement
Pressure Vessel Design Guide Glass Fiber Reinforced Inconel X750 STA 2219-T62 Aluminum Cryoformed 301 Stainless Steel	Unclassified Unlimited

19. Security Classif. (of this report)	20. Security Classif. (of this page)	21. No. of Pages	22. Price*
Unclassified	Unclassified	96	$3.00

* For sale by the National Technical Information Service, Springfield, Virginia 22151

FOREWORD

This report was prepared for The Boeing Company by R. E. Landes of Structural Composites Industries, Inc. (SCI) under the cognizance of E. E. Morris, Vice President. The report summarizes the first task of a three task program being conducted as a joint effort by SCI and the Research and Engineering Division of The Boeing Company under National Aeronautics and Space Administration Contract NAS 3-14380.

Guidance and many helpful suggestions were provided during the effort by The Boeing Company Technical Leader, Mr. W. D. Bixler, and the NASA Lewis Research Center Project Manager, Mr. James R. Faddoul.

TABLE OF CONTENTS

TABLE OF CONTENTS (continued)

TABLE OF CONTENTS (continued)

LIST OF FIGURES

LIST OF FIGURES (continued)

LIST OF FIGURES (continued)

LIST OF FIGURES (continued)

LIST OF FIGURES (continued)

LIST OF SYMBOLS

A	Minor semi-axis of an oblate spheroid, meters (feet)
B	Major semi-axis of an oblate spheroid, meters (feet)
C_i	Coefficients defined in text
D	Vessel diameter, meters (feet)
D_b	Boss diameter, cm (inch)
E	Modulus of elasticity, GN/m^2 (psi)
El	Secondary modulus of metal, computer input value, GN/m^2 (psi)
EL	Primary modulus of metal, computer input value, GN/m^2 (psi)
F_{bc}	Constrictive wrap buckling strength of a cylinder, MN/m^2 (psi)
F_{bo}	Constrictive wrap buckling strength of an oblate spheroid, MN/m^2 (psi)
F_{bs}	Constrictive wrap buckling strength of a sphere, MN/m^2 (psi)
F_{cl}	Classical elastic buckling strength, MN/m^2 (psi)
F_{ty}	Tensile yield strength, MN/m^2 (psi)
F'_{ty}	Offset tensile yield strength, MN/m^2 (psi)
F_{tu}	Ultimate tensile strength of metal, MN/m^2 (psi)
F_{tuf}	Ultimate strength of filaments, MN/m^2 (psi)
K_b	Burst pressure factor defined as $K_b = p_{b,T}/p_{o,T}$, dimensionless
K_e	Longitudinal filament thickness parameter defined as $K_e = t_e/t_l$, dimensionless

LIST OF SYMBOLS

K_h	Hoop filament thickness parameter defined as $K_h = t_h/t_l$, dimensionless
K_l	Metal shell thickness parameter defined as $K_l = p_s(D/t_l)$, N/cm^2 (psi)
K_p	Sizing pressure parameter defined as $K_p = p_s/p_{o,T}$, dimensionless
K_{sd}	Design value for metal shell operating to sizing stress ratio defined as $K_{sd} = \sigma_{o,max}/F'_{ty,T}$, dimensionless
K_w	Vessel performance factor defined as $K_w = p_{o,T}V/W$, J/g (in-lbf/lbm)
K_s	Metal shell operating to sizing stress ratio, dimensionless
L	Vessel overall length, meters (feet)
p_b	Burst pressure, N/cm^2 (psi)
p_o	Operating pressure, N/cm^2 (psi)
p_s	Sizing pressure, N/cm^2 (psi)
P_{vg}	Volume fraction of fibers in composite, dimensionless
R_a	Vessel radius at equator of head, meters (feet)
SYL	Metal tensile yield strength, computer input value, MN/m^2 (psi)
t_c	Longitudinal composite thickness, cm (inch)
t_e	Longitudinal filament thickness, cm (inch)
t_h	Hoop filament thickness, cm (inch)
t_{hc}	Hoop composite thickness, cm (inch)
t_l	Metal shell thickness, cm (inch)

LIST OF SYMBOLS

T_o	Operating temperature, ^oK (^oF)
V	Vessel internal volume, m^3 ($feet^3$)
W	Vessel weight, grams (lbm)
X	Radial distance from vessel axis of rotation to head contour point, meters (feet)
Z	Normalized coordinate defined as $Z \equiv X/R_a$, dimensionless
α_o	Longitudinal wrap angle, radians (degrees)
μ	Poisson's ratio, dimensionless
σ_c	Compressive stress in metal shell after sizing, MN/m^2 (psi)
σ_o	Tensile stress in metal shell at operating condition, MN/m^2 (psi)
σ_{of}	Tensile stress in filaments at operating condition, MN/m^2 (psi)
σ_s	Tensile stress in metal shell at sizing condition, MN/m^2 (psi)
σ_{wf}	Tensile stress in filaments at wrap condition, MN/m^2 (psi)

LIST OF SYMBOLS

SUBSCRIPTS:

A	Evaluated at ambient temperature
c	Hoop wrapped cylinder
cr	Critical value
e	Value for longitudinal filaments
h	Value for hoop filaments
H	Evaluated at liquid hydrogen temperature, $20^{o}K$ ($-423^{o}F$)
max	Maximum value
min	Minimum value
N	Evaluated at liquid nitrogen temperature, $77^{o}K$, ($-320^{o}F$)
o	Oblate spheroid
oc	Completely overwrapped cylinder
s	Sphere
T	Value at any temperature
θ	Hoop direction

CONVERSION OF U. S. CUSTOMARY UNITS TO THE INTERNATIONAL SYSTEM OF UNITS

Quantity	U.S. Customary Unit	Conversion Factor[1]	SI Unit
Density	$lbm/in.^3$	27.68×10^3	$kilograms/meter^3$ (kg/m^3)
Length	ft	0.3048	meters (m)
	in	0.0254	meters (m)
Stress, Pressure Modulus	psi	6.895×10^3	$newtons/meter^2$ (N/m^2)
Temperature	(^oF + 460)	5/9	degrees Kelvin (^oK)

Prefixes to indicate multiples of units are as follows:

Prefix	Multiple
giga (G)	10^9
mega (M)	10^6
kilo (k)	10^3
milli (m)	10^{-3}
micro (μ)	10^{-6}

1 Multiple value given in U. S. Customary Unit by conversion factor to obtain equivalent value in SI unit

I. INTRODUCTION AND SUMMARY

The potential of glass fiber reinforced (GFR) metal tanks for space vehicle application has been and continues to be demonstrated by a series of NASA-LeRC technology development programs conducted during the past ten years. The objectives of the current program, Contract NAS 3-14380, are to (1) evaluate designs of GFR metal tanks of three liner materials, (2) determine experimentally the critical and subcritical flaw growth of these metallic materials using uniaxial specimens, and (3) determine experimentally the applicability of the uniaxial specimen data by testing GFR metal tanks with flaws, to develop a design method for guaranteeing the cyclic life of overwrapped tanks based on the initial sizing cycle. The program is being conducted as a joint effort by the Research and Engineering Division of The Boeing Company and Structural Composites Industries, Inc. (SCI).

This handbook, summarizing the design evaluation phase, was prepared as a design guide for pressure vessel engineers concerned with a specific GFR metal tank design or a general tank trade-off study. Design philosophy and general equations and curves are provided for the safelife design of GFR metal tanks operating under anticipated Space Shuttle service conditions. The design guide covers spheres, oblate spheroids, and cylinders constructed of GFR Inconel X-750, 2219-T62 aluminum, and cryoformed 301 stainless steel. Efficiencies of designs for each configuration are compared at ambient and cryogenic temperatures for an operating pressure range of 690 to 2760 N/cm^2 (1000 to 4000 psi).

II. BACKGROUND

A. SPACE SHUTTLE TANKAGE

The Space Shuttle mission consists of delivery and retrieval of a variety of payloads to and from earth orbit on a regular and frequent schedule. It's primary objective is to lower present cost of a payload pound delivered to orbit by a factor of 100. This requires development of a manned vehicle, with cost-effective launch system which can be launched to earth orbit, perform specific logistics, and re-enter to a landing site adjacent to the pad. The Shuttle configuration has evolved to an orbiter vehicle, with disposal liquid oxygen/liquid hydrogen tank and solid rocket booster. As noted in Reference 1, the reusable orbiter vehicle must be refurbished to flight status following each mission, with a 100-mission life required, and a 500-mission life as a design objective.

The Space Shuttle Orbiter will have reusable, cyclically loaded, tanks to contain gases and liquids. Tankage comprises a significant portion of the structural weight, and because the orbiter is extremely weight critical, many of the vessels are candidate for high-strength, light weight, composite metal/filament overwrap construction.

B. GFR METAL TANK DESIGN PHILOSOPHY

The primary design objectives of a glass filament composite shell with an inner load carrying metal shell is to obtain maximum operating performance at minimum weight and to provide a comparable or improved safelife design over basic metal tank construction. Thick liners that share loads with the filament-wound shell offer an excellent approach to workable, low weight, fluid storage vessels. The functions and interactions of the parameters of filament reinforced metal shell vessels have been evaluated in detail by NASA and by SCI in past programs to establish optimum stress/strain relationships between the metal and fiber shells from strength, load, and strain compatibility viewpoints.

Analytical work and test evaluations have established many of the methods needed for analysis and rating of designs, and have indicated the technical problems which will be encountered with filament reinforced spheres, spheroids, and cylinders. They are related to the following factors:

(1) Load and strain capability of the two types of material.

(2) Constrictive wrap buckling strength of the metal shell.

(3) Prestress (filament tensioning) set up between the two materials during fabrication and proof testing (sizing).

(4) Effects of prestress into the plastic region of the metal shell.

(5) Thermal contraction characteristics of the various construction materials.

(6) Effects of cyclic and sustained loading on fatigue life and residual strength.

For a specific tank configuration and metal and filament shell materials, particular attention must be paid to relative shell thicknesses and winding tension prestress (during fabrication, or pressure-sizing past the metal shell yield point after fabrication) to obtain the following most significant conditions:

Condition (1): Suitable stress/strain relationships between the filament and metal shells to permit achievement of specified (optimum design) allowable operating/burst stresses in the filament and metal shells, simultaneously, at the operating/burst pressures and temperatures.

Condition (2): Suitable stress/strain relationships between the shells to permit attainment of a high fraction of the filament ultimate strength

- Prior to exceeding the metal shell biaxial ductility capability

- As the metal shells approaches its maximum strength capability

Condition (3): Preclude metal shell buckling due to constrictive wrap stresses.

A schematic stress/strain diagram for a GFR metal tank is presented in Figure 1, and is applicable to GFR spheres and spheroids, as well as hoop wrapped and completely wrapped closed-end cylinders. With reference to that figure, a "load-bearing metal shell" is defined as one capable of resisting buckling at the compressive stress level (E) shown there (produced by external pressure from the overwrapped shell), when no bond exists between the two shells. The two shells are designed to minimize the hysteresis loop of the liner in the operation-pressure-cycle stress range (E) to (J) to (E) [i.e., (E) to (J) is an elastic stress/strain curve] .

Significantly different stress/strain conditions are imposed on GFR metal tanks during application of the internal pressures associated with tank fabrication, proof testing, burst testing, and operation. Figure 1 depicts these states for both shells during fabrication, after mandrel removal, and at the proof-pressure prestress, zero pressure, operating pressure, and burst pressure. It provides a basis for the ensuing discussion, which repeatedly refers to points depicted there.

The metal shell may be held in a stress-free (strain-free) state of a rigid mandrel while being overwrapped with tensioned filaments [point (M)] . Upon mandrel removal, however, it will spring back into a compressive state, due to the overwrap pressure [point (O)] . The magnitude of compression at zero-internal-pressure equilibrium depends on the relative thicknesses and moduli of the overwrapped filaments and liners, as well as the biaxial stress-strain characteristics of the liner and the filament-winding tension used during filament-wound composite fabrication.

When the first pressure load (p_s) is applied, the GFR metal tank is strained to the point (A), which is fixed by material properties and thickness and by the load. For factors of safety associated with the tankage and with the glass-filament and metallic materials now available , point (A) can be beyond the metal-shell yield point and plastic deformation may occur. In general, it can be said that the biaxial tensile strain produced in the liner by the initial "sizing" pressure may exceed 1% and may be greater than 2%.

When the initial load is removed after plastic deformation, the liner will spring back along the offset, biaxial, elastic, strain-stress curve (A) - (E) and will be pushed into compression by external pressure from the overwrapped filaments until load equilibrium is reached at

point (E) [strain (G)]. The GFR metal tanks are designed so that point (E) does not exceed (a) the critical buckling-stress level of the liner in the absence of a bond between the two shells, or (b) a fixed fraction of the compressive elastic limit of the liner.

The operating-pressure level (p_o) will always be less than p_s. During the application of cyclic operating-pressure loads, therefore, the metal-liner strain range is between points (G) and (K).

C. COMPUTER PROGRAM FOR VESSEL DESIGN AND ANALYSIS

SCI developed the Reference 2 computer program, based on the preceeding discussion, for use in designing and analyzing complete GFR metal tanks wound with either geodesic or in-plane patterns along the cylinder and over the end domes and complemented by circumferential windings in the cylinder. The program treats the filament shell by means of a netting analysis, which assumes (1) constant stresses along the filament path, and (2) that the resin makes a negligible structural contribution. The filament shell and the constant-thickness metal liner are combined by equating strains in the longitudinal and hoop directions and by adjusting the radii of curvature to match the combined material strengths at the design pressure; both the elastic and plastic portions of the metal-liner stress-strain relationship are considered in this analysis.

The program establishes optimum head contours and defines component thicknesses and other dimensional coordinates, as well as the shell stresses and strains at zero pressure and the design pressures, the filament path lengths, and the weights and volumes of the components and complete vessels. Sufficient program flexibility is available to permit analysis of cylinders overwrapped in the circumferential direction only.

The computer program also determines stresses and strains in both shells throughout the service-cycling history from a series of input pressures, composite temperatures, and metal-liner temperatures. This feature permits analyses of pressure and temperature cycles imposed on the vessel during fabrication and environmental testing, taking into account previous strains and loads. The computer program was used to conduct the parametric study of GFR-metal tanks reported in Reference 3, for design and analysis of GFR Inconel X-750 tanks described in Reference 4, and to develop the information contained in this design guide.

D. FRACTURE MECHANICS CONSIDERATIONS

In order to assure adequate service performance of most aerospace structures and in particular metal tankage, it is necessary to apply the principles of fracture mechanics to establishing design and operation requirements for such pressure vessels. This requires knowledge of fracture toughness and subcritical flaw growth behavior of candidate materials. The guidelines to the design of metal pressure vessels based on fracture mechanics considerations are fully discussed in Reference 5. Briefly, the proof test is a means of establishing the maximum possible initial flaw that can exist in the structure. This knowledge plus the sustained load and cyclic load flaw growth characteristics of the material/environment combination can then be used to establish safe ratios of proof to operating stress level.

Fracture mechanics methods have not yet been established for light weight, high strength composite metal/filament overwrapped tankage, but must be if the weight saving advantages of this construction concept are to be successfully applied to aerospace programs. GFR metal tanks apparently offer unique advantages over the metal tank from a fracture mechanics viewpoint. During the sizing operation performed on a GFR metal tank the sizing stress exceeds the yield strength of the metal liner, thereby effectively screening a smaller flaw than possible in a comparable metal tank. The plastic deformation that takes place during the sizing operation may blunt the flaws and improve the subcritical flaw growth characteristics of the metal liner. Secondly, the metal liners of GFR metal tanks are about one-half to one-third the thickness of comparable all-metal tanks and, therefore, are more prone to a leakage failure mode. Tests of GFR metal tanks conducted to date, have shown that, during failure, the liner material can be contained by the overwrap resulting in a non-shatterable design. Damage containment in case of a malfunction or failure is a very desirable feature for Space Shuttle type applications. The filament overwrap, due to its restraining effect, might also offer some advantage in reducing crack growth.

Since no theoretical methods have been developed to handle flaws subjected to general plastic deformation, it is necessary to empirically evaluate data to better understand the mechanics of failure and subcritical flaw growth for these flaws. The required empirical data is

currently being established by Boeing/SCI under the second and third phases of this contract, NAS 3-14380. The end result of this program is to establish a fracture control method which would guarantee safe service life for GFR metal tanks.

III. SPECIFIC DESIGN CRITERIA

A complete discussion of the effects of each design variable associated with GFR metal tanks is contained in Reference 3. Specific design variables established for this study and the ranges in values of interest to NASA are summarized in the paragraphs that follow:

A. GEOMETRIC PARAMETERS

The selected vessel configurations include (1) spheres, (2) oblate spheroids, (3) circumferentially wrapped cylindrical vessels with hemispherical end closures, and (4) completely overwrapped cylindrical vessels with oblate spheroidal end closures. Schematics of each of the four configurations are presented in Figure 2. The pressure vessel internal volume range is 0.07 to 3.4 m^3 (2.5 to 120 ft^3), and the major axis inside diameter range is 0.15 to 1.8 meters (0.5 to 6.0 feet) for all configurations. Axial port diameters are fixed at 20% of the vessel major axis inside diameter.

B. SHELL MATERIALS

The composite reinforcement selected by NASA for this study was S-901 continuous glass filaments impregnated with an epoxy resin. Inconel X-750 (STA), 2219-T62 aluminum, and cryoformed 301 stainless steel were selected as the constant thickness load bearing liner materials based on their compatibility with the glass filament-overwrap and the resultant high GFR metal vessel weight efficiencies. Properties of these materials and the referenced literature from which they were obtained are presented in Table I.

Values for the tensile yield strength and "plastic" modulus of the metallic materials are not necessarily the same as the conventional values. Since the Reference 2 computer program requires a bi-linear form for the metal shell stress/strain relation, actual stress/strain curves must be linearized according to the schematic of Figure 3. To arrive at a value of the plastic modulus (E1) for a given metal, a straight line is passed through two stress/strain points on the real curve defined by the filament operating strain and the filament brust strain. The intersection of this linear "plastic" curve with the elastic curve (defined by the real elastic modulus, EL) fixes the computer value for yield strength (SYL).

C. FABRICATION CRITERIA

Filament Winding Patterns: Spheres - an axisymmetric, multiple angle wrap pattern which produces a constant thickness glass/epoxy composite shell. Oblate Spheroids - a longitudinal-in-plane pattern. Closed End Cylindrical Vessels - a circumferential pattern over the cylindrical section only; and, longitudinal-in-plane pattern complemented by circumferential pattern along cylindrical section. These patterns are shown schematically in Figure 2 for each configuration.

Filament Winding Tension: 2.2 Newtons/roving-end (1/2 lbf/roving-end) producing a filament prestress of 164 MN/m^2 (23.8 ksi) which may be increased to a maximum practical value of 8.9 Newtons/roving-end (2 lbf/roving-end) when required for optimization.

Winding Support Mandrel: Rigid support for all vessels except hoop wrapped cylinders; pressure support may be used for hoop wrapped cylinders if required.

D. SIZING CRITERIA

All vessels are sized (proof tested) prior to operation.

Metal Shell Sizing Stress: Computer derived optimum for filament reinforced metal; less than or equal to tensile yield strength for unreinforced metal portions of vessel.

Sizing Temperature: Ambient for GFR Inconel X-750 and 2219-T62 aluminum vessels; 77°K (-320°F) for GFR 301 stainless steel vessels (bare metal is initially cryostretched).

Zero Pressure After Sizing: Compressive stresses in the metal shall not exceed (1) the compressive allowable established for each type metal shells, or (2) the constrictive wrap buckling allowable stress-whichever is critical.

E. OPERATING CONDITIONS

Pressure: 690 to 2760 N/cm^2 (1000 to 4000 psi)

Temperature: Extremes are 344°K (+160°F) to liquid hydrogen at 20°K (-423°F).

Cyclic Loads: 2400 full zero to operating pressure cycles [100 flights x (5 checkout cycles prior to flight + 1 flight cycle) x scatter factor of 4 = 2400 cycles].

Filament Operating Stress: Shall be $\leq$ 1380 MN/m^2 (200,000 psi) at ambient (75°F) and $\leq$ 1720 MN/m^2 (250,000 psi) at cryogenic temperatures (see Table I).

Metal Shell Operating Stress Levels: 75, 85, and 95% of the metal shell offset yield stress (F'_{ty}).

F. FAILURE CRITERIA

For completely overwrapped metal vessels, the burst pressure is defined to be the pressure at which the longitudinal or hoop filament stress exceeds the ultimate strength of the fiber or the ultimate strain of the metal. For hoop wrapped cylindrical vessels, the burst pressure is defined to be the pressure at which (1) the hoop filament stress exceeds the ultimate fiber strength, or (2) the unreinforced metal shell stress exceeds the ultimate strength of the metal.

G. OPTIMUM VESSEL

Several methods of rating homogeneous metal pressure vessels, including use of the strength-to-density ratio and burst pressure, were reviewed. The study revealed that the most satisfactory method of judging the efficiency of metal, filament-wound, and GFR metal pressure vessels is one that incorporates all the basic parameters of the pressure vessel by means of the performance factor, $p_o V/W$, where p_o is the operating pressure (and could be the burst pressure, p_b): V is the vessel internal volume; and W is the pressure vessel weight. The performance factor dimensionally relates the vessel stored energy capability to the weight of the vessel.

This factor has an advantage over other design - rating methods in that complete vessels (heads, cylinders, bosses, attachments, etc.) may be rated by a single term, and a variety of designs can be

compared directly. Optimum designs are noted when the performance factor has a maximum value for a given set of design criteria.

H. BURST STRENGTH

Burst strength design factor of safety for the vessel was not a study design criterion. Safelife designs were developed from consideration of operating stresses in the metal and composite shells for the required service life conditions, to make maximum use of the allowable stresses. However, burst pressure capabilities of the various design configurations were determined, and they were usually less than 2.0 for the study range.

IV. DESIGN EQUATIONS AND CURVES

A. GENERAL CONSIDERATIONS

Using the design criteria outlined in Section III of this report, the Reference 2 computer program was used to conduct a parametric study of the type covered by Reference 3. Briefly, for each configuration and metal shell material, a sizing pressure and filament sizing stress was selected. Since it was desired to operate the vessel with the metal close to a 1:1 biaxial stress field, the sizing pressure and stress were used as computer input for the "design" pressure (PD) and stress (SFD), respectively. A series of metal shell thicknesses were then combined with the fixed parameters, for each specific case, to provide computer output for selection of a usable design. The prime criteria for usable design selection was that the metal shell must be at the allowable compressive stress level at zero pressure after sizing. For a design meeting this criteria, sizing to zero pressure/stress data were scanned for the design value of filament operating stress, in order to provide the required values for operating pressure and metal shell operating stresses. The computerized series was then repeated for several sizing pressures until sufficient data was available to establish design trends.

The study techniques and resultant data trends for weight optimum designs developed in the current study closely approximate the Reference 3 work; general differences and extensions in the work are discussed in the paragraphs that follow.

1. Metal Shell Operating To Sizing Stress Ratio Effects

Generally, metal shell stresses at the sizing pressure exceed the "elastic" tensile yield strength (F_{ty}) of the material, this inelastic condition produces an offset yield strength ($F'_{ty,T}$) in the metal shell which is greater than the elastic tensile yield strength of the material. Unless otherwise stated, metal shell sizing stress ($\sigma_{s,T}$) and offset yield strength ($F'_{ty,T}$) at the sizing temperature will be used interchangeably in the text. (i.e., $F'_{ty,T} \equiv \sigma_{s,T}$).

The computer program defined in Reference 2 was used to establish metal shell sizing stresses by solution of an equation which

may be represented by the functional relation

$$\sigma_s = f(K_{sd}, \sigma_{wf}, \sigma_{of}) \qquad (1)$$

Design criteria, outlined in Section III, dictate that the filament operating stress level (σ_{of}) shall not exceed 1380 MN/m^2 (200,000 psi) at ambient or 1720 MN/m^2 (250,000 psi) at cryogenic temperatures, and it was desired to overwrap all vessels at a filament prestress (σ_{wf}) of 164 MN/m^2 (23,800 psi); design values of the metal shell operating to sizing stress ratio (K_{sd}) were fixed at 0.75, 0.85, and 0.95 (K_{sd} is the parameter which is used to relate fracture mechanics data to composite tank design for a specific safelife operating requirement). These criteria, substituted into the functional relation (equation 1), established values of σ_s (for each K_{sd}) which are bi-directionally constant over the entire vessel contour for all vessel shapes, except hoop wrapped cylinders. Although σ_s is invariant over the contour, the metal shell operating stress (σ_o) and the corresponding metal stress ratio K_s, in both directions may vary from the design value, K_{sd}.

Hoop wrapped cylinders have the additional design requirement that stresses in unreinforced areas of the metal shell may not exceed the elastic yield strength (F_{ty}) of the metal. Thus, hoop and longitudinal stresses in the metal shell at the sizing pressure are not equal; conversely, a 1:1 stress state does exist in the entire metal shell at the operating pressure (and sizing temperature). The variable sizing stress causes K_s to again vary from the design value, K_{sd}, similar to the completely GFR metal vessels.

In summary, the geometric location of the singular value of K_{sd} and the bi-directional variation over a given contour is dependent on the vessel shape, how much of the contour is reinforced, and the orientation of the reinforcement (hoop and/or longitudinal wraps). These factors make it necessary to discuss each shape separately, and this is done in the sections dealing with each metal shell material.

One final effect from sizing requirements concerns the fact that two distinct winding patterns are necessary for a completely overwrapped cylindrical vessel: (1) a longitudinal in-plane pattern complemented by (2) a simple hoop pattern in the cylinder. The computer program uses the design value for the longitudinal filament wrap stress ($\sigma_{wf,e}$) and adjusts the hoop filament wrap stress ($\sigma_{wf,h}$) to meet sizing requirements and the design filament operating stress level. Computer output indicates $\sigma_{wf,h} \sim 0.2\ \sigma_{wf,e}$ which is still in the range of practical winding tensions.

2. Constrictive Wrap Buckling Equations

Design criteria dictates that at zero pressure after sizing the stresses in the metal shell shall not exceed (1) the compressive allowable in the cylinder or at any point on the head contour (from the equator to a normalized radial distance, Z, equal to 40% of the vessel radius, or (2) the constrictive wrap buckling allowable stress - whichever is critical. The effect of the buckling criteria on each shape is discussed in the following paragraphs.

a. Completely GFR Metal Cylindrical Vessels

The coefficient in the equation for the constrictive wrap buckling allowable strength of completely GFR metal cylindrical vessel used in the Reference 3 parametric study was 150,000. Subsequent data reported in Reference 4 indicated a more conservative value of 106,000. For this study the conservative value will be used, and the resultant constrictive wrap buckling allowable stress equation is

$$F_{bc} = 106,000\ E/\ (D/t_1)^3 \qquad (2)$$

Thus, when the compressive stress in the metal shell at zero pressure after sizing equals the constrictive wrap buckling stress (F_{bc}), the design is defined to be "buckling sensitive".

b. Hoop Wrapped Cylinders

Sizing criteria dictate the design of hoop wrapped cylinders, and compressive stresses at zero pressure after sizing are always less than the compressive yield strength of the material for all K_{sd} values. Thus, hoop wrapped cylinders are not critical in compression until the induced compressive stress (σ_c) in the metal shell reaches a value defined by the critical constrictive wrap buckling strength (F_{bc}), equation 2.

c. Spheres

As previously discussed, experimental work undertaken by NASA and SCI/Aerojet has verified that the constrictive wrap buckling strength of thin metal cylindrical shells (F_{bc}) may be determined from the emperical relation defined by equation 2. Comparison of this relation with the classical relation for elastic buckling strength of cylinders ($F_{cl,c}$) subjected to radial pressure

$$F_{cl,c} = \frac{E}{(1-\mu^2)} \Big/ (D/t_1)^2 \qquad (3)$$

indicates the difference in structural stability of shells subjected to the two types of "external radial" loading.

Because of the lack of data on the constrictive wrap buckling strength of doubly curved thin metal shells, it is assumed that the buckling strength ratio for cylinders ($F_{bc}/F_{cl,c}$) may also be applied to shells of double curvature. Thus, the relation for the constrictive wrap buckling strength of a sphere (F_{bs}) may be defined as

$$F_{bs} = F_{bc} \ (F_{cl,s} / F_{cl,c}) \qquad (4)$$

where,

$$F_{cl,s} = \frac{2E}{[3(1-\mu^2)]^{1/2}} \Big/ (D/t_1) \qquad (5)$$

is the classical equation for the elastic buckling strength of thin metal spheres subjected to hydrostatic pressure. Combining equations 2, 3, 4, and 5 with the approximation

$$\left[(1-\mu^2)/3\right]^{1/2} \sim 0.5$$

yields the following relation for determining the constrictive wrap buckling strength of spheres

$$F_{bs} = 106,000\ E/(D/t_1)^2 \qquad (6)$$

d. Oblate Spheroids

Experimental and theoretical studies summarized in Reference 6 indicate the elastic buckling strength of thin metal oblate spheroidal shells is similar to that for a sphere of diameter

$$D = 2(B^2/A) \tag{7}$$

where,

B = major semiaxis

A = minor semiaxis

Noting that (2B) is the major diameter of the oblate spheroid and the ratio (B/A) is approximately 1.25 for oblates, equation 6 may be rewritten to give a relation for the constrictive wrap buckling strength of oblate spheroids (F_{bo})

$$F_{bo} = 68,000\ E/\ (D\ /t_1)^2 \tag{8}$$

3. Internal Volume Relations

Preliminary design criteria for pressure vessels generally include the envelope dimensions of diameter (D) and overall length (L), or diameter and internal volume (V) requirements. The most common method used to present these parameters is a series of curves which relate V/D^3 and L/D. In this study the envelope parameter relations are presented in the form of equations for more complete design versatility.

The volume of sphere is directly related to its diameter by the classical equation

$$V_s = \pi D^3/6 \tag{9}$$

Evaluation of a number of computer runs for the three metal shell materials indicates the volume relation for oblate spheroids is

$$V_o = \pi D^3/\ 7.30 \tag{10}$$

The maximum error in equation 10 is $< 3\%$; this occurs when small diameter, high pressure oblate spheroids operate at high K_{sd} values.

The volume relation for hoop wrapped cylinders is also a function of L/D ratio and may be calculated from the expression

$$V_c = \frac{\pi D^3}{12} \left[3(L/D) - 1 \right] \quad (11)$$

Completely overwrapped cylindrical vessel volumes are additionally influenced by the oblate spheroidal end domes which vary in shape for different metal shells and L/D ratios. Inspection of computer output indicates the equation

$$V_{oc} = \frac{\pi D^3}{12} \left[3(L/D) - .855 \right] \quad (12)$$

is satisfactory for $L/D \geq 1.0$. The maximum error is approximately 3%.

B. GFR 2219-T62 ALUMINUM VESSELS

1. Sizing/Operating Details

Figure 4 presents vessel sizing to operating pressure ratio (K_p) as a function of K_{sd} and operating temperature for all GFR 2219 aluminum vessel configurations. Values for sizing pressure may be calculated from the expression

$$p_s = K_p p_{o,T} \quad (13)$$

Metal shell offset yield stresses, induced by the sizing cycle, at ambient and cryogenic temperatures are shown in Figure 5 as a function of K_{sd} for spherical vessels. The invariant metal shell operating stresses in the spherical vessel may be calculated, as a function of operating temperature, from the expression

$$\sigma_{o,T} = K_{sd} F'_{ty,T} \quad (14)$$

Figure 6 presents metal shell offset yield stresses at each operating temperature for oblate spheroids and completely GFR cylinders as a function of K_{sd}. Equation 14 may be used to calculate the maximum stress in the metal shell at the operating condition. At ambient temperature the maximum operating stress is in the hoop direction located at the equator of the head for both configurations. Maximum operating stresses at cryogenic temperatures occur (a) in the hoop direction of the

cylinder for completely GFR cylindrical vessels, and (b) in the meridional direction at contour coordinate Z = 0.4 for oblate spheroids. At all other locations/directions on these two shapes metal shell operating stresses are less than the maximum values calculated from equation 14.

Figure 7 presents metal shell offset yield stresses for hoop GFR cylindrical vessels as a function of K_{sd} and operating temperature. The yield stress in the longitudinal direction of the cylinder and bidirectionally in the hemispherical heads is not altered by the sizing cycle; metal stresses at unreinforced locations/directions remain elastic during vessel sizing and operation. In order to maintain this elasticity in the metal shell, the differential hoop strain from the wrap condition to the operating condition had to be decreased for $K_{sd} > 0.838$. Thus, in the range $0.838 > K_{sd} > 0.923$, filament prestress was increased from 164 MN/m^2 (23.8 ksi) to the maximum value of 666 MN/m^2 (96.6 ksi) and for $K_{sd} > 0.923$, filament operating stress was additionally decreased as required. The resultant decrease in differential hoop strain caused a corresponding decrease in the metal cylinder hoop offset yield stress as is noted by the discontinuity in the curves of Figure 7.

At ambient temperature the invariant operating stress in the metal shell of the hoop GFR cylindrical vessel may be calculated from the expression

$$\sigma_{o,A} = K_{sd} F_{ty,A} \tag{15}$$

As noted in the above equation, the offset yield stress ($F'_{ty,A}$) has been replaced by the yield stress corresponding to unreinforced areas ($F_{ty,A}$). Maximum operating stress in the metal shell at cryogenic temperatures occurs in the hoop direction of the cylinder and may be calculated from equation 14. Cryogenic operating stress levels in the meridional direction at any point on the metal shell and in the hoop direction at all points on the hemispherical heads are less than the calculated maximas.

2. Metal Shell Thickness

Figure 8 presents the product (K_1) of sizing pressure (p_s) and metal shell diameter to thickness ratio (D/t_1) as a function of K_{sd} for all vessel configurations. Previously established values of sizing pressure and vessel diameter permit the metal shell thickness to be calculated from the expression

$$t_1 = p_s D/K_1 \tag{16}$$

All configurations of GFR aluminum vessels are not sensitive to constrictive wrap buckling in the study operating pressure range. Buckling sensitive vessel designs will occur when the value of (D/t_l) exceeds (a) 304 for complete GFR cylinders, (b) 5302 for spheres, and (c) 4246 for oblate spheroids; these D/t_l ratios correspond to operating pressures less than 690 N/cm^2 (1000 psi).

Sizing criteria dictate the design of hoop GFR aluminum cylinders, and compressive stresses at zero pressure after sizing are always less than the allowable compressive strength of the aluminum shell for all values of K_{sd}. Thus, the value of (D/t_l) which causes buckling sensitivity (a) is greater in value than that listed for complete GFR aluminum cylinders, and (b) varies over the range of K_{sd}. Values are not listed since these designs fall below the present study range of operating pressures.

3. Longitudinal Composite Thickness

Values of longitudinal filament thickness to metal shell thickness ratio (K_e) for completely GFR aluminum vessels are presented in Figure 9 as a function of K_{sd}. For spherical vessels the corresponding uniform composite thickness is given by the expression

$$t_c = 2K_e t_l / P_{vg} \tag{17}$$

The longitudinal composite thickness at the equator of the oblate spheroid and in the cylindrical section of the completely GFR cylindrical vessel is given by the expression

$$t_c = K_e t_l / (P_{vg} \cos^2 \alpha_o) \tag{18}$$

where,

P_{vg} = volume fraction of glass = 0.673

$\tan \alpha_o = (D_b/D) / (L/D)$

D_b/D = boss to chamber diameter ratio = 0.2

4. Hoop Composite Thickness

Figure 10 presents hoop filament thickness to metal shell thickness ratio (K_h) as a function of K_{sd} for both types of GFR cylindrical vessels. For hoop GFR cylindrical vessels a discontinuity occurs in the curve at a value of $K_{sd} = 0.923$. The change in slope of the curve at this point is a direct result of the decrease in filament operating stress discussed in Section IV-B-1.

Hoop composite thickness for both types of cylindrical vessels may be calculated from the expression

$$t_{hc} = K_h t_l / P_{vg} \tag{19}$$

independent of the L/D ratio.

5. Vessel Burst Pressure

Analysis of stress/strain output from the computer indicated the primary mode of failure for completely GFR aluminum vessels is fracture of the longitudinal filaments. Burst to operating pressure ratios (K_b), based on this failure mode, for completely GFR aluminum vessels are presented in Figures 11, 12, and 13 for operating temperatures of 297°K (+75°F), 77°K (-320°F), and 20°K (-423°F), respectively.

Figure 14 presents burst to operating pressure ratios for ambient and cryogenic operated hoop GFR cylindrical vessels. Modes of failure are also defined in the figure for each operating temperature. The rapid increase in hoop filament thickness for $K_{sd} > 0.923$ has no effect on burst pressure for vessels operating at ambient and 77°K (-320°F) because the controlling mode of vessel failure is the ultimate strength of the aluminum shell. Conversely, the large value of aluminum ultimate strength at 20°K (-423°F) permits the increased hoop filament thickness to have an effect on burst pressure for $0.923 < K_{sd} < 0.955$. For 20°K (-423°F) operation of the vessel at $K_{sd} \geq 0.955$, ultimate aluminum strength defines the failure mode as may be noted in the figure.

The curves may be used to establish vessel burst pressure for all configurations and operating conditions from the expression

$$P_{b,T} = K_b P_{o,T} \tag{20}$$

6. Vessel Performance and Weight

Performance factors ($K_w = p_o V/W$) for ambient operated GFR aluminum vessels are presented in Figure 15 for each configuration as a function of K_{sd}. Similar plots for the 77°K (-320°F) and 20°K (-423°F) operating temperatures are presented in Figures 16 and 17, respectively.

Bands of performance, are shown for completely overwrapped and hoop GFR cylindrical vessels, since the performance of these vessels depends on the vessel length to diameter ratio (L/D). Lower bounds of cylinder performance are based on L/D = 1.0 for completely GFR cylinders and L/D = 2.0 for hoop GFR cylinders; both lower bound values were established from practical considerations.

Weights of vessels (excluding bosses, attachments, and fluids) with specific volume and operating requirements may be established from the curves by the expression

$$W = p_{o,T} V/K_w \tag{21}$$

C. GFR INCONEL X-750 VESSELS

1. Sizing/Operating Details

Figure 18 presents vessel sizing to operating pressure ratios (K_p) as a function of K_{sd} and operating temperature for all configurations of GFR Inconel pressure vessels. The required sizing pressure for each desired operating condition may be determined from the expression

$$p_s = K_p p_{o,T} \tag{13}$$

Since metal shell sizing stresses for hoop GFR Inconel cylinders are strongly influenced by buckling sensitivity, the stress relations for hoop GFR and completely GFR Inconel vessels are discussed under separate sections in the following paragraphs.

a. Completely GFR Vessels

Metal shell offset yield stresses induced by the sizing pressure at ambient and cryogenic temperature are shown in Figure 19 as a function of K_{sd} for spherical vessels. The invariant operating stress in the Inconel metal shell of the spherical vessel may be

calculated, as a function of operating temperature, from the expression

$$\sigma_{o,T} = K_{sd} F'_{ty,T} \qquad (14)$$

Figure 20 presents metal shell offset yield stresses at each operating temperature for oblate spheroids and completely GFR cylinders as a function of K_{sd}. Equation 14 may be used to calculate the maximum stress in the Inconel metal shell at the operating condition. At ambient temperature the maximum operating stress is in the hoop direction located at the equator of the head for both configurations. Maximum operating stresses at cryogenic temperatures occur (a) in the hoop direction of the cylinder for completely GFR cylindrical vessels, and (b) in the meridional direction at contour coordinate Z = 0.4 for oblate spheroids. At all other locations/directions on these two shapes metal shell operating stresses are less than the maximum values calculated from equation 14.

b. Hoop GFR Cylinders

Yield stresses in the longitudinal direction of the hoop GFR Inconel cylinder and bidirectionally in the hemispherical heads are not altered by the sizing cycle; metal shell stresses at unreinforced locations/directions remain elastic during vessel sizing and operation. Conversely, the yield stress in the hoop direction of the Inconel metal shell is increased by the sizing cycle; the magnitude of the hoop directed offset yield stress is influenced by K_{sd} and by the sensitivity of the specific design to buckling.

The curve of Figure 21 defines the boundary between non-buckling and buckling sensitive designs in terms of critical sizing pressure ($p_{s,cr}$), and the K_{sd} range of interest. For designs with $p_s \geq p_{s,cr}$ (see Figure 21), the metal shell offset yield stresses in the hoop direction of the cylinder at ambient and cryogenic temperatures are defined by the solid curve in Figure 22. Designs in this sizing pressure range are not sensitive to buckling, and for all $K_{sd} \leq 0.935$ the filament operating stress is 1380 MN/m^2 (200 ksi) and the filament prestress is 164 MN/m^2 (23.8 ksi); for $K_{sd} > 0.935$ optimum differential strain requirements forced filament operating stresses to be decreased and/or filament prestress to be increased.

For designs in the buckling sensitive sizing pressure range, $p_s < p_{s,cr}$, an interpolation technique using Figures 21 and 22 must be used to determine metal shell offset yeild stresses in the hoop direction

of the cylinder. The procedure is as follows:

(1) Locate the desired point defined by ρ_s and K_{sd} on Figure 21.

(2) Interpolate between the dashed curves for a value of ambient filament operating stress level (σ_{of}).

(3) Enter Figure 22 with σ_{of} and K_{sd} and read the corresponding hoop directed offset yield stress in the Inconel shell at the desired operating temperature.

Sizing pressures defined in Figure 21 by the solid curve labeled (4) produce designs that exhibit metal shell hoop stresses equal to the yield strength of the Inconel metal, (i.e., the entire metal shell remains elastic during the sizing cycle). Designs which require sizing pressures less than those defined in Figure 21 by the curve labeled (4) have been omitted since they are impractical for a composite application on a weight basis.

The invariant operating stress in the metal shell of the hoop GFR cylindrical vessel may be calculated from the expression

$$\sigma_{o,A} = K_{sd} F_{ty,A} \tag{15}$$

As noted in the above equation, the offset yield stress ($F'_{ty,A}$) has been replaced by the yield stress corresponding to unreinforced areas ($F_{ty,A}$). Maximum operating stress in the metal shell at cryogenic temperatures occurs in the hoop direction of the cylinder and may be calculated from equation 14. Cryogenic operating stress levels in the meridional direction at any point on the metal shell and in the hoop direction at all points on the hemispherical heads are less than the cacluated maximas.

2. Metal Shell Thickness

Figure 23 presents the prouct (K_1) of sizing pressure (p_s) and Inconel metal shell diameter to thickness ratio (D/t_1) as a function of K_{sd} for all vessel configurations not sensitive to constrictive wrap buckling criteria. Previously established values of sizing pressure and vessel diameter permit the metal shell thickness to be calculated from the expression

$$t_1 = p_s D_i / K_1 \tag{16}$$

Completely overwrapped spheres and oblate spheroids are not constrictive wrap buckling stress sensitive in the study operating pressure range; GFR Inconel shells with these shapes are designed so that compressive stresses at zero pressure after sizing do not exceed the compression allowables at the operating temperatures. The transition metal shell diameter to thickness ratio, where constrictive wrap buckling strength controls the design, is 5516 for spheres and 4418 for oblate spheroids; both of these ratios correspond to operating pressures less than 690 N/cm^2 (1000 psi).

a. Completely GFR Cylindrical Vessels

Computer output used to establish the curve for completely overwrapped cylindrical vessels (Figure 23) indicated that for sizing pressure greather than

$$p_{s,cr} = C_1 + C_2 K_{sd} \tag{22}$$

Inconel shell designs are based on the ambient compressive allowables. (The coefficients in equation (22) are: C_1 = 1209 N/cm^2 (1754 psi) and C_2 = 74 N/cm^2 (107 psi). For sizing pessures less than

$$p_{s,min} = C_3 - C_4 K_{sd} \tag{23}$$

the longitudinal filament thickness is zero, thus excluding the weight optimized completely overwrapped cylindrical vessels from this pressure range. (The coefficients in equation (23) are: C_3 = 1150 N/cm^2 (1668 psi) and C_4 = 90 N/cm^2 (131 psi). In the sizing pressure range $p_{s,cr} \geq p_s \geq p_{s,min}$ the metal shell designs are based on constrictive wrap buckling strength; the corresponding transition diameter to thickness ratio is 312.

Based on these results, Figure 24 was prepared to provide metal shell design information for buckling sensitive completely GFR cylindrical vessels. The figure presents metal shell diameter to thickness ratio as a function of sizing pressure and three selected values of K_{sd}. Metal shell thickness is calculated directly from the diameter to thickness ratio corresponding to the required sizing pressure. Interpolation between curves may be used to establish metal shell designs for other values of K_{sd} within the study range.

b. Hoop GFR Cylindrical Vessels

Hoop wrapped cylinder designs exhibit metal shell compressive stresses at zero pressure after sizing which are a function of K_{sd} and always less than the compressive allowables. The shells become constrictive wrap buckling sensitive at ratios of D/t_1 which depend on the magnitude of the induced compressive stress. Since the induced compressive stress is controlled by the sizing cycle, the sizing pressure has been used as a buckling sensitivity indicator (refer to the discussion of Section IV-C-1-b).

Figure 25 presents metal shell diameter to thickness ratio as a function of sizing pressure and three selected values of K_{sd} for the range of designs sensitive to buckling. Metal shell thickness is calculated directly from the diameter to thickness ratio corresponding to the required sizing pressure and value of K_{sd}. Interpolation between K_{sd} curves is possible, but care should be exercised since the curves are highly non-linear in this sizing pressure range. A cutoff, based on the $p_{s,min}$ discussion of Section IV-C-1-b, has been placed on the curves to show the upper boundary of hoop GFR Inconel D/t_1 ratios considered in this study, (i.e. $(D/t_1)_{max} = 4\sigma_o/p_o$).

3. Longitudinal Composite Thickness

Values of longitudinal filament thickness to metal shell thickness ratio (K_e) for compressive allowable designs of completely overwrapped Inconel vessels are presented in Figure 26 as a function of K_{sd}.

The curve for completely GFR Inconel cylindrical vessels is valid for sizing pressures greater than or equal to $p_{s,cr}$ as defined by equation (22). For sizing pressures in the range $p_{s,cr} > p_s \geq p_{s,min}$, the longitudinal filament thickness to metal shell thickness ratio may be calculated from the expression

$$K_e = C_5 (p_s - p_{s,min}) \qquad (24)$$

where, $p_{s,min}$ is defined by equation (23) and $C_5 = 0.363 \times 10^{-3} cm^2/N$ $(0.250 \times 10^{-3}/psi)$. It is evident that the $p_{s,min}$ are the sizing pressures corresponding to zero longitudinal filament thickness for each K_{sd}.

For spherical vessels the corresponding uniform composite thickness (t_c) is given by the expression

$$t_c = 2 K_e t_1 / P_{vg} \tag{17}$$

The longitudinal composite thickness (t_c) at the equator of the oblate spheroid and in the cylindrical section of the completely GFR cylindrical vessel is given by the expression

$$t_c = K_e t_1 / (P_{vg} \cos^2 \alpha_o) \tag{18}$$

$P_{vg} = 0.673$

$D_b/D = 0.2$

$\tan \alpha_o = (D_b/D) \; / \; (L/D)$

4. Hoop Composite Thickness

Figure 27 presents hoop filament to metal shell thickness ratios (K_h) for compressive allowable designs of both types of GFR cylindrical vessels as a function of K_{sd}.

The curve labeled (2) is valid for all completely GFR cylindrical vessels sized at pressures greater than $p_{s,cr}$, as defined by equation (22). For sizing pressures less than $p_{s,cr}$, but greater than $p_{s,min}$, the value of K_h may be calculated from the expression

$$K_h = C_6 p_s + 0.283 K_{sd} - 0.390 \tag{25}$$

where, $C_6 = 7.1 \times 10^{-4}$ cm^2/N (4.9×10^{-4}/psi).

Figure 27 also presents values of K_h for hoop wrapped Inconel cylindrical vessels as a function of K_{sd}. The curve labeled (3) applies to all compressive allowable designs of hoop GFR Inconel cylinders. For designs in the buckling sensitive range, $p_s < p_{s,cr}$, values of K_h may be calculated from the expression

$$K_h = F_{tyA} K_{sd} / \sigma_{of} \tag{26}$$

where the filament operating stress (σ_{of}) was previously determined in Section IV-C-1-b.

Hoop composite thickness (t_{hc}) for both types of cylindrical vessels may be calculated from the expression

$$t_{hc} = K_h t_l / P_{vg} \tag{19}$$

independent of L/D ratio.

5. Vessel Burst Pressure

Burst to operating pressure ratios (K_b) for all configurations of GFR Inconel vessels not sensitive to buckling are presented in Figures 28, 29, and 30 for operating temperatures of 297°K (+75°F), 77°K (-320°F), and 20°K (-423°F), respectively. The primary mode of failure for all completely GFR vessels is fracture of the longitudinal filaments; the mode of failure for hoop GFR cylindrical vessels is fracture of the hoop filaments.

Ambient values of K_b for buckling sensitive design of completely GFR cylindrical vessels are presented in Figure 31 as a function of sizing pressure and three selected values of K_{sd}. For constant K_{sd} and decreasing sizing pressure, the decrease in K_b from the constant value associated with non-buckling sensitive designs is not significant. The deviation is less significant at cryogenic operating temperatures ($< 5\%$), and values of K_b for non-buckling sensitive designs (Figures 29 and 30) may be used for buckling sensitive designs without appreciable error.

No clear relationship was developed in this study for presenting values of K_b for buckling sensitive designs of hoop GFR Inconel cylindrical vessels. These designs are significantly influenced by the mode of vessel failure and, for each K_{sd}, the corresponding value of K_l and K_h (both of which vary with filament operating stresss level). A conservative estimate of K_b for buckling sensitive hoop GFR Inconel cylinders can be obtained from the non-buckling sensitive design curves, Figures 28, 29, and 30. The maximum value of K_b for each K_{sd} may be calculated from the expression

$$(K_b)_{max} = 4(K_p/K_l)F_{tu} \tag{27}$$

Once K_b has been established, vessel burst pressure for all configurations and operating conditions may be calculated from the relation

$$p_{b,T} = K_b p_{o,T} \tag{2}$$

6. Vessel Performance and Weight

Performance factors (K_w) for all configurations of GFR Inconel vessels are presented in Figures 32, 33, and 34 for operating temperatures of 297°K (+75°F), 77°K (-320°F), and 20°K (-423°F), respectively. Bands of performance are shown for both types of GFR cylindrical vessels, since the performance of these vessels depends on the vessel length to diameter ratio (L/D). Lower bounds of cylinder performance are based on L/D = 1.0 for completely GFR cylinders and L/D = 2.0 for hoop GFR cylinders.

Dry weights of vessels with specific volume and operating pressure requirements may be established from the curves by the relation

$$W = p_{o,T} V/K_w \tag{21}$$

Values of performance and weight obtained from the curves for buckling sensitive GFR cylinder designs are not exact, but do provide a very good first approximation.

D. GFR 301 STAINLESS STEEL VESSELS

Unlike either the Inconel or aluminum metals, 301 stainless steel must be stretched at 77°K (-320°F) to a stress level of approximately 930 NM/m^2 (135 ksi) before overwrapping in order to gain the structural properties listed in Table I. A complete discussion of the cryoforming technique, resultant material properties, and test results from GFR 301 stainless steel spheres is contained in Reference 7. Following the initial cryostretch, overwrapping, and cure cycle, the GFR 301 stainless steel vessel is sized, similar to GFR aluminum and Inconel vessels, except that the sizing is conducted at liquid nitrogen temperature.

1. Sizing/Operating Details

Figure 35 presents vessel sizing to operating pressure ratio (K_p) as a function of K_{sd} and operating temperature for all

configurations of GFR stainless steel pressure vessels. The required 77°K (-320°F) sizing pressure for each desired operating condition may be determined from the expression

$$p_s = K_p p_{o,T} \tag{13}$$

Since metal shell sizing stresses for hoop GFR stainless steel cylinders are strongly influenced by buckling sensitivity, the stress relations for hoop GFR and completely GFR stainless steel vessels are discussed under separate sections in the following paragraphs.

a. Completely GFR Vessels

Metal shell offset yield stresses induced by the sizing pressure at ambient and cryogenic temperature are shown in Figure 36 as a function of K_{sd} for spherical vessels. The invariant operating stress in the stainless steel metal shell of the spherical vessel may be calculated, as a function of operating temperature, from the expression

$$\sigma_{o,T} = K_{sd} F'_{ty,T} \tag{14}$$

Figure 37 presents metal shell offset yield stresses at each operating temperature for oblate spheroids and completely GFR cylinders as a function of K_{sd}. Equation 14 may be used to calculate the maximum stress in the stainless steel metal shell at the operating condition. The maximum operating stress at all operating temperatures is in the hoop direction located at the equator of the head for both configurations. At all other locations/directions on these two shapes metal shells operating stresses are less than the maximum values calculated from equation 14.

b. Hoop GFR Cylinders

Yield stresses in the longitudinal direction of the hoop GFR stainless steel cylinder and bidirectionally in the hemispherical heads are not altered by the sizing cycle; metal shell stresses at unreinforced locations/directions remain elastic during vessel sizing and operation. Conversely, the yield stress in the hoop direction of the stainless steel metal shell is increased by the sizing cycle; the magnitude of the hoop directed offset yield stress is influenced by K_{sd} and by the sensitivity of the specific design to buckling.

The curve of Figure 38 defines the boundary between non-buckling and buckling sensitive designs in terms of critical sizing pressure ($p_{s,cr}$), and the K_{sd} range of interest. For designs with $p_s \geq p_{s,cr}$ (See Figure 38), the metal shell offset yield stresses in the hoop direction of the cylinder at ambient and cryogenic temperatures are defined by the curve of Figure 39. Designs in this sizing pressure range are not sensitive to buckling and for all $K_{sd} \leq 0.932$ the filament operating stress at $77^{o}K$ ($-320^{o}F$) is 1450 MN/m^2 (210 ksi), and the ambient filament prestress is 164 MN/m^2 (23.8 ksi); for $K_{sd} > 0.932$ optimum differential strain requirements forced filament operating stresses at $77^{o}K$ ($-320^{o}F$) to be decreased and/or ambient filament prestresses to be increased.

For designs in the buckling sensitive pressure range, $p_s < p_{s,cr}$, the differential strain from the ambient winding condition to the cryogenic operating condition must be further decreased by an amount which depends on the induced compressive stress in the metal at ambient temperature. This complicated interrelation between design parameter at each K_{sd} coupled with time and funding limits on the study phase of the program precluded further investigation of buckling sensitive hoop GFR stainless steel cylinder designs.

The invariant operating stress in the metal shell of non-buckling sensitive hoop GFR cylindrical vessels at both cryogenic operating temperatures may be calculated from the expression

$$\sigma_{o,T} = K_{sd} F_{ty,T} \qquad (15a)$$

As noted in the above equation, the offset yield stress ($F'_{ty,T}$) has been replaced by the yield stress corresponding to unreinforced areas ($F_{ty,T}$). Maximum operating stress in the metal shell at ambient temperature occurs in the unreinforced locations/directions and may also be calculated from equation 15a; the operating stress level in the hoop direction is less than the calculated maximas.

2. Metal Shell Thickness

Figure 40 presents the product (K_1) of sizing pressure (p_s) and stainless steel metal shell diameter to thickness ratio (D/t_1) as a function of K_{sd} for all vessel configurations not sensitive to constrictive wrap buckling criteria. Previously established values of sizing pressure

and vessel diameter permit the metal shell thickness to be calculated from the expression

$$t_1 = p_s D_1 / K_1 \qquad (16)$$

Completely overwrapped spheres and oblate spheroids are not constrictive wrap buckling stress sensitive in the study operating pressure range, GFR stainless steel shells with these shapes are designed so that compressive stresses at zero pressure after sizing do not exceed the compression allowables at the operating temperatures. The transition metal shell diameter to thickness ratio, where constrictive wrap buckling strength controls the design, is 4240 for spheres and 3396 for oblate spheroids; both of these ratios correspond to operating pressures less than 690 N/cm^2 (1000 psi).

a. Completely GFR Cylindrical Vessels

Computer output used to establish the curve for completely overwrapped cylindrical vessels (Figure 40) indicated that for sizing pressures greater than

$$p_{s,cr} = C_7 + C_8 K_{sd} \qquad (28)$$

stainless steel shell designs are based on the ambient compressive allowable. The coefficients in equation (28) are: C_7 = 1895 N/cm^2 (2748 psi) and C_8 = 726 N/cm^2 (1053 psi). In the sizing pressure range, $p_s \leq p_{s,cr}$, designs are sensitive to the constrictive wrap buckling strength of the stainless steel shell; the corresponding transition diameter to thickness ratio is 262. The program time/funding factor discussed in Section IV-D-1-b also precluded further investigation of the buckling sensitive completely GFR stainless steel cylindrical vessels, and these designs have not been included in this guide.

b. Hoop GFR Cylindrical Vessels

Hoop wrapped stainless steel cylinder designs exhibit metal shell compressive stresses at zero pressure after sizing which are a function of K_{sd} and always less than the compressive allowables. The shells become constrictive wrap buckling sensitive at ratios of D/t_1 which depend on the mangitude of the induced compressive stress. Since the induced compressive stress is controlled by the sizing cycle, the critical sizing pressure curve (Figure 38) may be used as a buckling sensitivity indicator.

3. Longitudinal Composite Thickness

Values of longitudinal filament thickness to metal shell thickness ratio (K_e) for GFR stainless steel spheres are presented in Figure 41 as a function of K_{sd}. The corresponding uniform composite thickness is given by the expression

$$t_c = 2K_e t_l / p_{vg} \tag{17}$$

Figure 42 presents K_e for GFR oblate spheroids and compressive allowable designs of completely overwrapped cylindrical vessels. The longitudinal composite thickness at the equator of the oblate spheroid and in the cylindrical section of the completely GFR cylindrical vessel is given by the expression

$$t_c = K_e t_l / (p_{vg} \cos^2 \alpha_o) \tag{18}$$

where,

$p_{vg} = 0.673$

$D_b/D = 0.2$

$\tan \alpha_o = (D_b/D) \ / \ (L/D)$

4. Hoop Composite Thickness

Figure 43 presents hoop filament thickness to metal shell thickness ratios (K_h) as a function of K_{sd} for both types of GFR cylindrical vessels. For hoop GFR cylindrical vessels, a discontinuity occurs in the curve at a value of $K_{sd} = 0.955$. The change in slope of the curve at this point is a direct result of the decrease in filament operating stress discussed in Section IV-D-1-b.

Hoop composite thickness for both types of cylindrical vessels may be calculated from the expression

$$t_{hc} = K_h t_l / p_{vg} \tag{19}$$

independent of the L/D ratio.

5. Vessel Burst Pressure

Analysis of stress/strain output from the computer indicated the primary mode of failure for completely GFR stainless steel vessels is fracture of the longitudinal filaments. Burst to operating pressure ratios (K_b), based on this failure mode, for completely GFR stainless steel vessels not sensitive to buckling are presented in Figures 44, 45, and 46 for operating temperatures of 297°K (+75°F), 77°K (-320°F), and 20°K (-423°F), respectively.

Figure 47 presents burst to operating pressure ratios for compressive yield designs of ambient and cryogenic operated hoop GFR cylindrical vessels. Modes of failure are also defined in the figure for each operating temperature.

The curves may be used to establish vessel burst pressure for all configurations and operating conditions from the expression

$$p_{b,T} = K_b p_{o,T} \tag{20}$$

6. Vessel Performance and Weight

Performance factors (K_w) for ambient operated GFR stainless steel vessels are presented in Figure 48 for each configuration as a function of K_{sd}. Similar plots for the 77°K (-320°F) and 20°K (-423°F) operating temperatures are presented in Figures 49 and 50, respectively.

Bands of performance, are shown for both types of GFR cylindrical vessels, since the performance of these vessels depends on the vessel length to diameter ratio (L/D). Lower bounds of cylinder performance are based on L/D = 1.0 for completely GFR cylinders and L/D = 2.0 for hoop GFR cylinder; both lower bound values were established from practical considerations.

Weights of vessels (excluding bosses, attachments, and fluids) with specific volume and operating requirements may be established from the curves by the expression

$$W = p_{o,T} V / K_w \tag{21}$$

E. SAMPLE DESIGNS

The design equations and curves presented in this report are used here to illustrate the procedure for preliminary design of GFR metal tanks.

Design No. 1 (Buckling Sensitive)

In addition to the basic study design criteria, the following hypothetical design requirements are assumed:

Operating pressure at 297°K (+75°F)	965 N/cm^2 (1400 psi)
Required volume	2.83 m^3 (100 ft^3)
Available tank space	1.22 m (4.0 ft) x 1.22 m (4.0 ft) x 6.10 m (20.0 ft)
Metal shell material	Inconel X-750
Metal shell maximum operating stress to sizing stress ratio (hypothetically derived from fracture mechanics data)	0.80

Volume and envelope dimensions indicate the configuration should be cylindrical (it could be stacked spheres) and efficiency considerations lead to a completely GFR pattern. For a volume of 2.83 m^3 (100 ft^3), Equation 12 is used to arrive at a diameter, D = 0.91 m (3 ft), and an overall vessel length, L = 4.55 M (15 ft) (L/D = 5), which meet the envelope requirements.

With the above information, the equations and curves of Section IV-C are used to establish the vessel design parameters. The table below summarizes resulting data and references the governing equation or figure.

	Parameter	Value SI Units	Value US Units	Data Source
	K_{sd}	0.80	0.80	Given
	K_p	1.250	1.250	Figure 18
Sizing pressure	p_s	1210 N/cm^2	1750 psi	Equation 13
Metal shell sizing stress	$\sigma_s = F'_{ty,A}$	890 MN/m^2	129.1 ksi	Figure 20
Metal shell maximum operating stress	$(\sigma_{0,max})_A$	712 MN/m^2	103.3 ksi	Equation 14
Buckling sensitivity sizing pressure	$p_{s,cr}$	1270 N/cm^2	1840 psi	Equation 22
Minimum allowable sizing pressure	$p_{s,min}$	1080 N/cm^2	1560 psi	Equation 23
	K_l - not applicable; $p_s < p_{s,cr}$ indicates design is buckling sensitive			
	D/t_l	317.5	317.5	Figure 24
Metal shell thickness	t_l	0.287 cm	0.113 inch	direct calculation
	K_e	0.0475	0.0475	Equation 24
Longitudinal composite thickness	t_c	0.020 cm	0.008 inch	Equation 18
	K_h	0.694	0.694	Equation 25
Hoop composite thickness	t_{hc}	0.296 cm	0.117 inch	Equation 19
	K_b	1.360	1.360	Equation 31
Ambient burst pressure	$P_{b,A}$	1310 N/cm^2	1900 psi	Equation 20
Performance factor	K_w	67 J/g	0.27 x 10^6 in-lb/lb	Figure 32
Vessel weight	W	407 kg	896 lbs	Equation 21

Analysis of the above design details for this hypothetical example indicates the longitudinal composite thickness (t_c) is quite small, if not impractical for this size tank. Thus, a better choice for this application might have been a hoop GFR cylindrical vessel. Other comments could be made about the specific details, but this would serve no purpose since the assumed criteria was chosen to maximize use of general procedures.

Design No. 2 (Not Sensitive to Buckling)

In order to show a typical design path for a non-buckling sensitive design, the following hypothetical requirements are assumed:

Operating Pressure at 77°K (-320°F)	2070 N/cm^2 (3000 psi)
Required Shape	Sphere
Maximum Diameter	0.914 m (3 ft)
Metal Shell Material	2219-T62 Aluminum
Metal Shell Maximum Operating to Sizing Stress Ratio	0.70

Based on the required diameter, Equation 9 is used to arrive at a volume of 0.40 m^3 (14 ft^3). With the above information, the equations and curves of Section IV-B are used to establish the vessel design parameters summarized in the following table.

Parameter		Value SI Units	US Units	Data Source
	K_{sd}	0.70	0.70	Given
	K_p	1.188	1.188	Figure 4
Sizing pressure	p_s	2460 N/cm^2	3560 psi	Equation 13
Metal shell sizing stress	$\sigma_s = F'_{ty, A}$	367 MN/m^2	53.2 ksi	Figure 5
Metal shell offset yield stress at 77°K (-320°F)	$F'_{ty, N}$	446 MN/m^2	64.7 ksi	Figure 5
Metal shell operating stress at 77°K (-320°F)	$\sigma_{o, N}$	312 MN/m^2	45.3 ksi	Equation 14
	K_l	3.1×10^5 N/cm^2	4.5×10^5 psi	Figure 8
Metal shell thickness	t_l	0.724 cm	0.285 inch	Equation 16
	K_e	0.275	0.275	Figure 9
Composite thickness	t_c	0.592	0.233	Equation 17
	K_b	2.05	2.05	Figure 12
Burst pressure at 77°K (-320°F)	$p_{b, N}$	4240 N/cm^2	6150 psi	Equation 20
Performance factor at 77°K (-320°F)	K_w	98 J/g	0.39×10^6 in-lbf/lbm	Figure 16
Vessel weight	W	84.4 kg	186 lbm	Equation 21

The above design (although hypothetical) is probably very realistic for the K_{sd} selected; the burst pressure of the unit is approximately twice the cryogenic operating pressure.

V. SAFELIFE VERSUS BURST FACTOR OF SAFETY DESIGNS

As noted earlier, vessel criteria for this Guide are based on safelife design. Complementing fracture data generated under other tasks of the program permit selection of appropriate K_{sd} values for vessel service cycle requirements. Vessel designs developed for values of K_{sd} down to 0.70 generally had burst factors of safety less than 2.0.

Subsequent to preparation of most material in this Guide, Space Shuttle requirements in Reference 1 specified that pressure vessels other than major propellant tanks should have a burst factor of ≥ 2.0. Designing for a minimum burst factor of safety ≥ 2.0, as well as safelife, introduces a new criterion which increases thicknesses, and increases reliability of the vessels. This is an important and quite significant situation, working in favor of GFR metal vessel applications to the Space Shuttle as follows:

(a) The required burst factor of safety of ≥ 2.0 results in an "overdesigned" GFR metal tank compared to current best estimates of the required metal shell operating stress ratio, K_{sd}, for safelife design.

(b) Conventional metal tanks also have a factor of safety of ≥ 2.0 so that the inherent weight saving of GFR metal tanks is not biased by any lower factor of safety for the metal tank.

(c) The required GFR metal tank "overdesign" for burst pressure results in a reduction in the metal and/or filament overwrap stresses from their maximum safe operating values at the vessel operating pressure.

(d) Since the lightest vessel is the one with the least metal, weight minimization dictates making the liner as thin as possible consistent with GFR metal tank criteria. If this is done in conjunction with a 2.0 burst factor of safety, composite tank weight saving compared with homogeneous metal tanks will increase over the performance factors presented in this Guide.

VI. CONCLUDING REMARKS

A. The information contained in this design guide permits rapid preliminary sizing of GFR metal tanks, including the determination of values for proof pressure, metal shell and composite overwrap thicknesses, vessel diameter and length, and weight for given values of (1) internal volume, (2) operating pressure, (3) operating temperature, and (4) typical Space Shuttle service cycle requirements.

B. During the conduct of the study the three singular values of metal shell operating to sizing stress ratio (K_{sd}), dictated by study criteria, were increased to cover the entire range of K_{sd} between 0.70 and 1.00. This generalization provides GFR tank design capability for any K_{sd} value, within this range, which may come from fracture mechanics consideration.

C. Pressure vessel operating performance factors are high compared with homogeneous metal tanks. Generally, the GFR stainless steel vessels exhibit the highest performance followed by GFR aluminum and GFR Inconel vessels. At ambient operating temperature the GFR sphere is (1) 20 to 25% more efficient than a long completely overwrapped cylinder, (2) 25 to 30% more efficient than a GFR oblate spheroid, and (3) 30 to 40% more efficient than a long hoop GFR cylindrical vessel. At cryogenic operating temperatures, a smaller efficiency spread between configurations exists.

D. Although performance is a major consideration, selection of the metal material should be based on analysis of fracture data and suitability of the metal shell for the service temperature range and contained fluid.

E. The operating pressure range considered in this design guide was 690 to 2760 N/cm^2 (1000 to 4000 psi), and care should be exercised in using the guide to establish designs outside this pressure range. Many of the design variables appear to be constant at operating pressures above 2760 N/cm^2 (4000 psi), but in many cases "thick wall" effects lead to non-conservative estimates.

TABLE 1

MATERIAL PROPERTIES USED IN PARAMETRIC STUDY
(Reference 3, except as noted)

Material	Density		Coefficient of Thermal Expansion		Tensile Yield Strength		Derivative of yield strength with respect to temperature	
	g/cm^3	lbm/in^3	$\mu/^oK$	$in/in/^oF \times 10^6$	MN/m^2	ksi	$N/cm^2/^oK$	$psi/^oF$
Inconel X-750 (STA)	8.30	0.300	8.98	4.99	814	118	-74.6	-60.1
Aluminum 2219-T62	2.82	0.102	16.05	8.915	293	42.5	-36.1	-29.1
Cryoformed 301 Stainless Steel (b)	7.47	0.270	8.26	4.59	1190(a)	172(a)	-94.3(a)	-76.0(a)
Glass-Filaments	1.99(c)	0.072(c)	3.62	2.01	-	-	-	-

(a) Reference 8
(b) Reference 7
(c) Composite value based on $P_{vg} = 0.673$
(d) Reference 4

TABLE 1 (continued)

MATERIAL PROPERTIES USED IN PARAMETRIC STUDY
(Reference 3, except as noted)

Material	Elastic modulus		Derivative of elastic modulus with respect to temperature		Plastic modulus		Derivative of plastic modulus with respect to temperature	
	GN/m^2	psi $\times 10^{-6}$	$GN/m^2/^oK$	$psi/^oF$	GN/m^2	ksi	$MN/m^2/^oK$	$psi/^oF$
Inconel X-750 (STA)	214	31.0	-0.0249	-2010	3.03(d)	440(d)	-0.0012	-0.1
Aluminum 2219-T62	72.4	10.5	-0.0311	-2510	2.76(d)	400(d)	-2.66	-214
Cryoformed 301 Stainless Steel (a)	131	19.0	-0.207	-16700	4.14	600	-0.78	-63
Glass-Filaments	85.5	12.4	-0.0299	-2410	-	-	-	-

(a) Reference 8
(d) Reference 4

TABLE 1 (continued)

MATERIAL PROPERTIES USED IN PARAMETRIC STUDY
(Reference 3, except as noted)

Material	Poisson's ratio	Derivative of Poisson's ratio with respect to temperature	Maximum allowable operating stress (Compressive in metal, tensile in filaments)					
			297°F	(75°F)	77°K	(-320°F)	20°K	(-423°F)
	Dimensionless	Dimensionless	MN/m^2	ksi	MN/m^2	ksi	MN/m^2	ksi
Inconel X-750 (STA)	0.290	0.0	745	108	889	129	931	135
Aluminum 2219-T62	0.325	-0.2005×10^{-4}	273	39.6	342	49.6	360	52.2
Cryoformed 301 Stainless Steel (a)	0.290 (b)	0.0 (b)	772	112	903	131	938	136
Glass-Filaments (a)	-	-	1380	200	1720	250	1720	250

(a) Reference 8
(b) Reference 7

TABLE 1 (continued)

MATERIAL PROPERTIES USED IN PARAMETRIC STUDY
(Reference 3, except as noted)

Material	Ultimate Strength					
	297°K	(75°F)	77°K	(-320°F)	20°K	(-423°F)
	MN/m^2	ksi	MN/m^2	ksi	MN/m^2	ksi
Inconel X-750 (STA)	1200	174	1480	214	1610	234
Aluminum 2219-T62	407	59	538	78	634	92
Cryoformed 301 Stainless Steel (a)	1410	204	1930	280	2030	295
Glass-Filaments (d)	2280	330	2840	412	2840	412

(a) Reference 8
(d) Reference 4

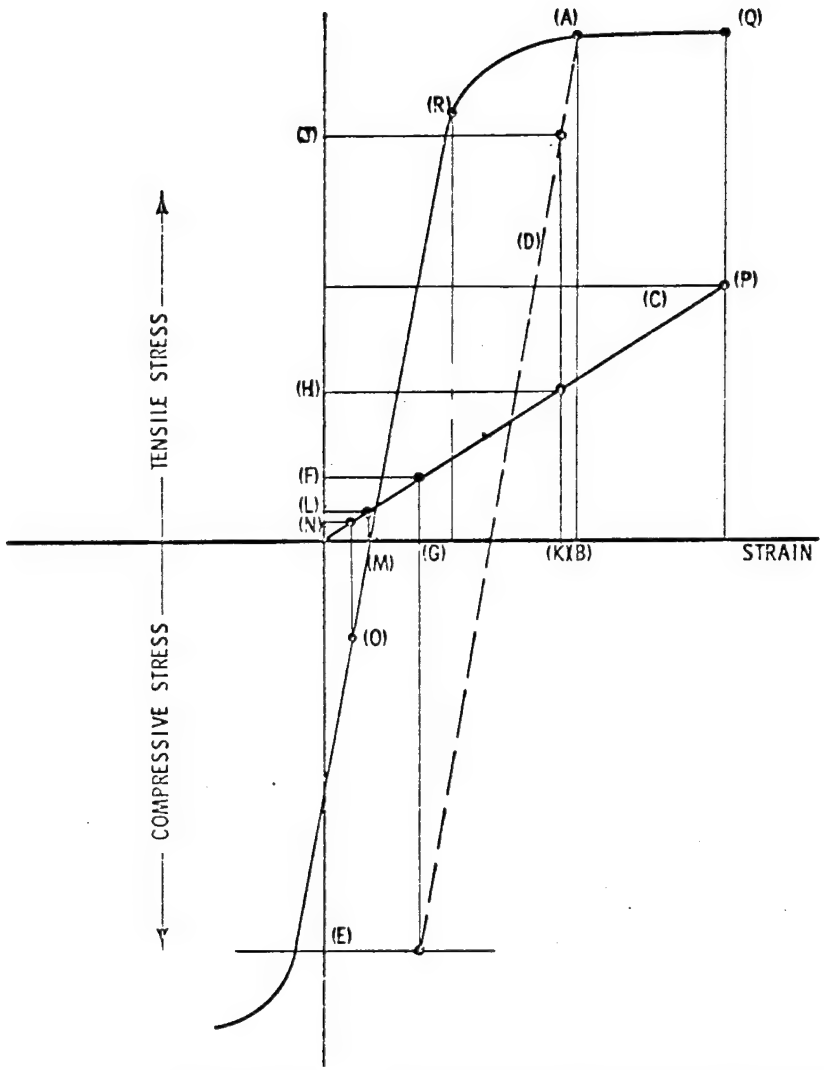

(A) STRESS-STRAIN CURVE FOR METAL SHELL - FIRST CYCLE
(B) MAXIMUM STRAIN REQUIRED OF COMPLETE SHELL - FIRST CYCLE
(C) STRESS-STRAIN CURVE FOR GLASS-FIBER SHELL - ALL CYCLES
(D) STRESS-STRAIN CURVE FOR METAL SHELL-UNLOADING FROM FIRST CYCLE
(E) COMPRESSIVE STRESS ACHIEVED IN METAL SHELL WHEN VESSEL PRESSURE IS ZERO AFTER STRAIN TO (A)
(F) TENSION STRESS IN GLASS FIBER SHELL THAT BALANCES COMPRESSION STRESS (E) IN METAL SHELL
(G) RESIDUAL STRAIN IN GLASS FIBER AND METAL SHELLS WHEN VESSEL PRESSURE IS ZERO AFTER STRAIN TO (A)
(H) OPERATING STRESS IN GLASS FIBER SHELL - ALL CYCLES SUBSEQUENT TO THE FIRST
(J) OPERATING STRESS IN METAL SHELL - ALL CYCLES SUBSEQUENT TO FIRST
(K) OPERATING STRAIN IN GLASS-FIBER AND METAL SHELLS - ALL CYCLES SUBSEQUENT TO FIRST
(L) STRESS IN GLASS FIBER SHELL FROM WINDING ON RIGID MANDREL
(M) STRAIN IN GLASS FIBER SHELL FROM WINDING ON A RIGID MANDREL; ZERO STRAIN POINT OF METAL SHELL BEFORE WINDING
(N) STRESS IN GLASS FIBER SHELL AFTER MANDREL REMOVAL WHEN VESSEL PRESSURE IS ZERO
(O) STRAIN IN METAL AND GLASS FIBER SHELLS AFTER MANDREL REMOVAL WHEN VESSEL PRESSURE IS ZERO
(P) ULTIMATE STRESS OR STRAIN OF GLASS FIBER SHELL
(Q) ULTIMATE STRESS OR STRAIN OF METAL SHELL WHEN FILAMENTS FRACTURE
(R) ARBITRARY STRAIN POINT IN METAL SHELL AND GLASS FIBER SHELL BELOW METAL SHELL PROPORTIONAL LIMIT

FIGURE 1: STRESS-STRAIN DIAGRAM FOR GLASS FILAMENT REINFORCED METALLIC SHELL

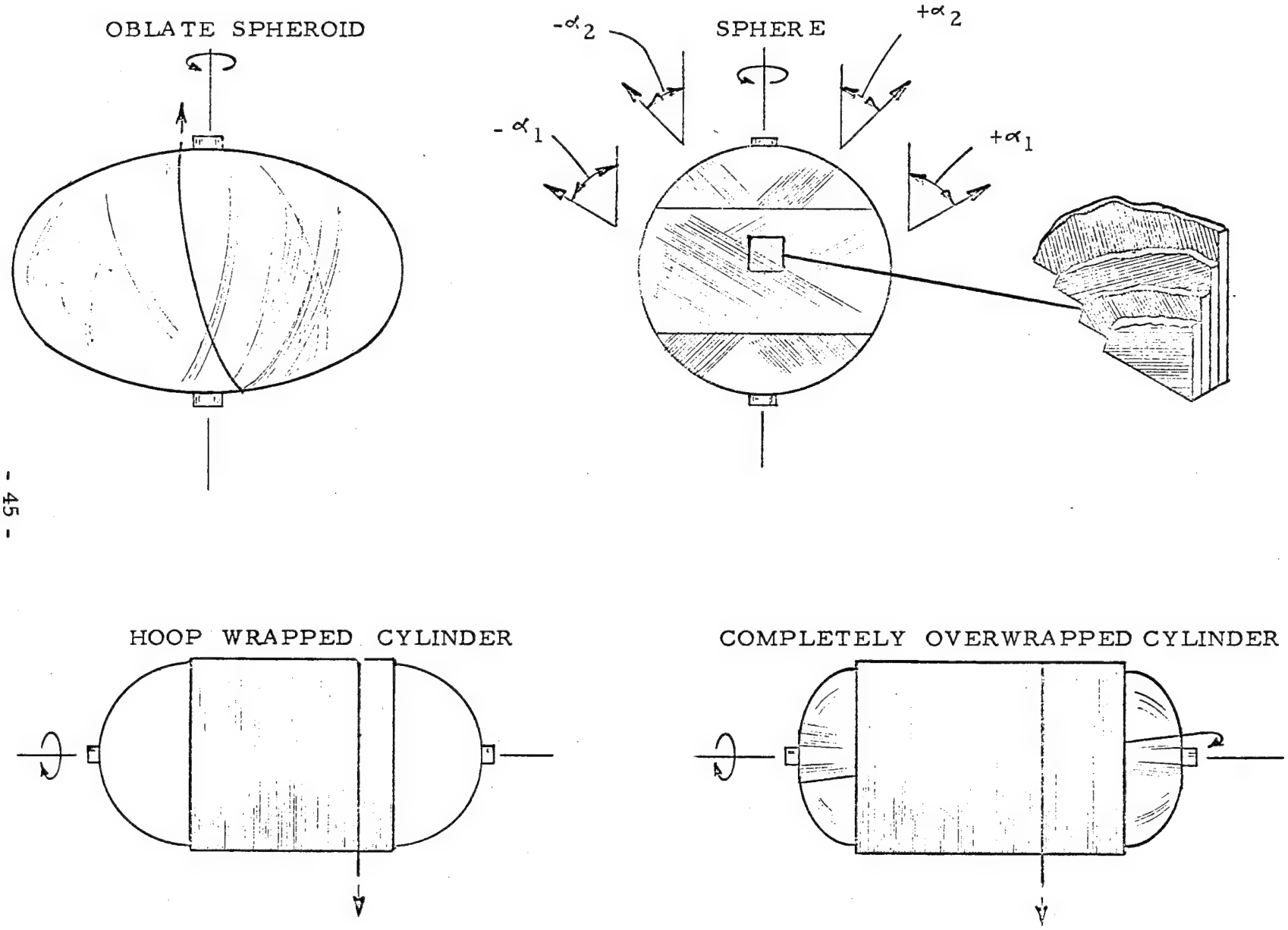

FIGURE 2: VESSEL CONFIGURATIONS AND WRAP PATTERNS

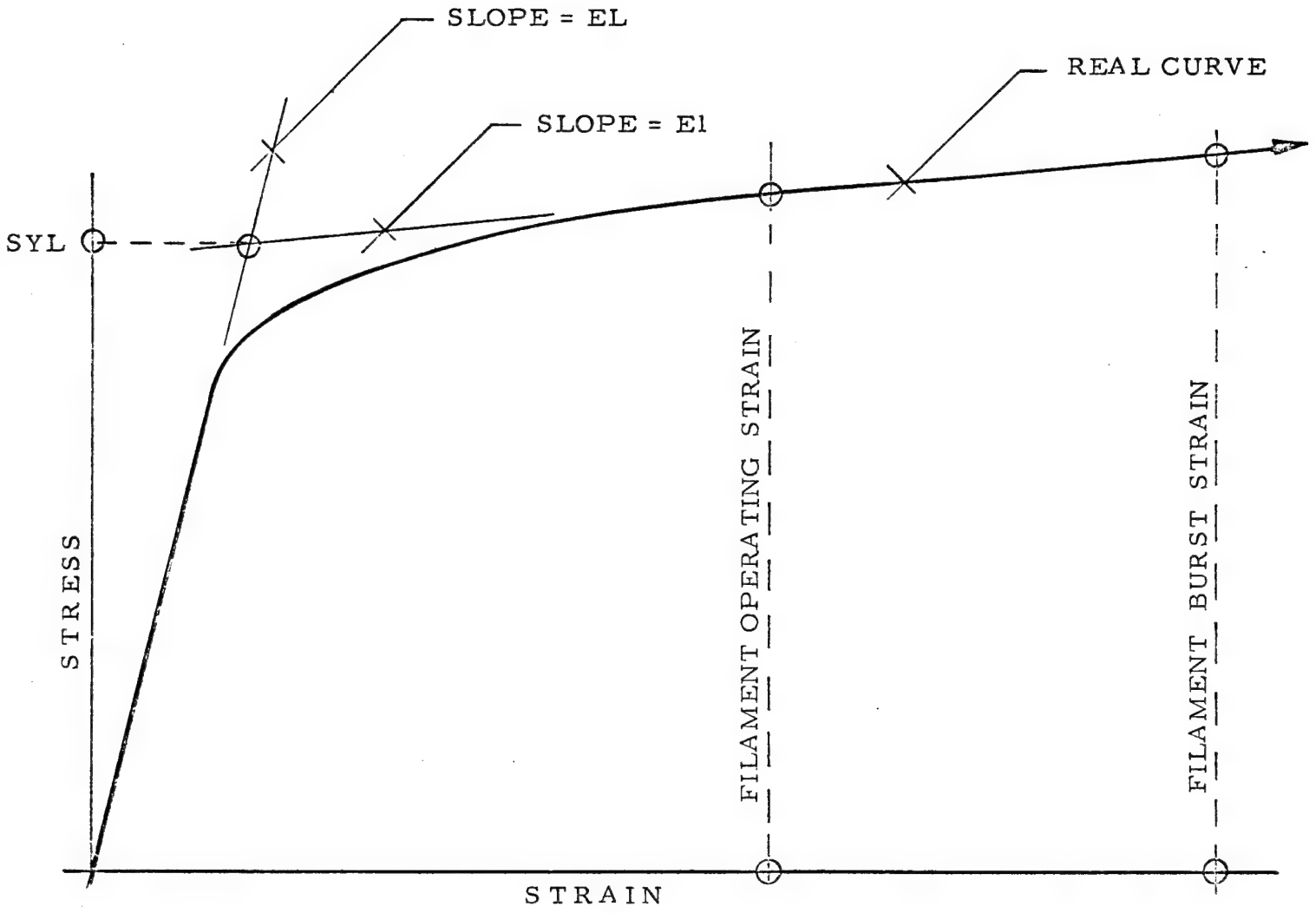

FIGURE 3: LINEARIZATION OF METAL SHELL STRESS/STRAIN CURVE

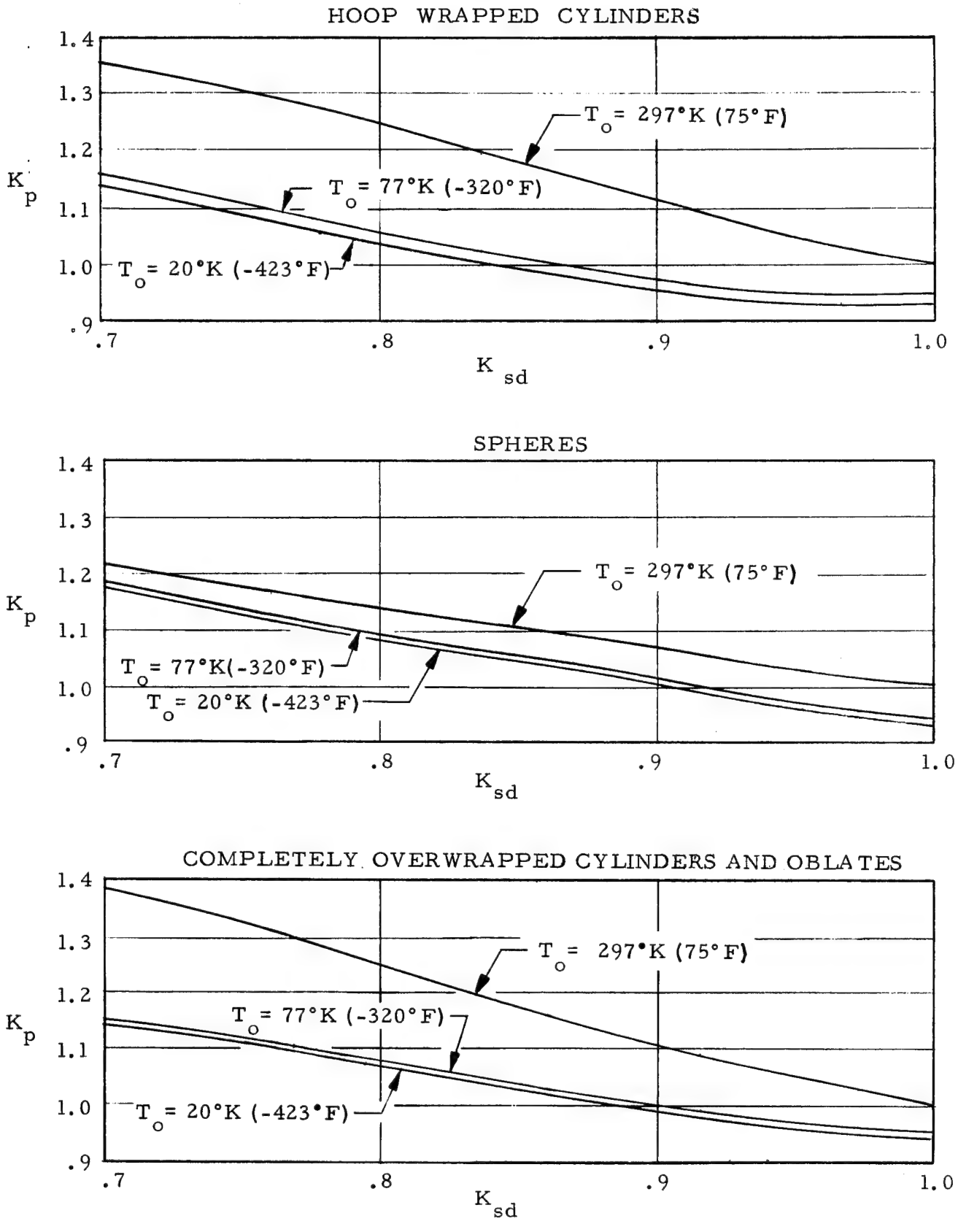

FIGURE 4: SIZING PRESSURE REQUIREMENTS FOR AMBIENT AND CRYOGENIC OPERATED GFR 2219-T62 ALUMINUM PRESSURE VESSELS

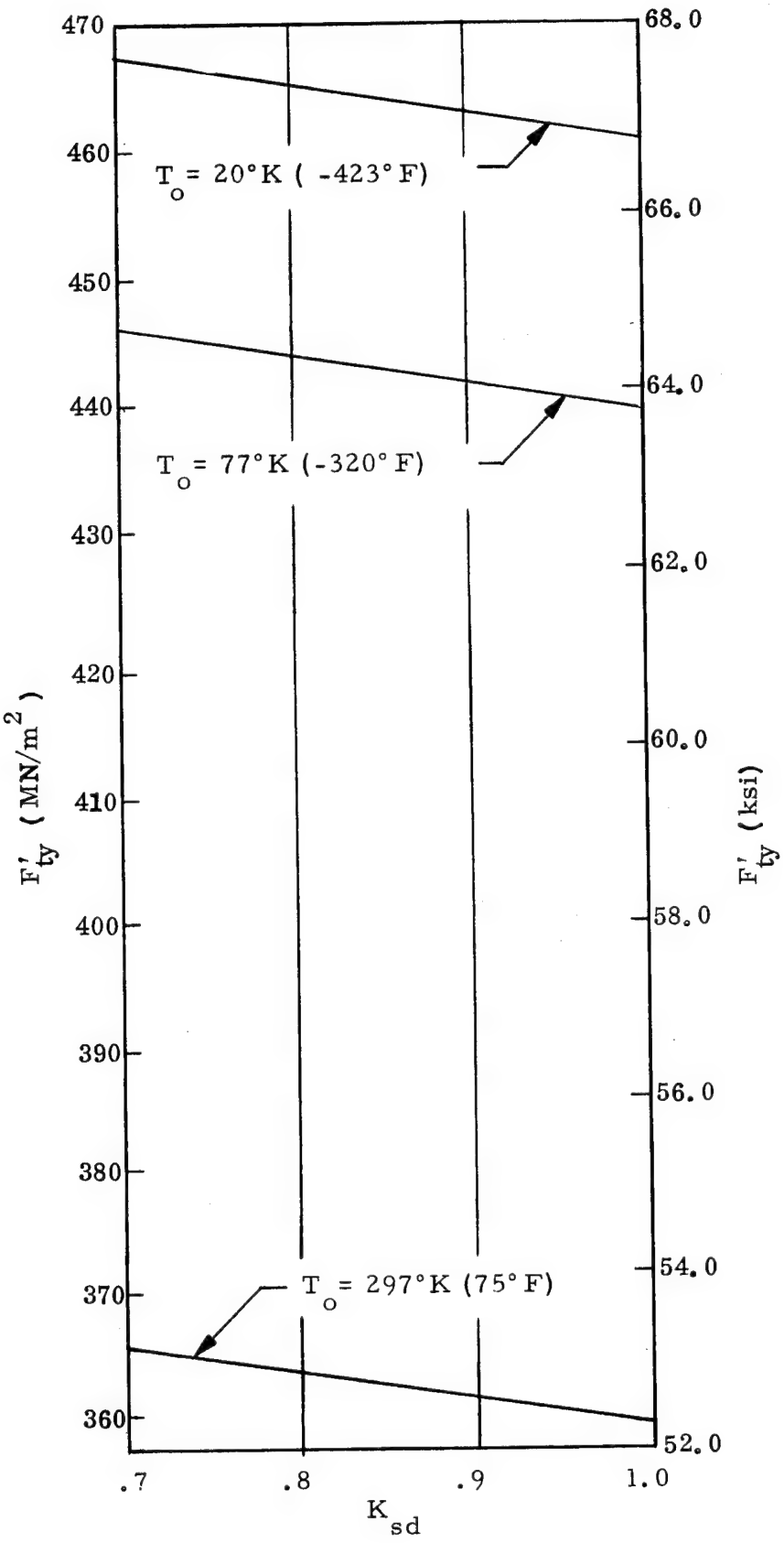

FIGURE 5: METAL SHELL OFFSET YIELD STRENGTH AT AMBIENT AND CRYOGENIC TEMPERATURE FOR SIZED GFR 2219-T62 ALUMINUM SPHERES

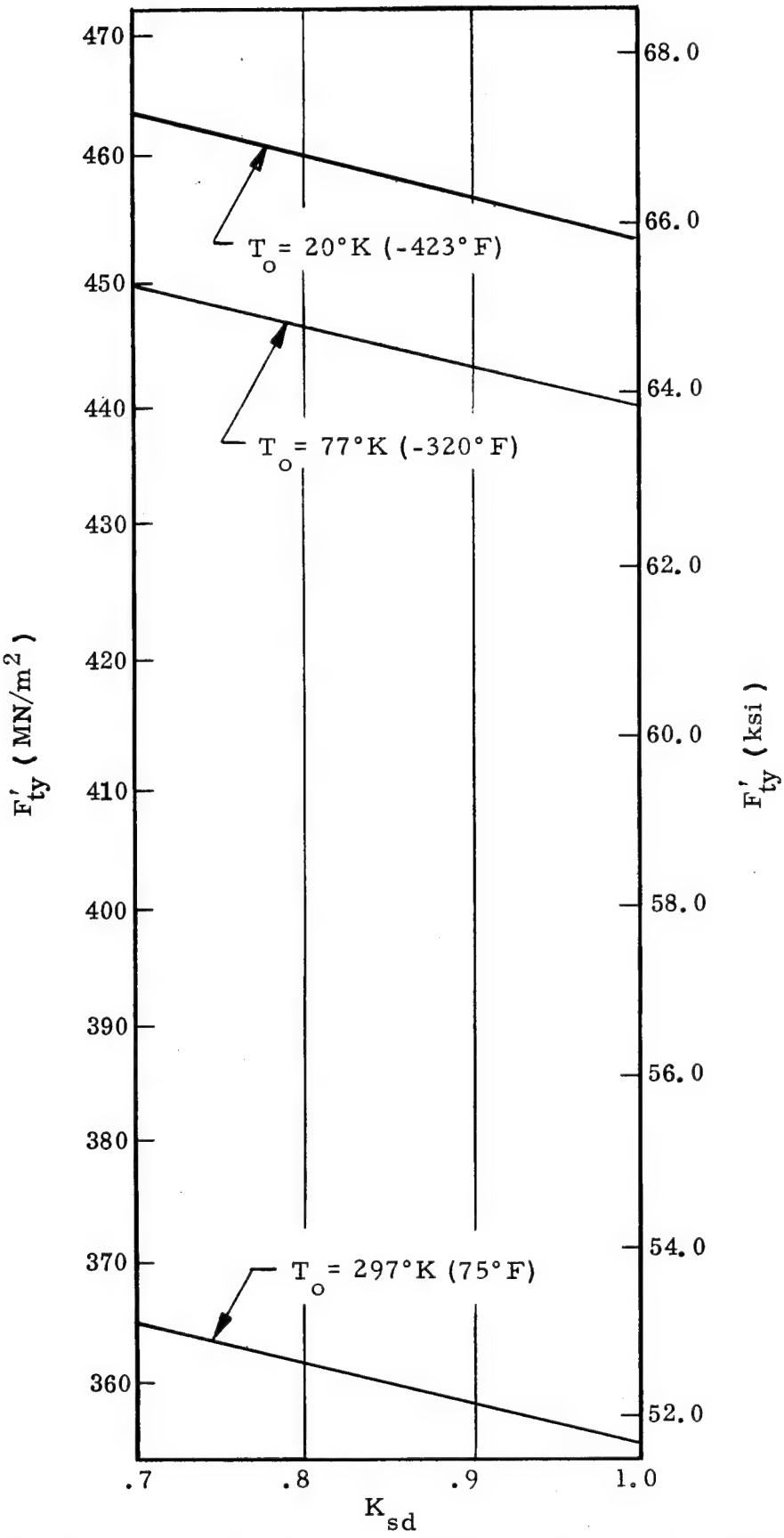

FIGURE 6: METAL SHELL OFFSET YIELD STRENGTH AT AMBIENT AND CRYOGENIC TEMPERATURE FOR SIZED COMPLETELY GFR 2219-T62 ALUMINUM OBLATE SPHEROIDS AND CYLINDRICAL VESSELS

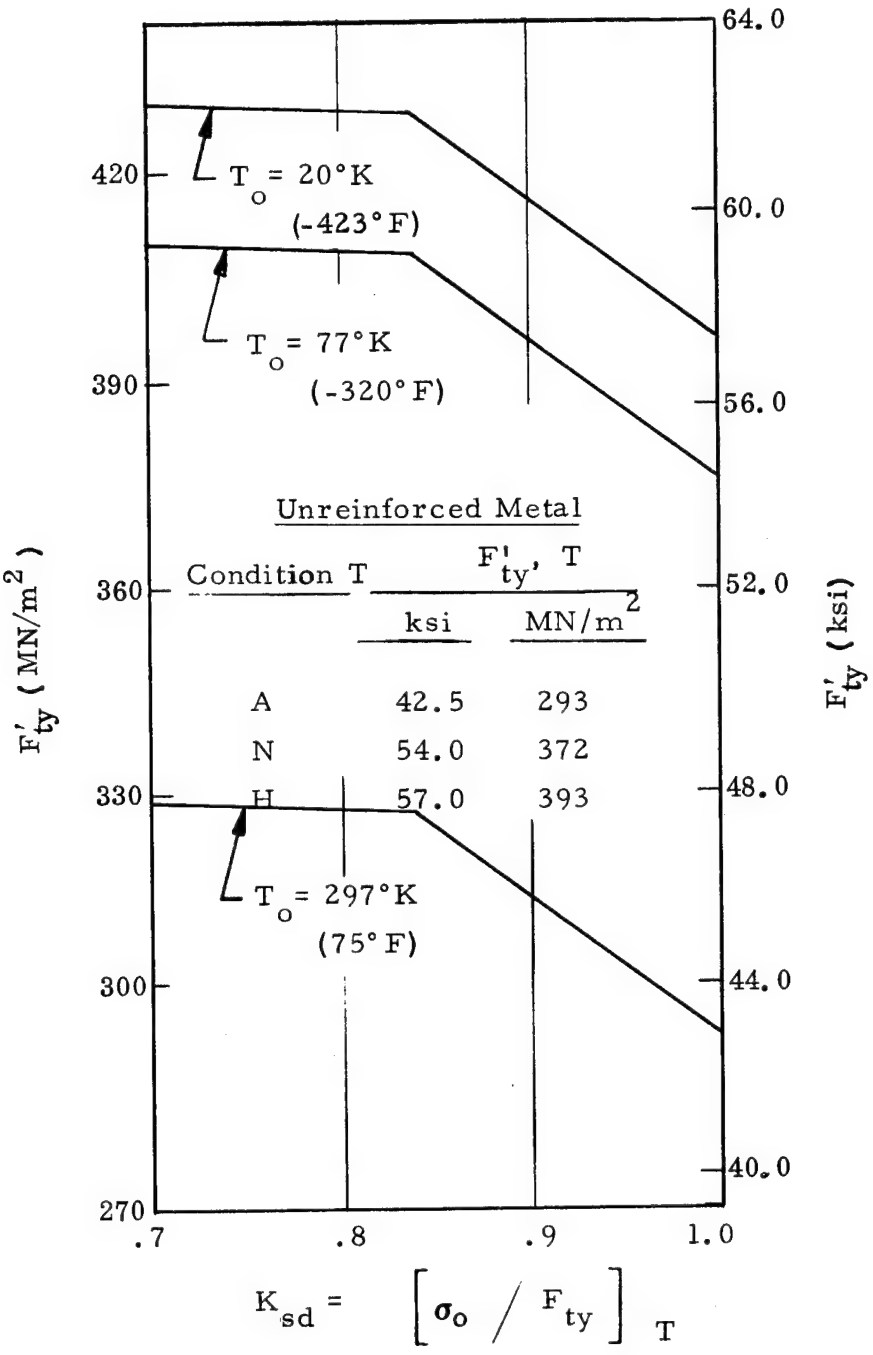

FIGURE 7: METAL SHELL OFFSET YIELD STRENGTH AT AMBIENT AND CROYGENIC TE,MPERATURE FOR SIZED HOOP GFR 2219-T62 ALUMINUM CYLINDERS

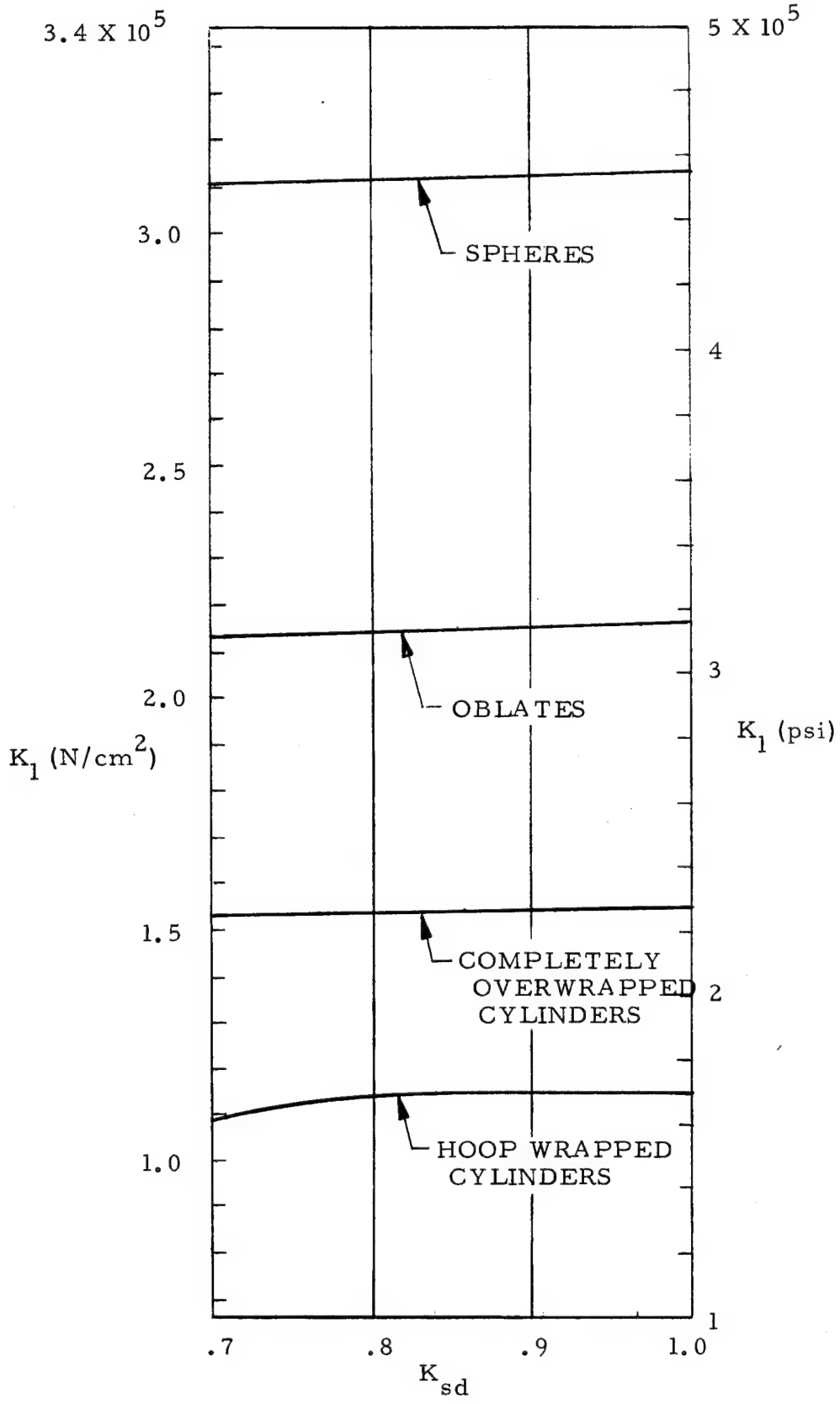

FIGURE 8: METAL SHELL THICKNESS PARAMETER FOR GFR 2219-T62 ALUMINUM PRESSURE VESSELS

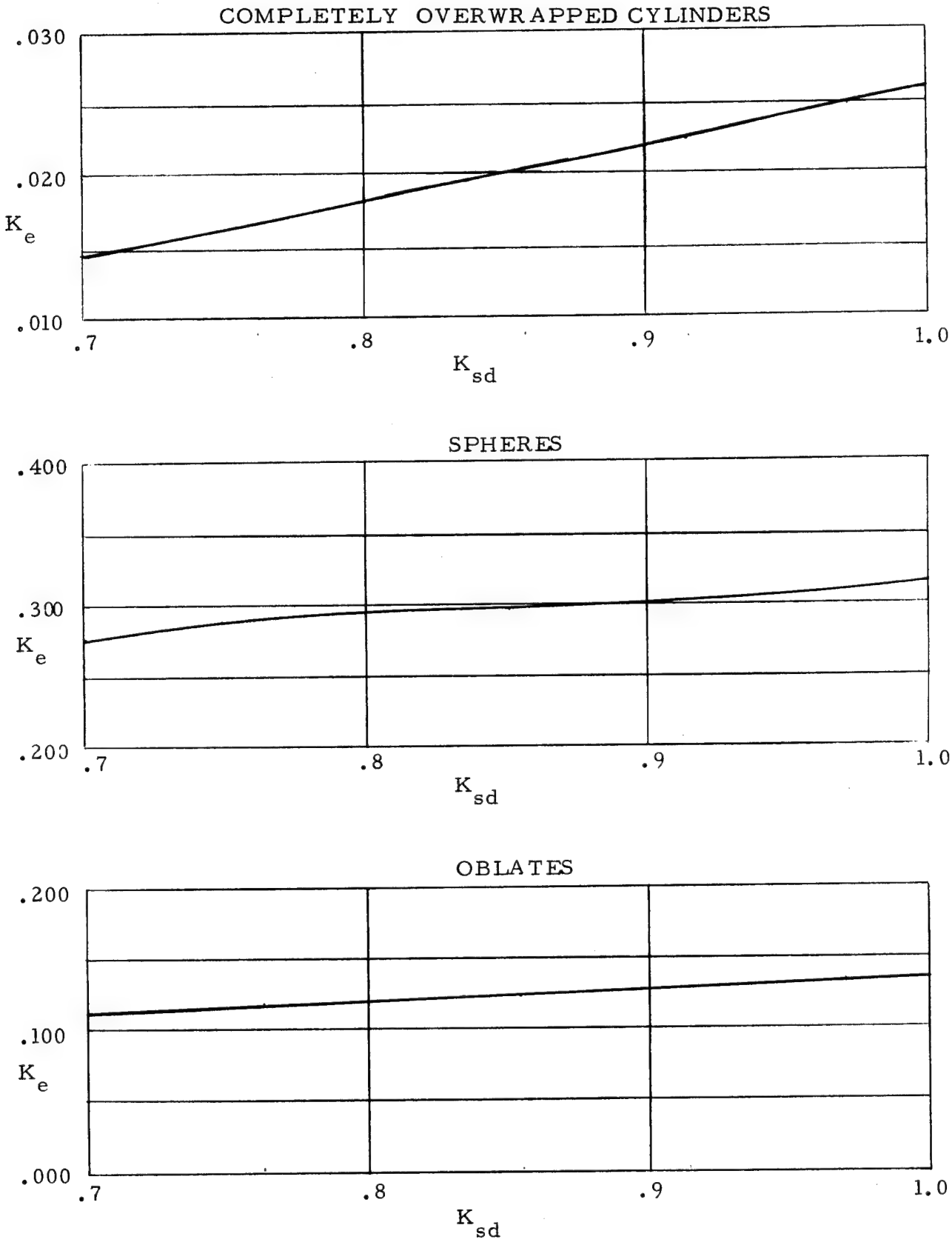

FIGURE 9: LONGITUDINAL FILAMENT THICKNESS PARAMETER FOR COMPLETELY GFR 2219-T62 ALUMINUM PRESSURE VESSELS

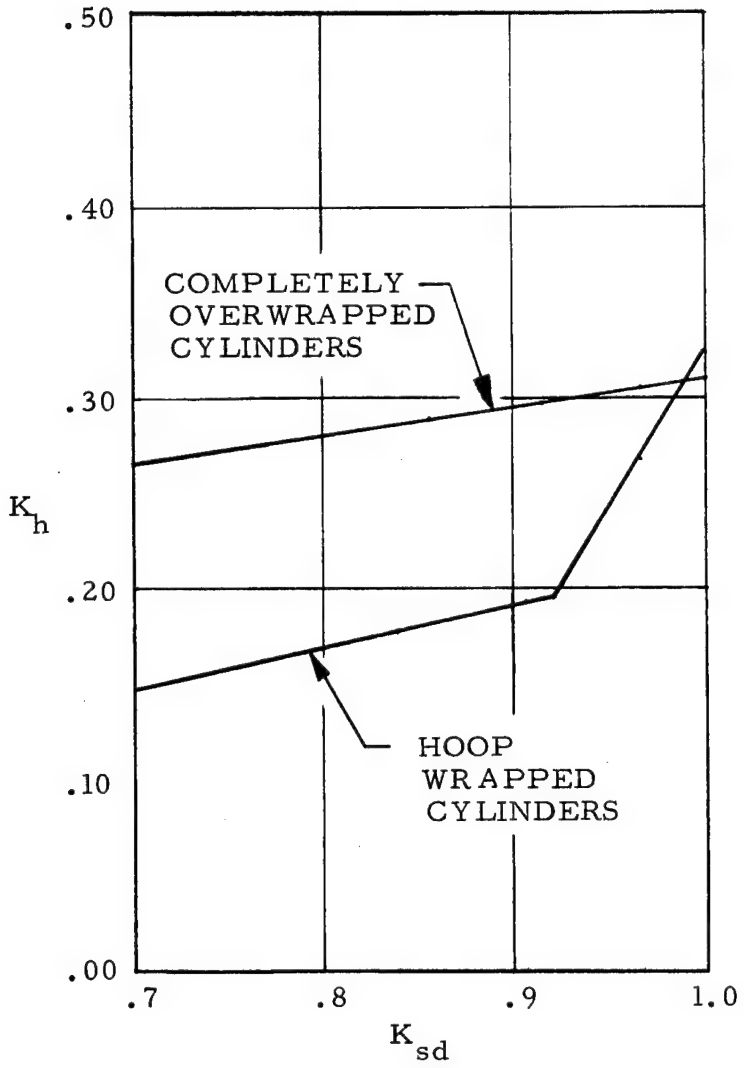

FIGURE 10: HOOP FILAMENT THICKNESS PARAMETER FOR GFR 2219-T62 ALUMINUM CYLINDRICAL VESSELS

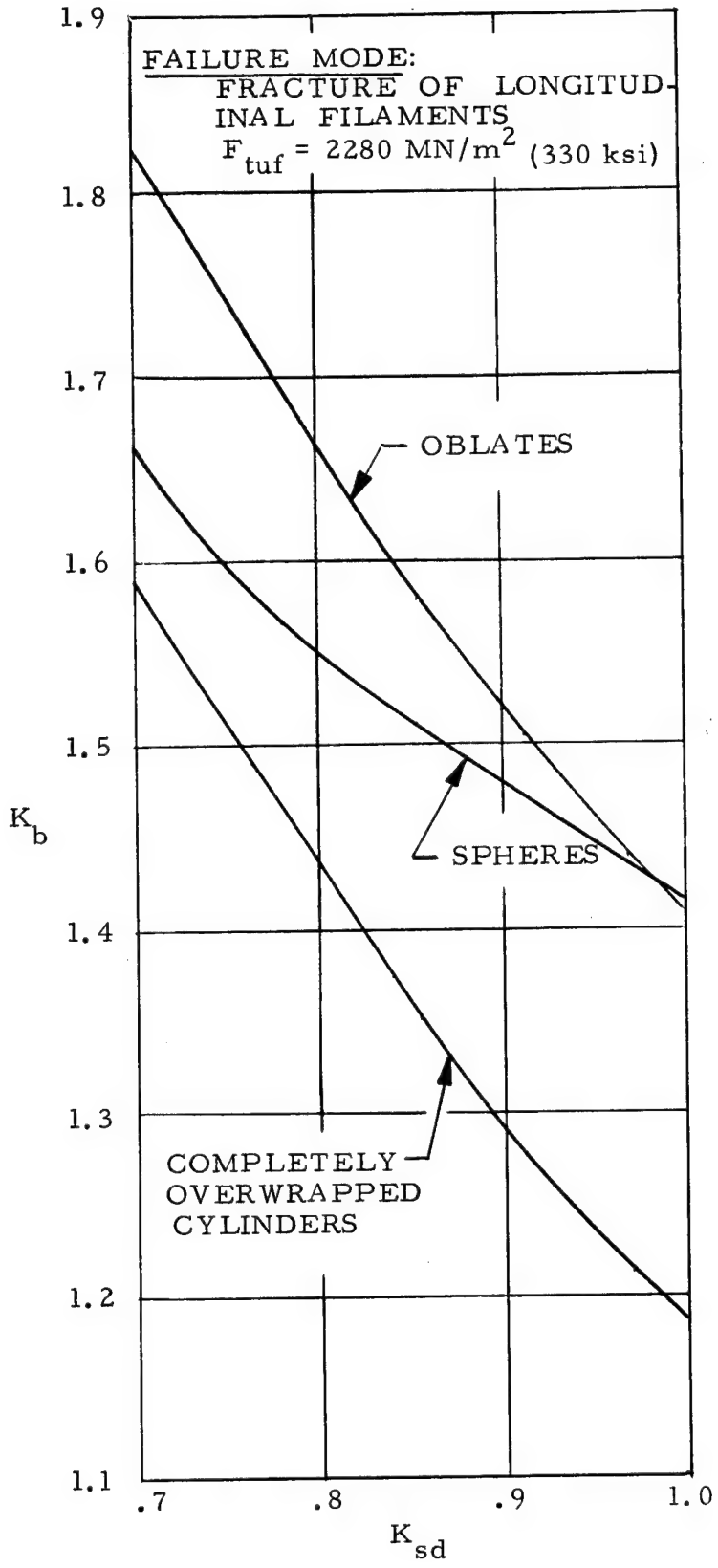

FIGURE 11: AMBIENT BURST PRESSURE FACTORS FOR COMPLETELY GFR 2219-T62 ALUMINUM PRESSURE VESSELS

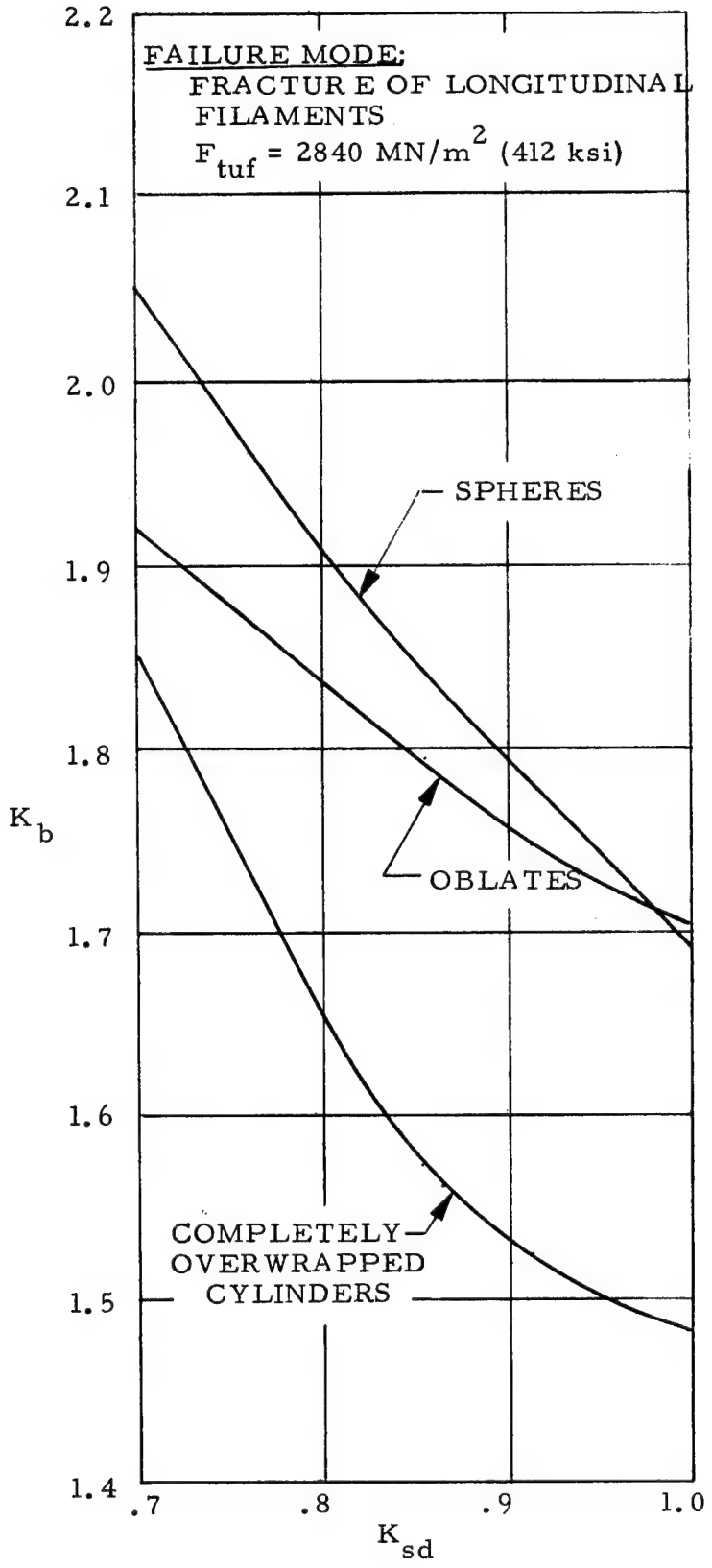

FIGURE 12: BURST PRESSURE FACTORS AT 77°K (-320°F) FOR COMPLETELY GFR 2219-T62 ALUMINUM PRESSURE VESSELS

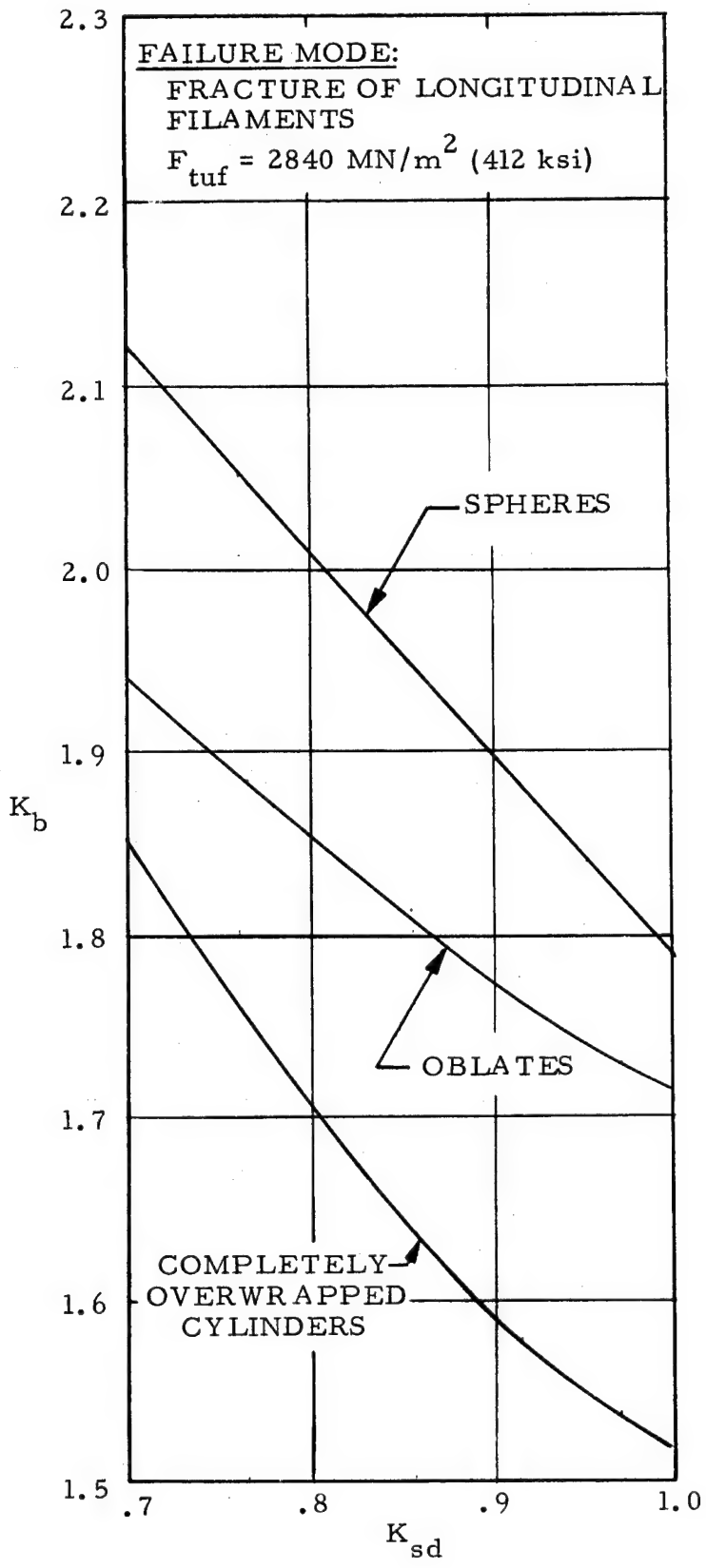

FIGURE 13: BURST PRESSURE FACTORS AT 20°K (-423°F) FOR COMPLETELY GFR 2219-T62 ALUMINUM PRESSURE VESSELS

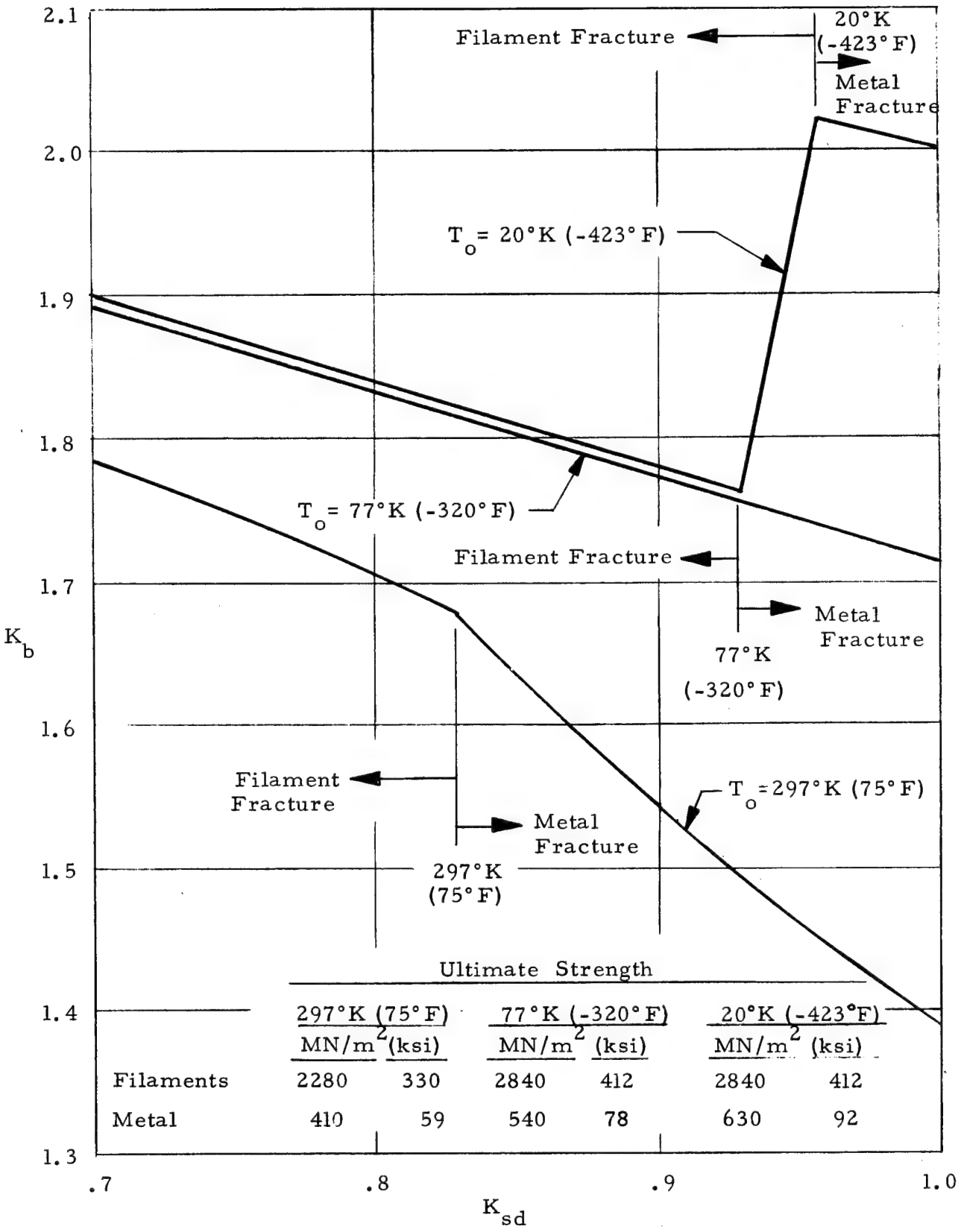

FIGURE 14: AMBIENT AND CRYOGENIC BURST PRESSURE FACTORS FOR HOOP GFR 2219-T62 ALUMINUM PRESSURE VESSELS

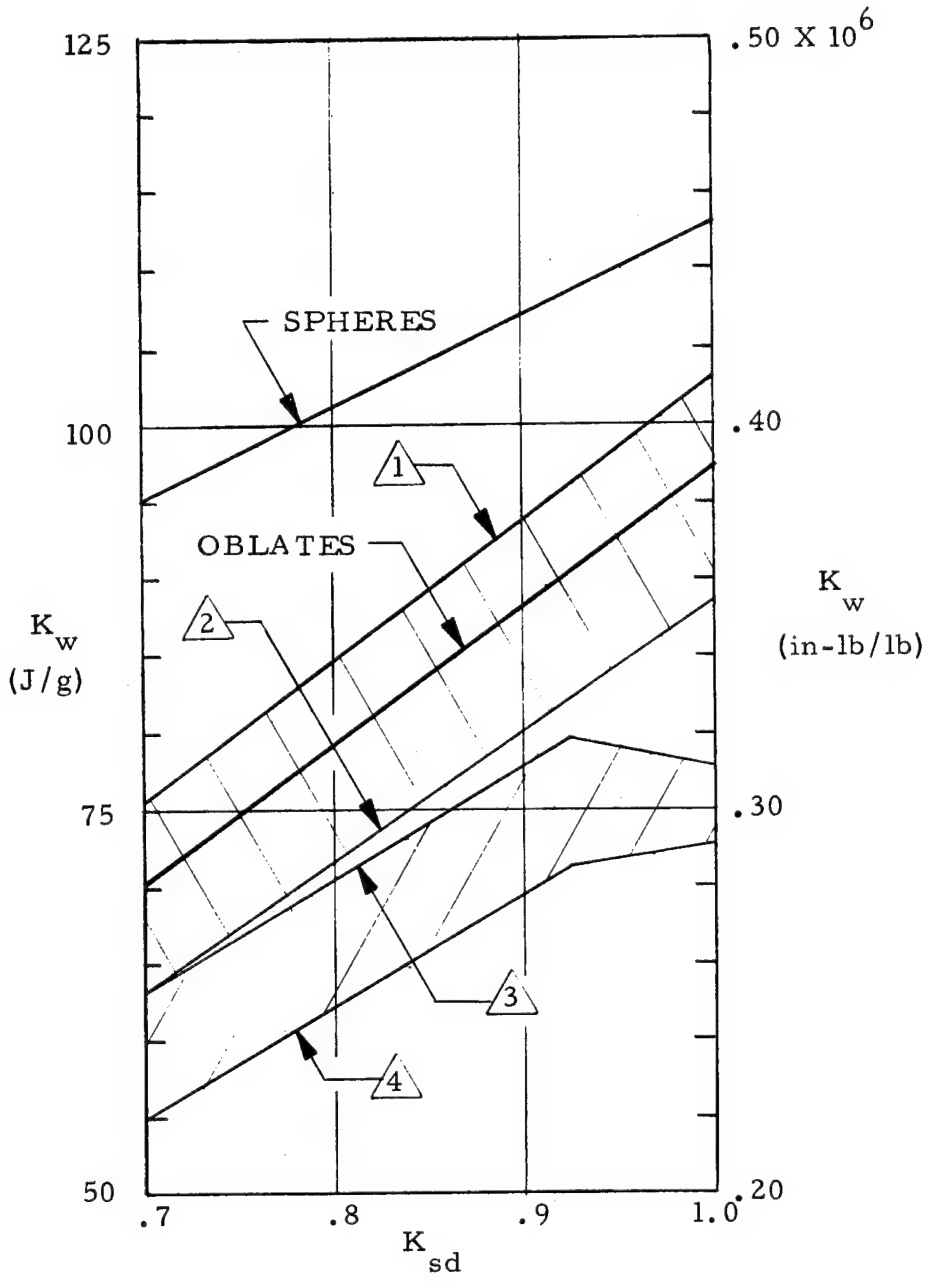

FIGURE 15: PERFORMANCE FACTOR FOR AMBIENT OPERATED GFR 2219-T62 ALUMINUM PRESSURE VESSELS

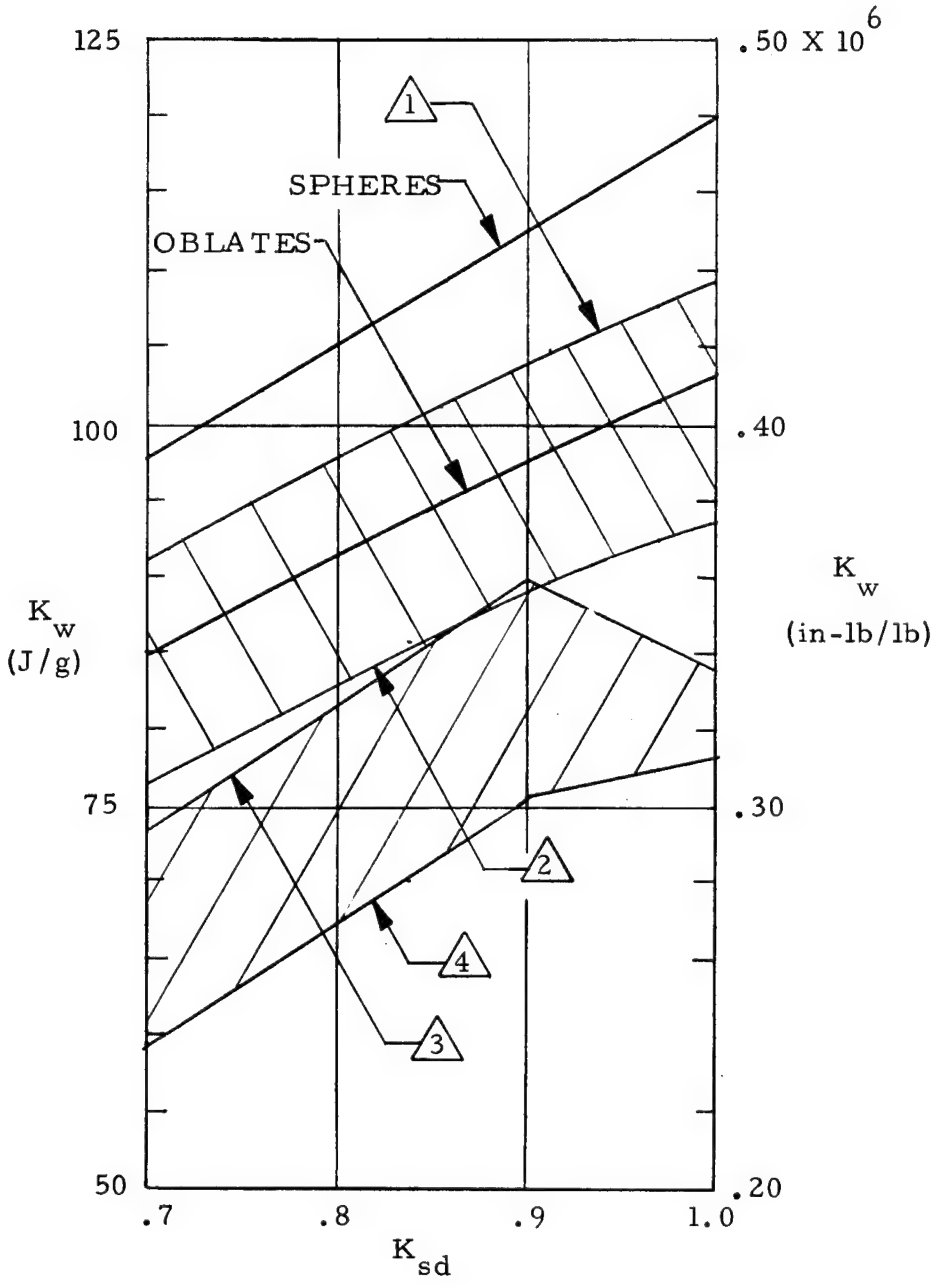

FIGURE 16: PERFORMANCE FACTORS FOR GFR 2219-T62 ALUMINUM VESSELS OPERATED AT 77°K (-320°F)

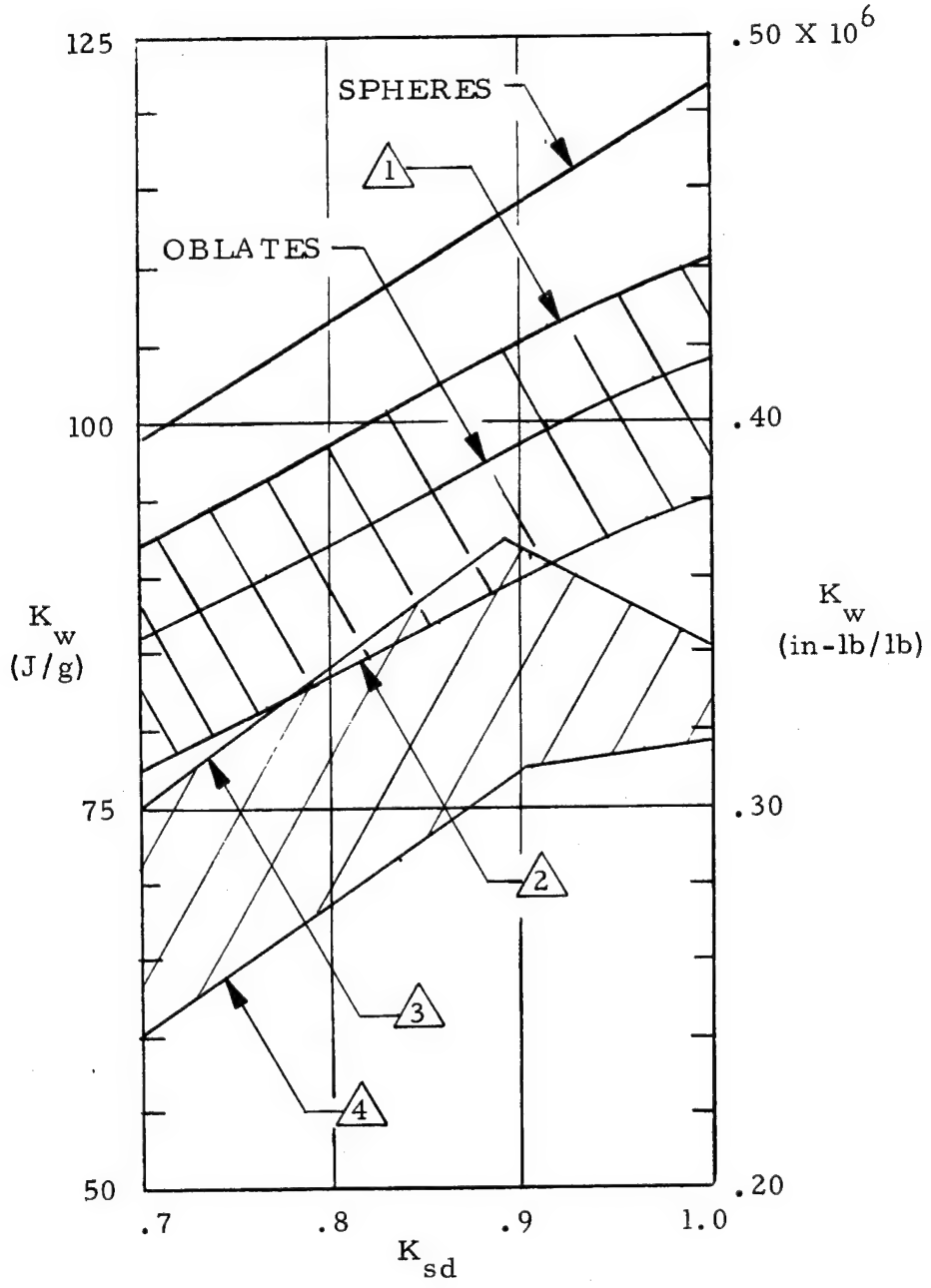

FIGURE 17: PERFORMANCE FACTORS FOR GFR 2219-T62 ALUMINUM VESSELS OPERATED AT 20°K (-423° F)

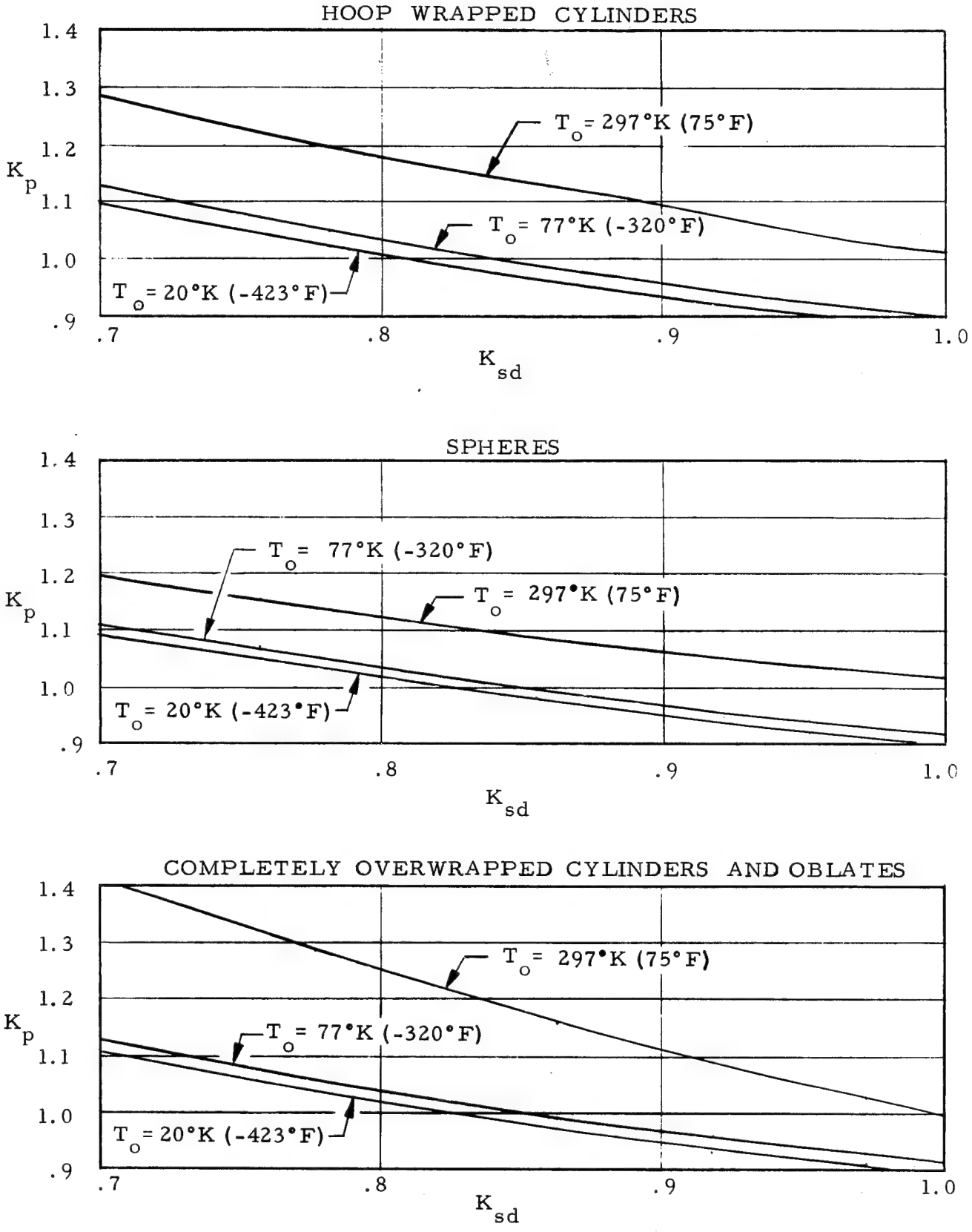

FIGURE 18: SIZING PRESSURE REQUIREMENTS FOR AMBIENT AND CRYOGENIC OPERATED GFR INCONEL X-750 PRESSURE VESSELS

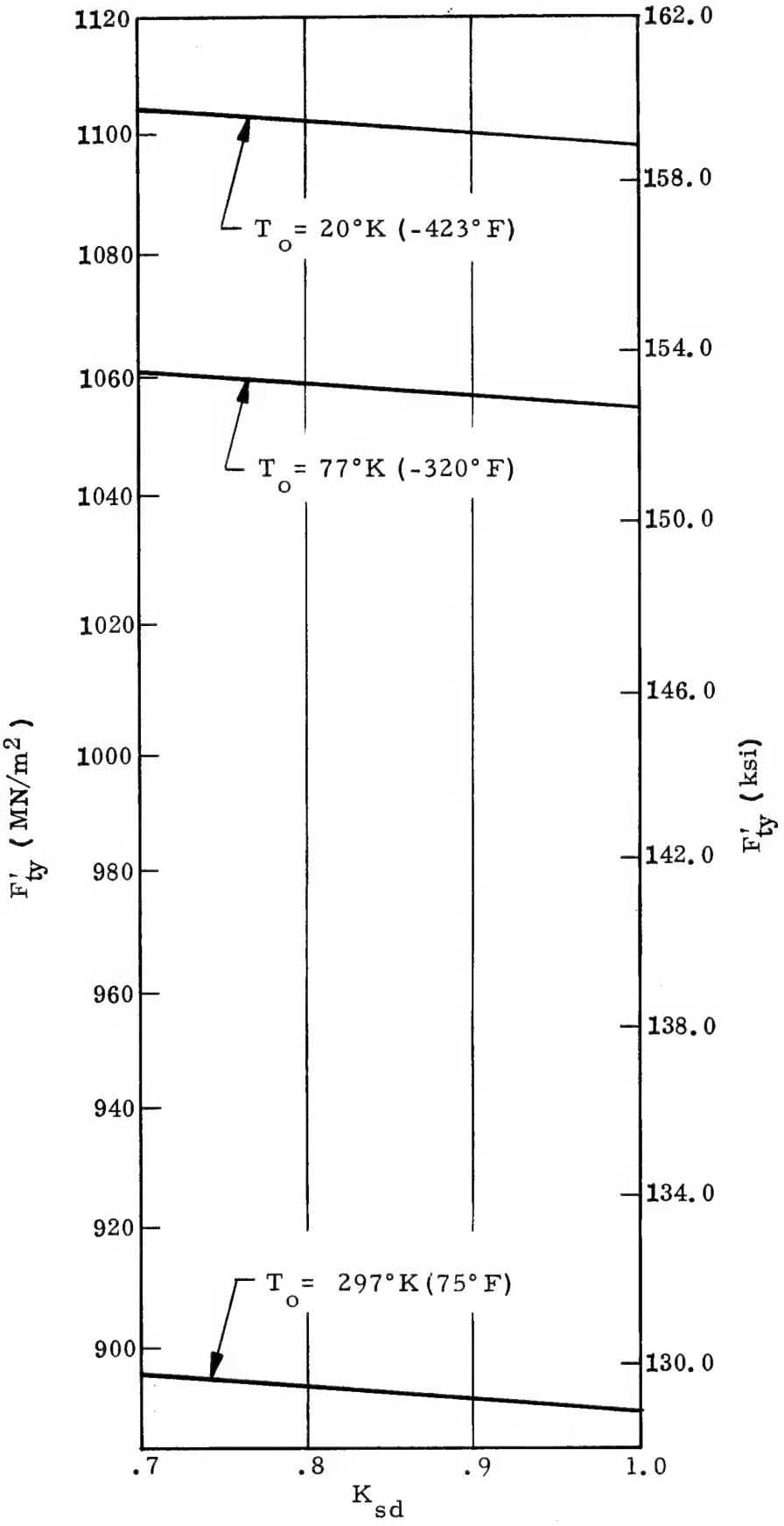

FIGURE 19: METAL SHELL OFFSET YIELD STRENGTH AT AMBIENT AND CRYOGENIC TEMPERATURE FOR SIZED GFR INCONEL X-750 SPHERES

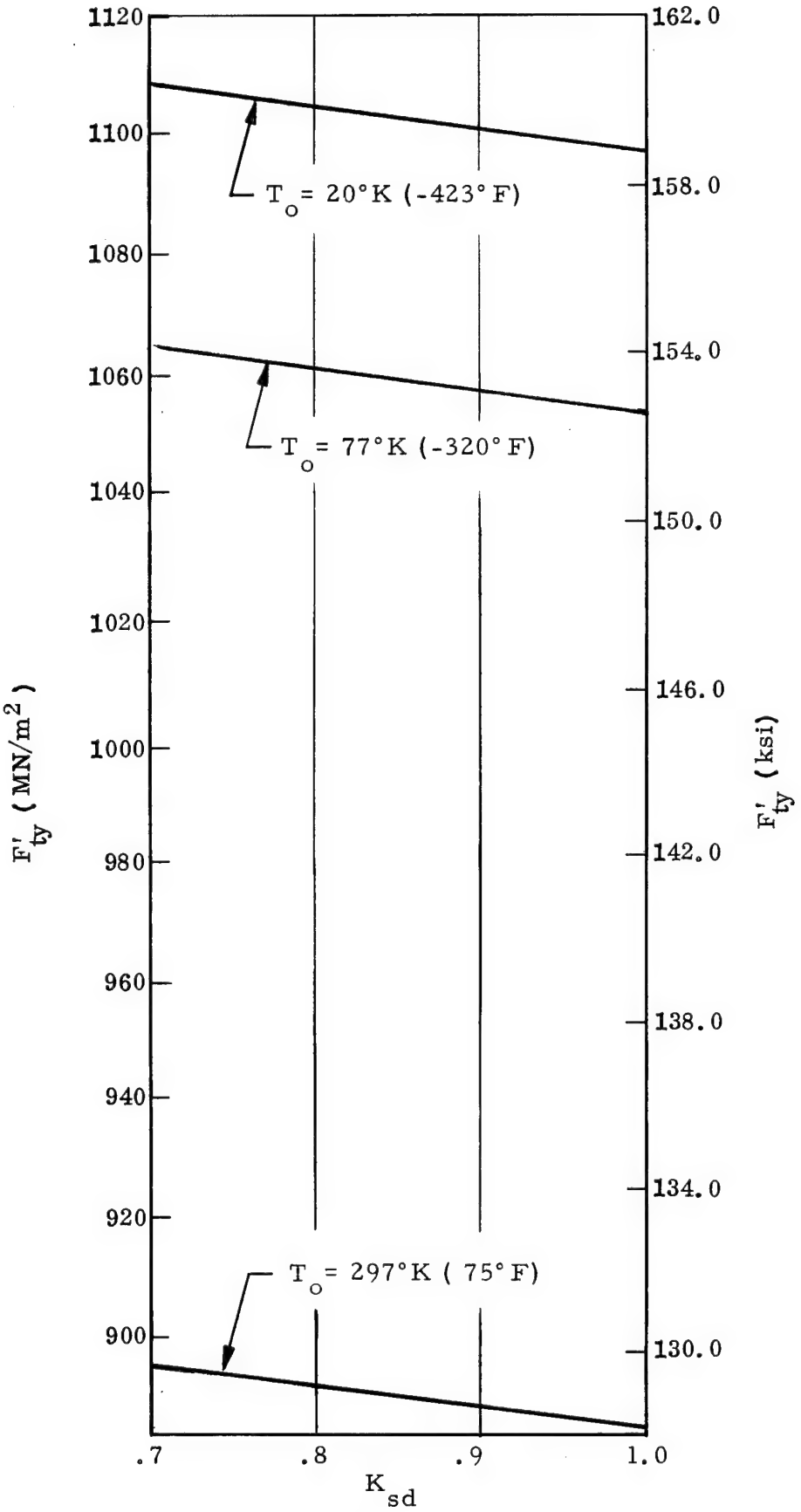

FIGURE 20: METAL SHELL OFFSET YIELD STRENGTH AT AMBIENT AND CRYOGENIC TEMPERATURE FOR SIZED COMPLETELY GFR INCONEL X-750 OBLATE SPHEROIDS AND CYLINDRICAL VESSELS

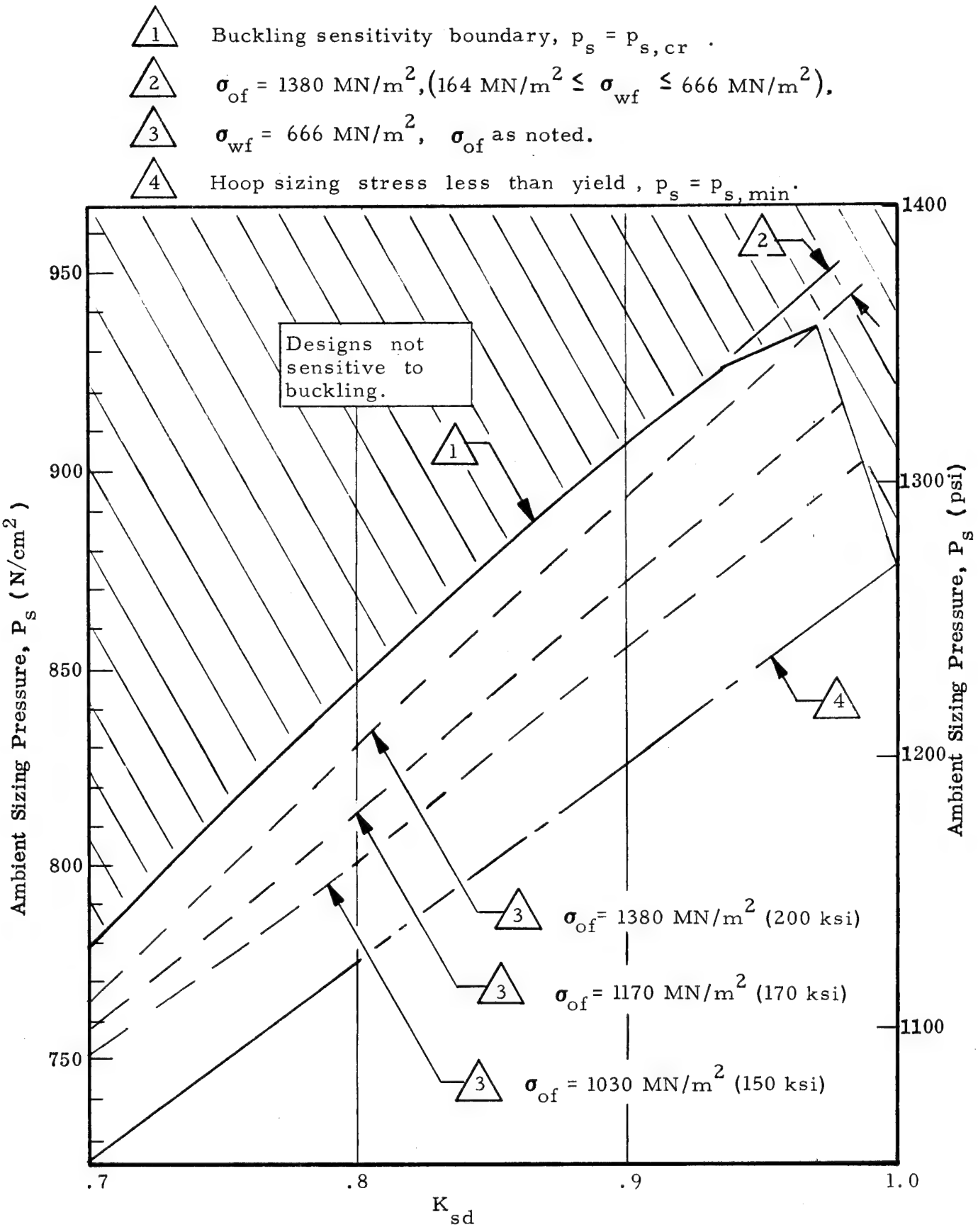

FIGURE 21: BUCKLING SENSITIVITY INDICATOR FOR HOOP GFR INCONEL X-750 PRESSURE VESSELS

UNREINFORCED METAL

F_{tyA} = 814 MN/m^2 (118 ksi)

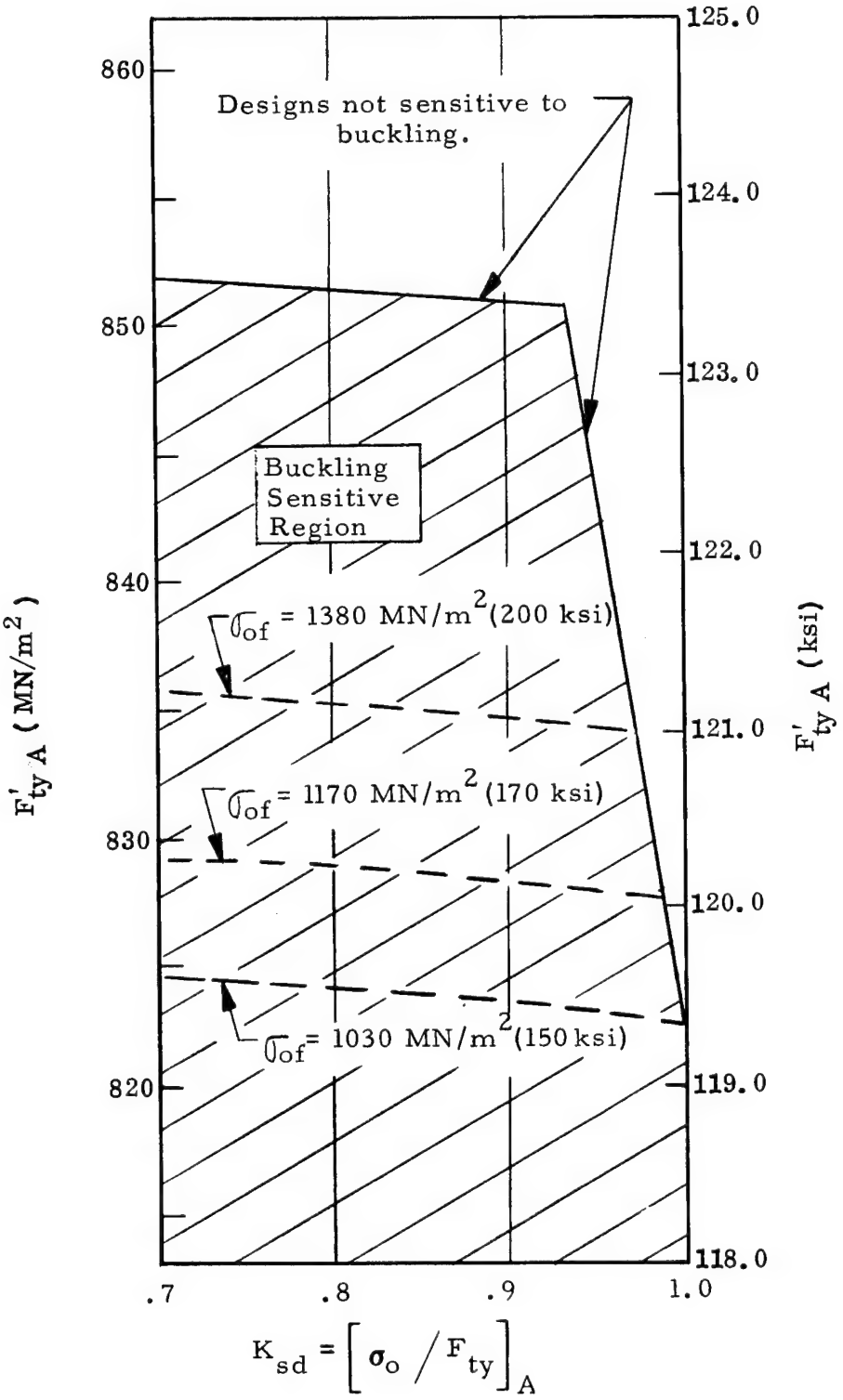

FIGURE 22A: METAL SHELL OFFSET YIELD STRENGTH AT AMBIENT TEMPERATURE FOR SIZED HOOP GFR INCONEL X-750 CYLINDERS

UNREINFORCED METAL

F_{tyN} = 977 MN/m^2 (141.7 ksi)

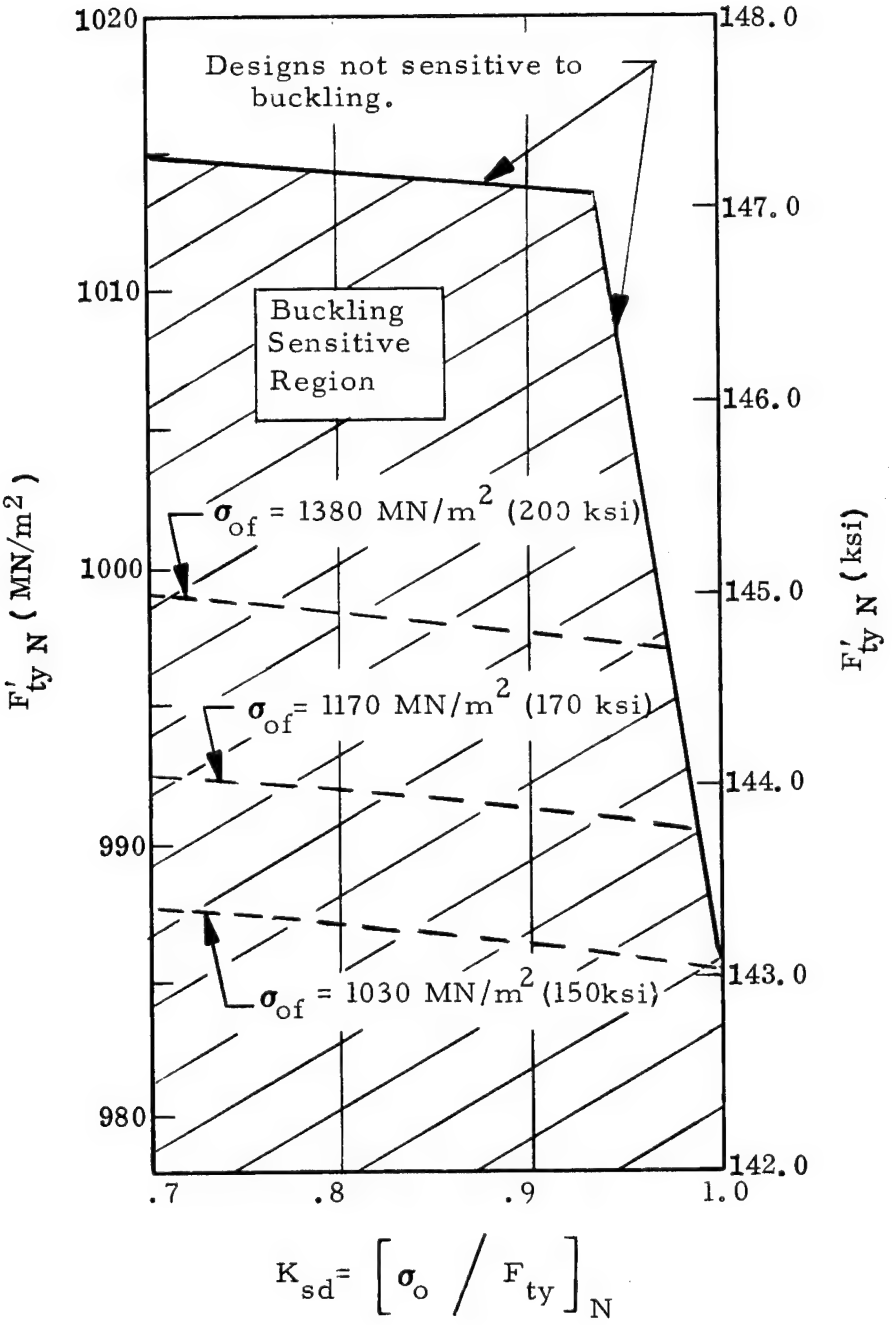

FIGURE 22B: METAL SHELL OFFSET YIELD STRENGTH AT LIQUID NITROGEN TEMPERATURE FOR SIZED HOOP GFR INCONEL X-750 CYLINDERS

UNREINFORCED METAL

F_{tyH} = 1019 MN/m^2 (147.9 ksi)

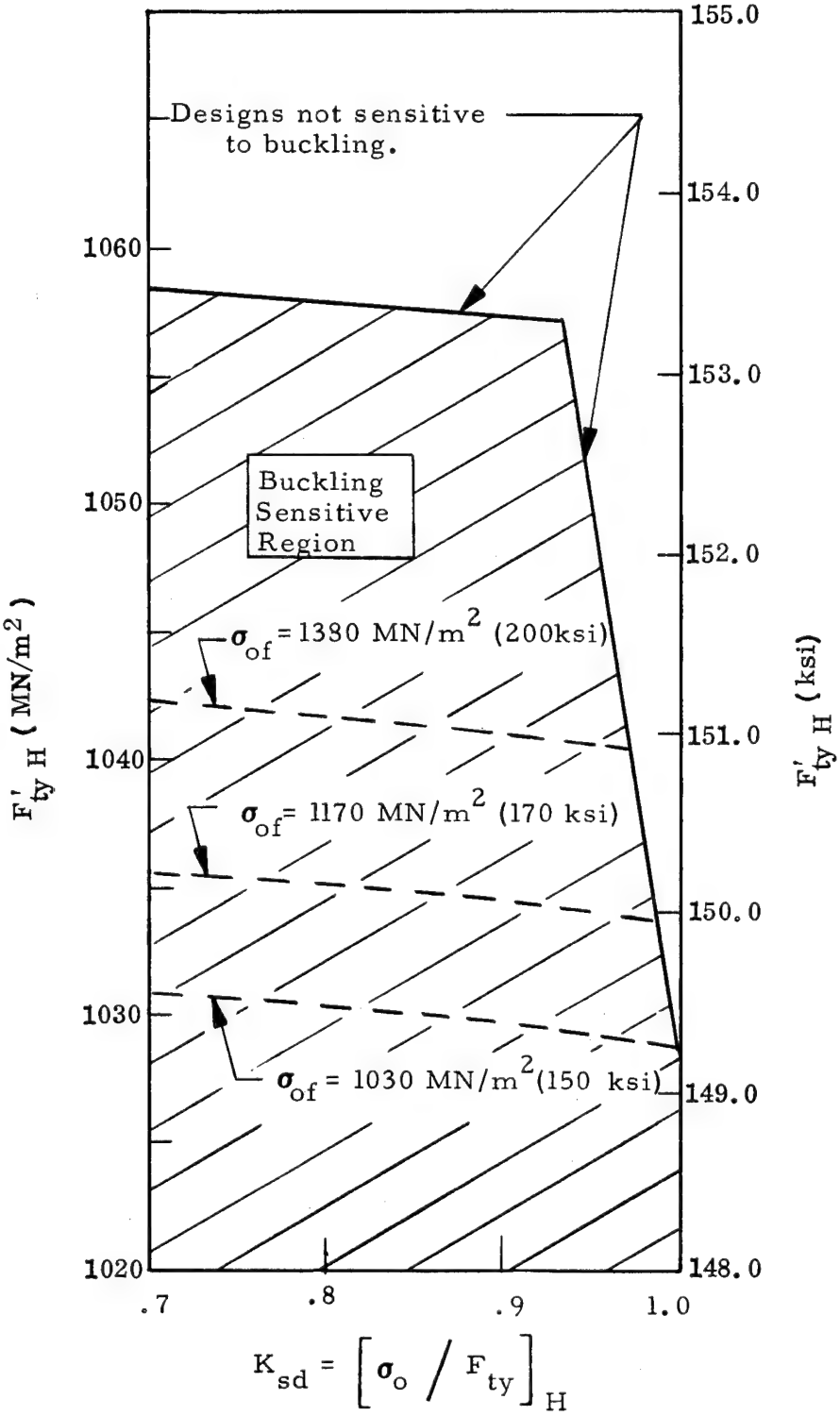

FIGURE 22C: METAL SHELL OFFSET YIELD STRENGTH AT LIQUID HYDROGEN TEMPERATURE FOR SIZED HOOP GFR INCONEL X-750 CYLINDERS

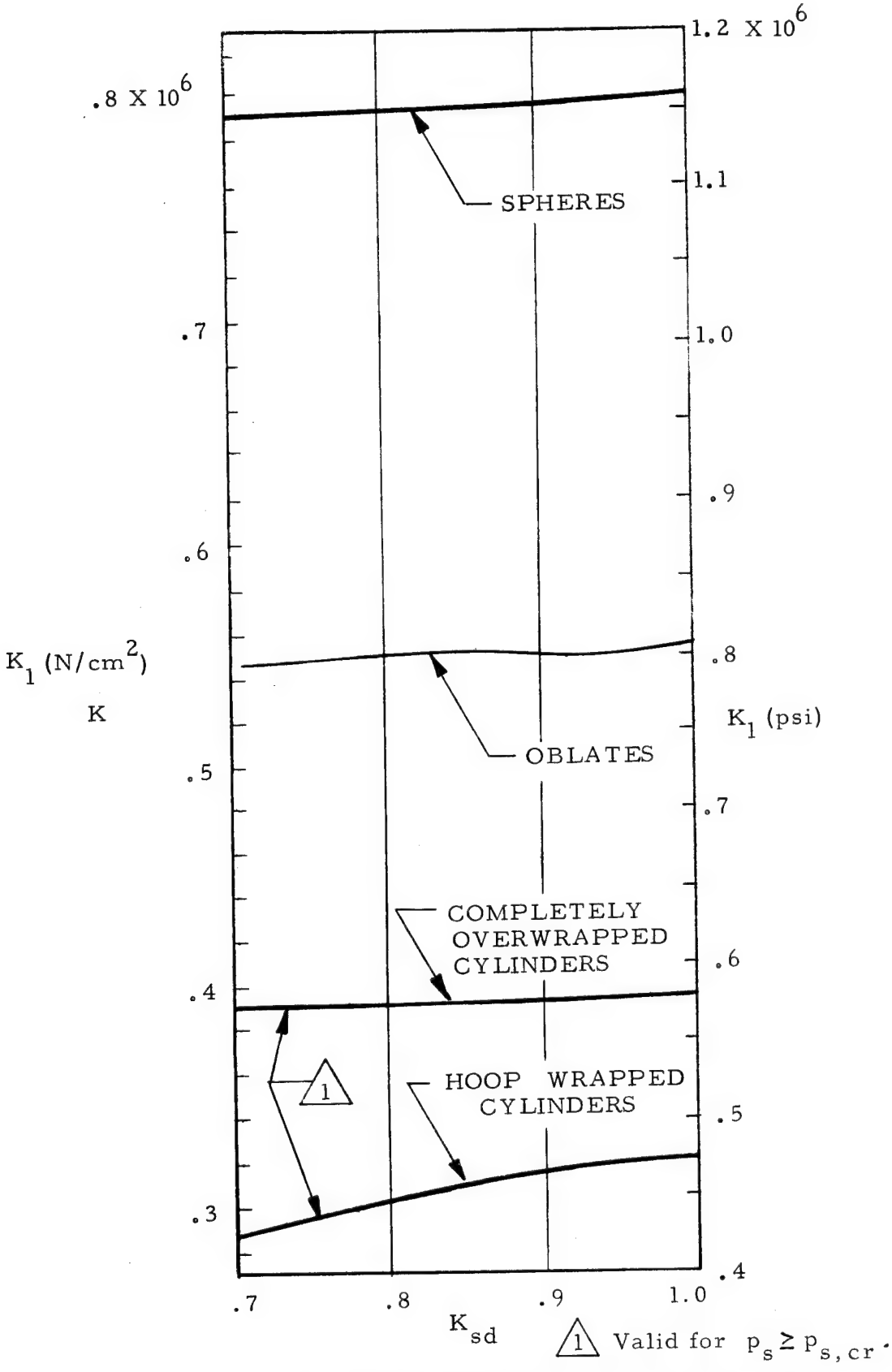

FIGURE 23: METAL SHELL THICKNESS PARAMETER FOR GFR INCONEL X-750 PRESSURE VESSELS

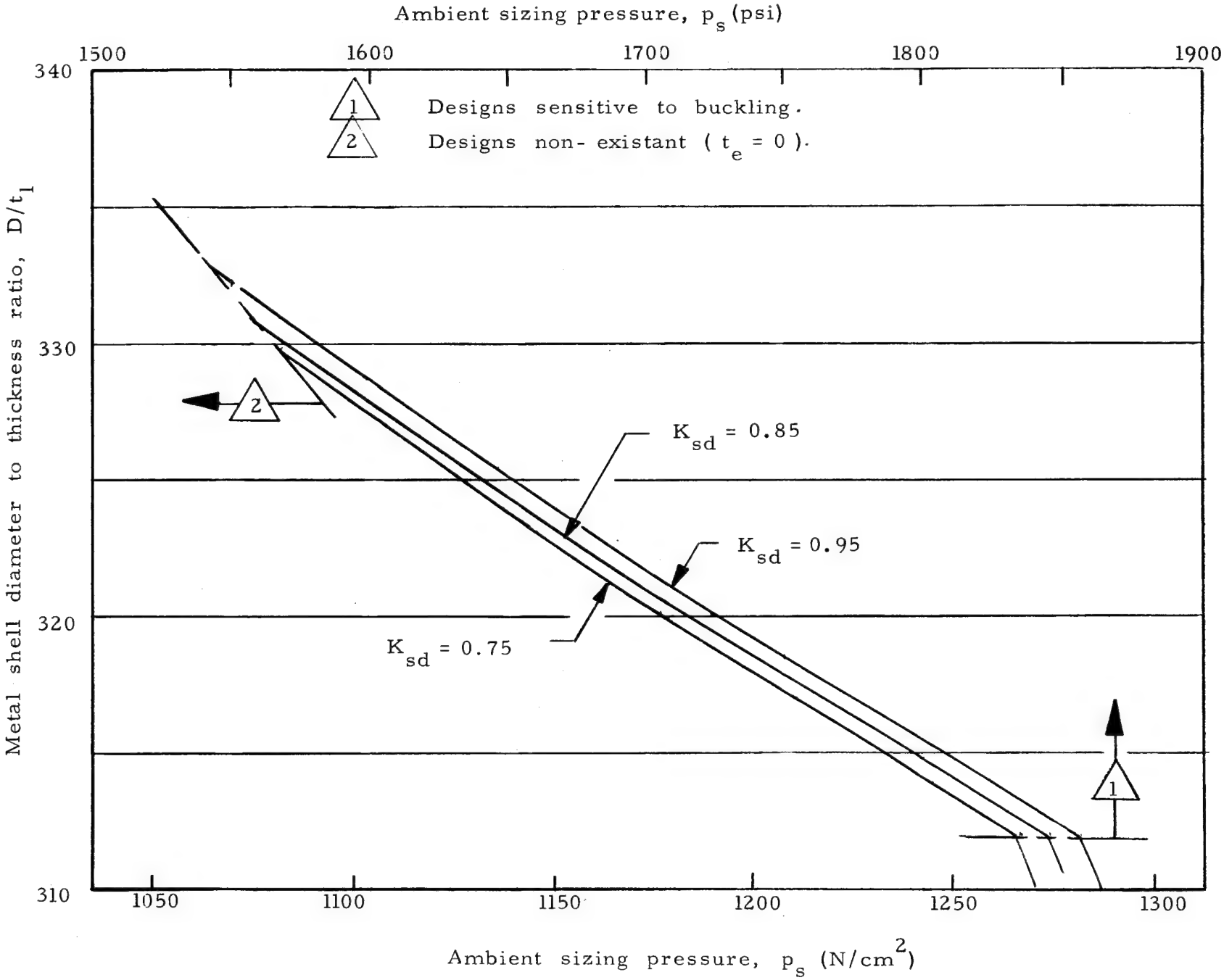

FIGURE 24: METAL SHELL DIAMETER TO THICKNESS RATIOS FOR BUCKLING SENSITIVE COMPLETELY GFR INCONEL X-750 PRESSURE VESSELS

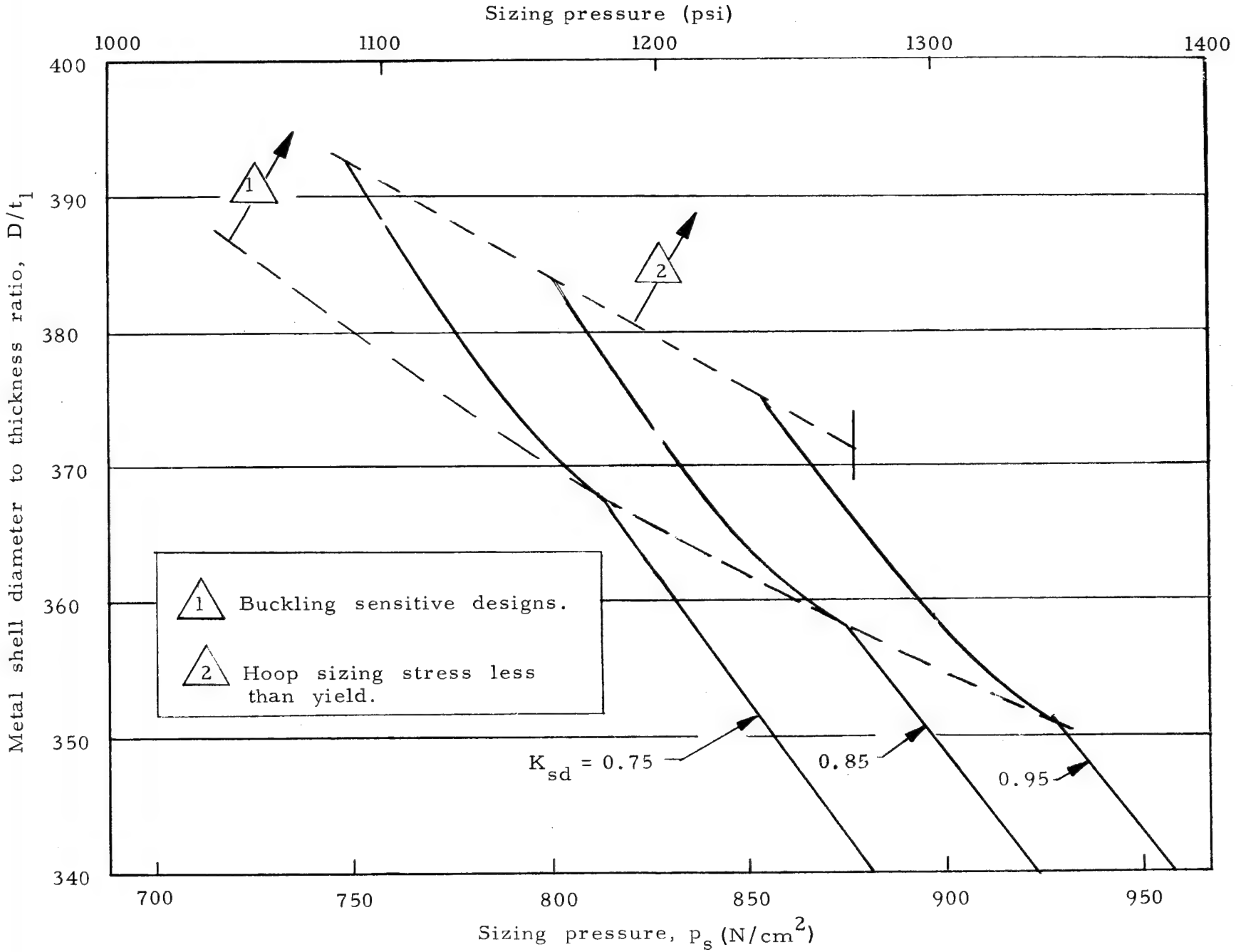

FIGURE 25: METAL SHELL DIAMETER TO THICKNESS RATIOS FOR BUCKLING SENSITIVE HOOP GFR INCONEL X-750 PRESSURE VESSELS

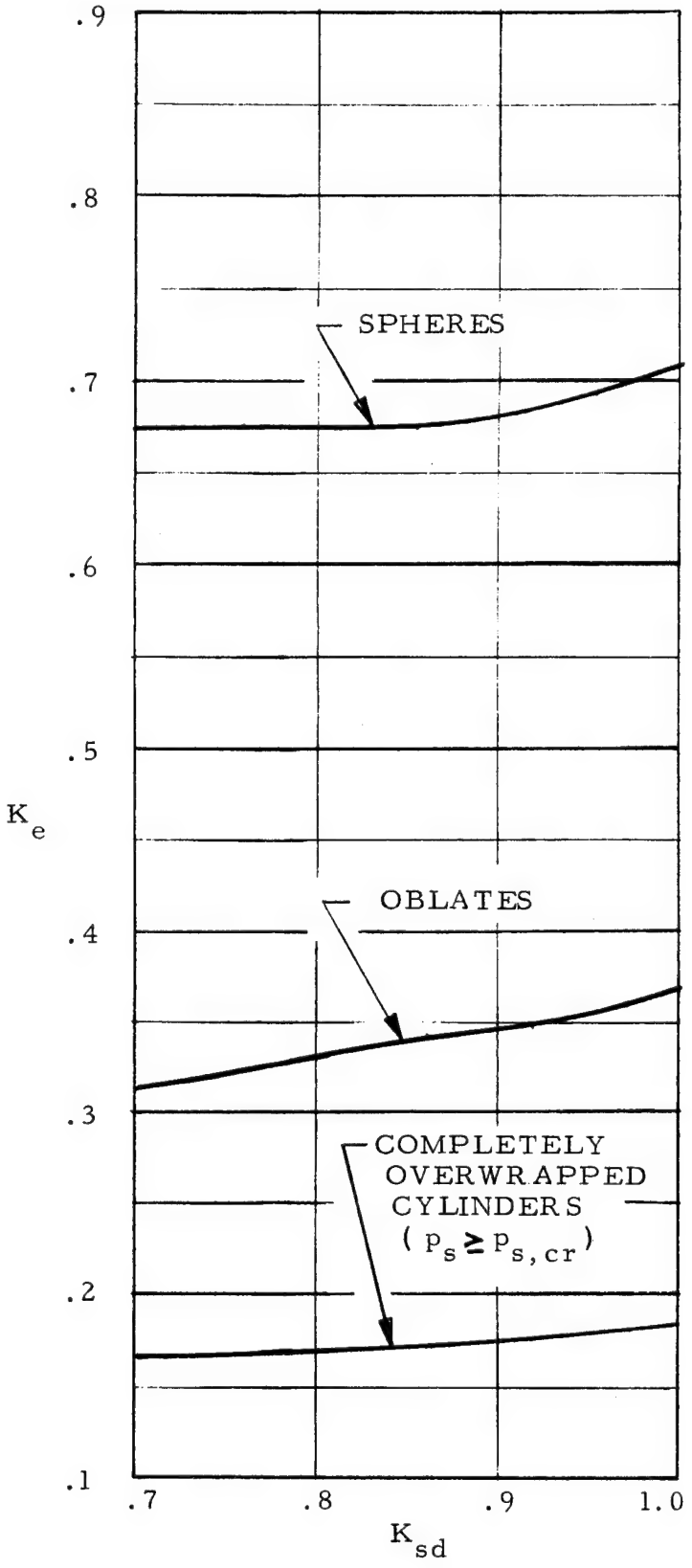

FIGURE 26: LONGITUDINAL FILAMENT THICKNESS PARAMETER FOR COMPLETELY GFR INCONEL X-750 PRESSURE VESSELS

Notes:

1. Curves valid for all $p_s \geq p_{s,cr}$.

2. Completely overwrapped cylindrical vessels.

3. Hoop wrapped cylinders.

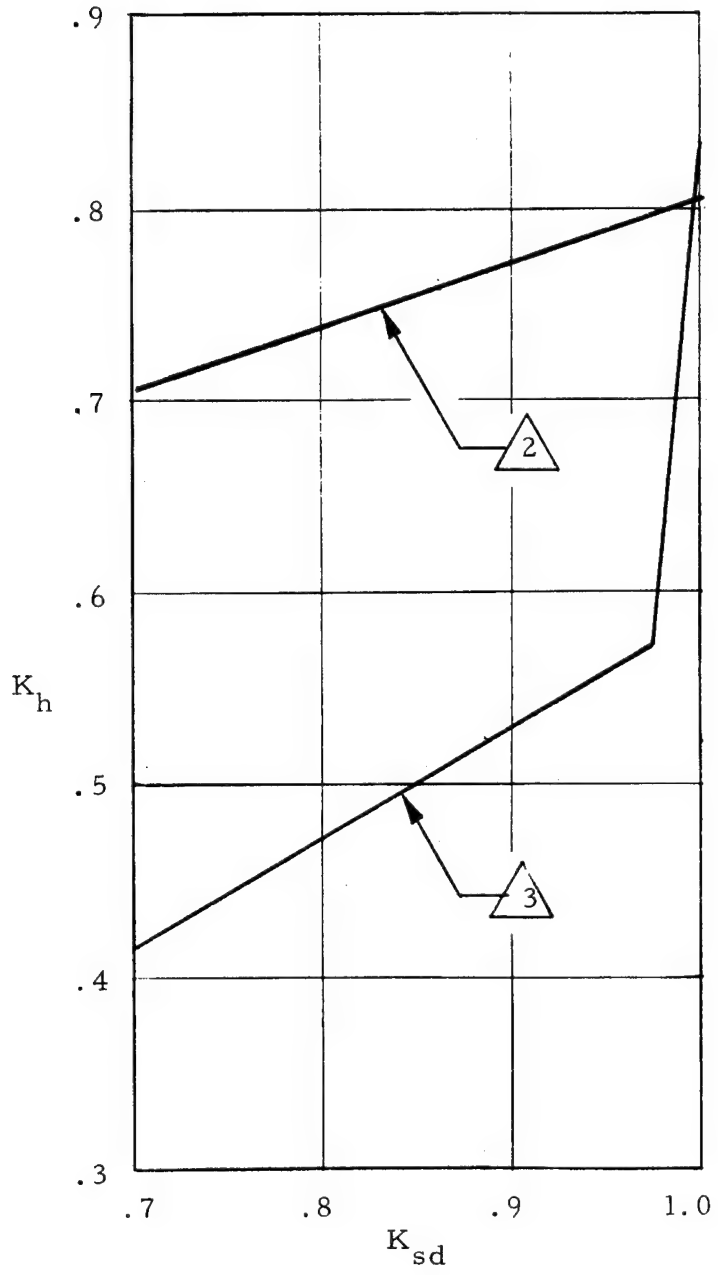

FIGURE 27: HOOP FILAMENT THICKNESS PARAMETER FOR GFR INCONEL X-750 CYLINDRICAL VESSELS

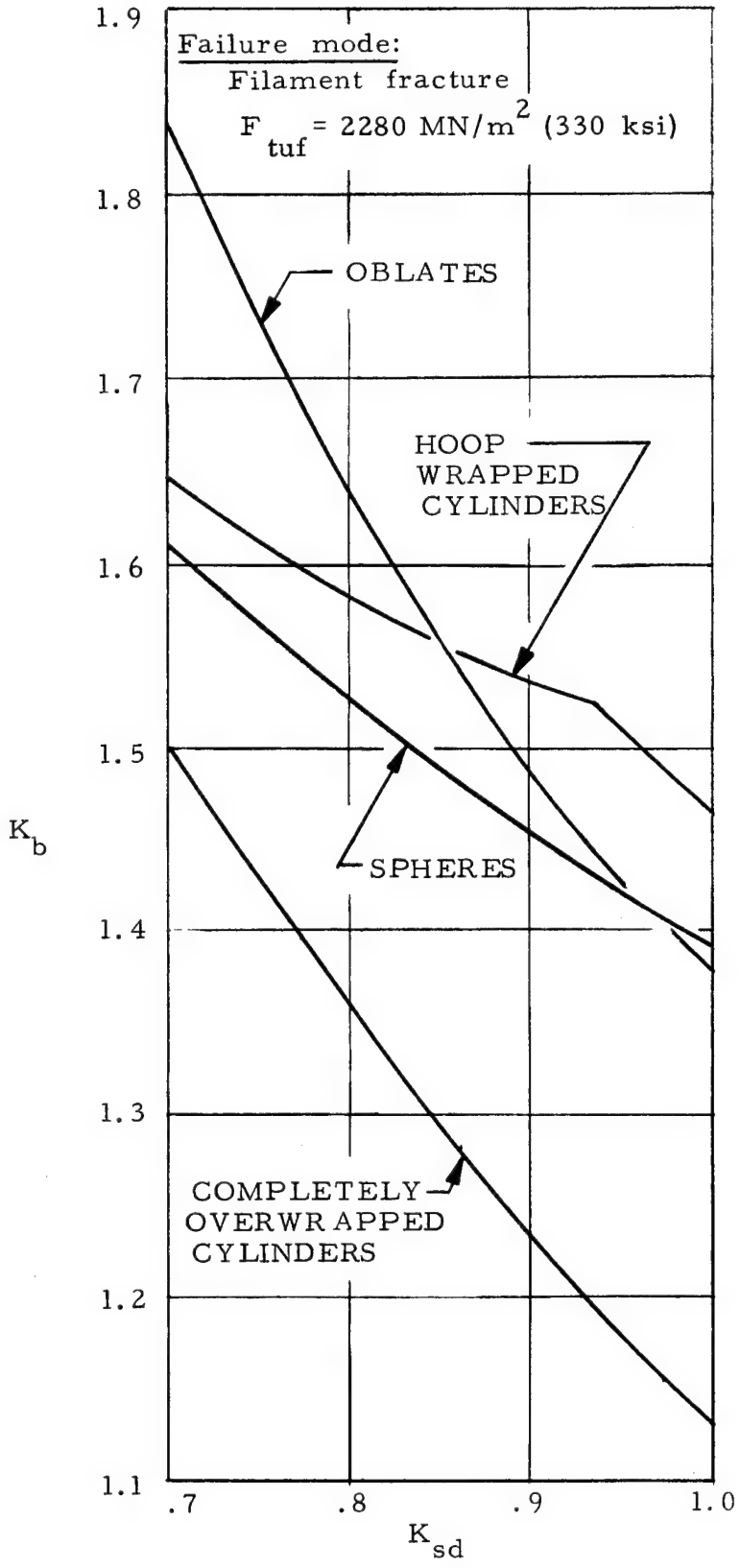

FIGURE 28: AMBIENT BURST PRESSURE FACTORS FOR COMPLETELY GFR INCONEL X-750 PRESSURE VESSELS

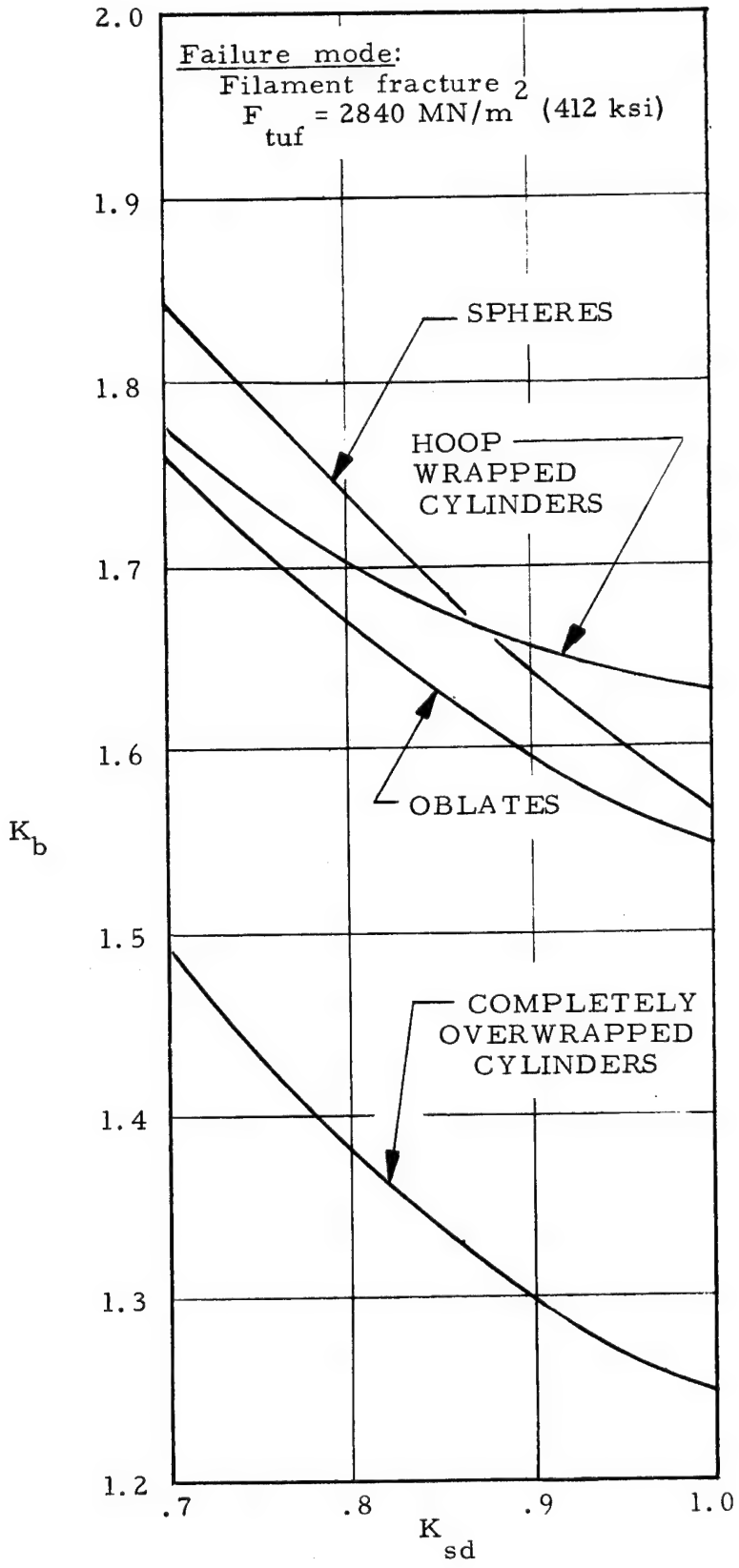

FIGURE 29: BURST PRESSURE FACTORS AT 77°K (-320°F) FOR GFR INCONEL X-750 PRESSURE VESSELS

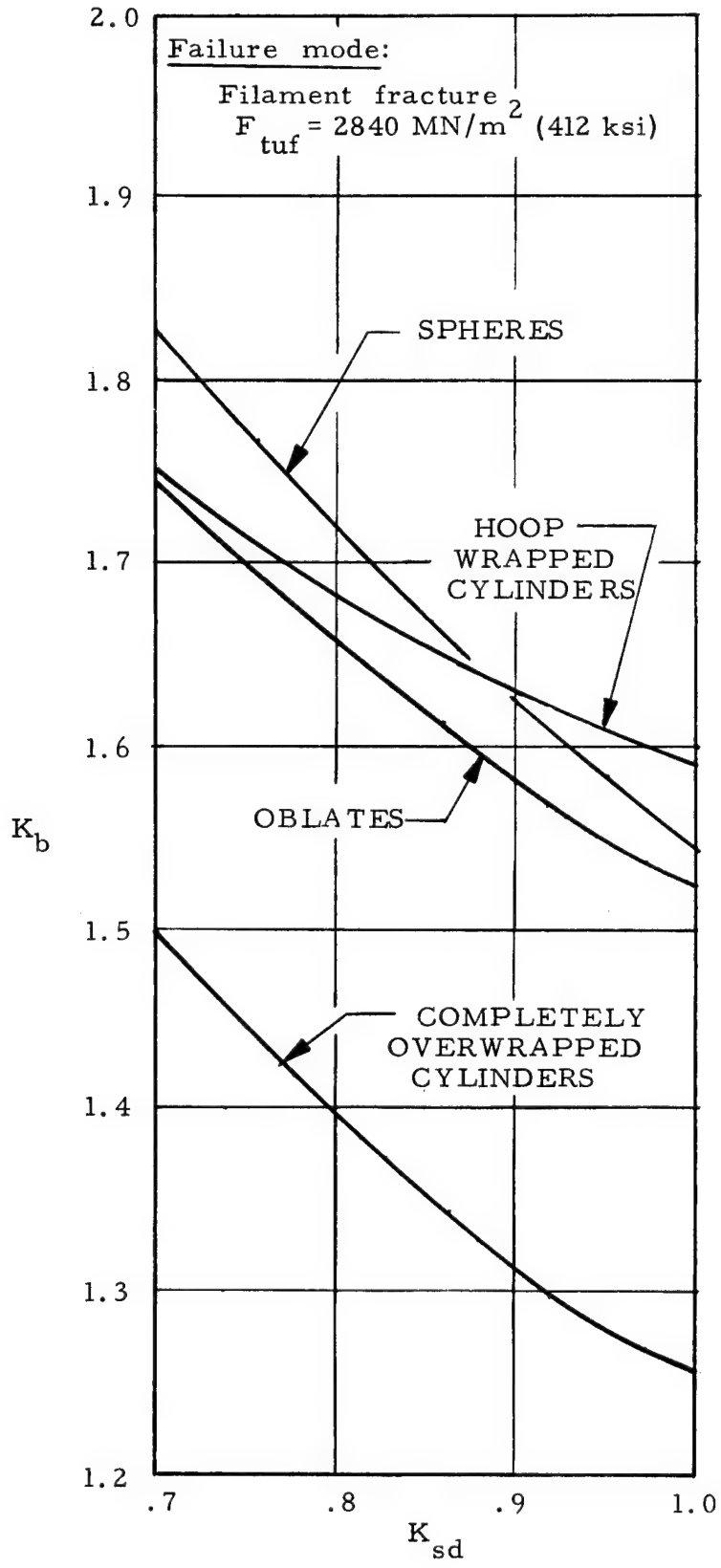

FIGURE 30: BURST PRESSURE FACTORS AT 20°K (-423°F) FOR GFR INCONEL X-750 PRESSURE VESSELS

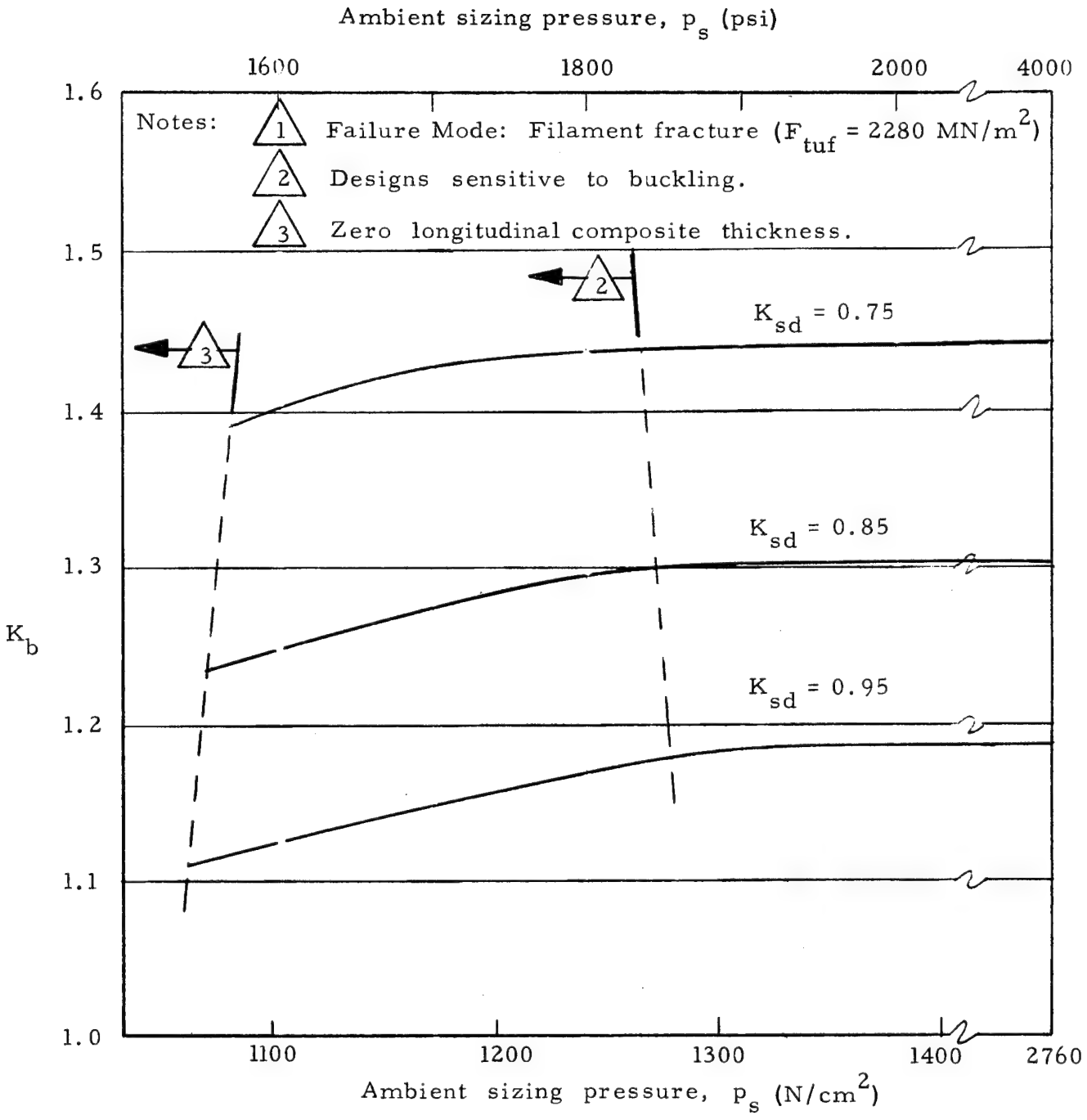

FIGURE 31: BURST PRESSURE FACTOR VARIATION FOR BUCKLING SENSITIVE COMPLETELY GFR INCONEL X-750 CYLINDRICAL PRESSURE VESSELS

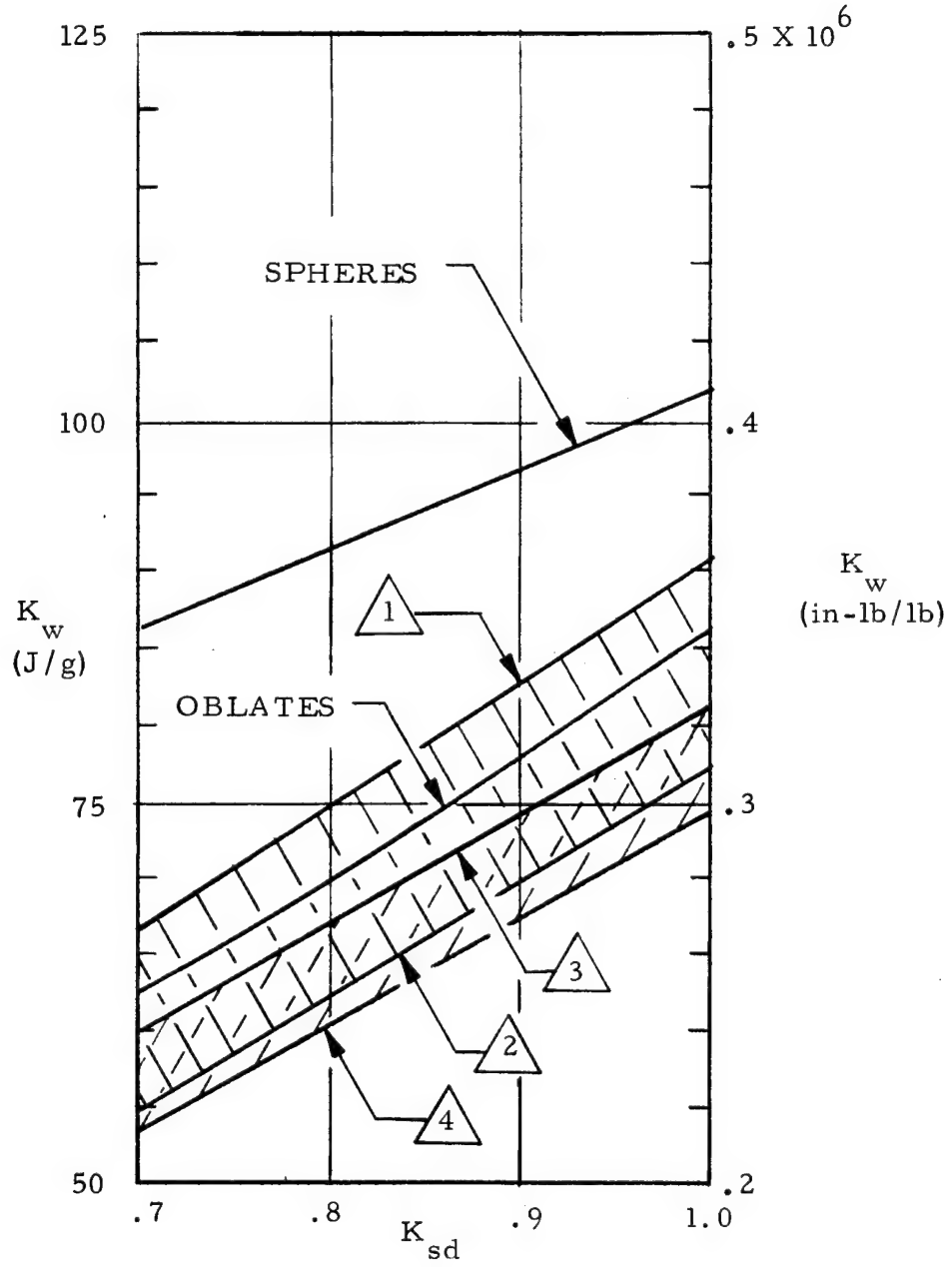

FIGURE 32: PERFORMANCE FACTORS FOR AMBIENT OPERATED GFR INCONEL X-750 PRESSURE VESSELS

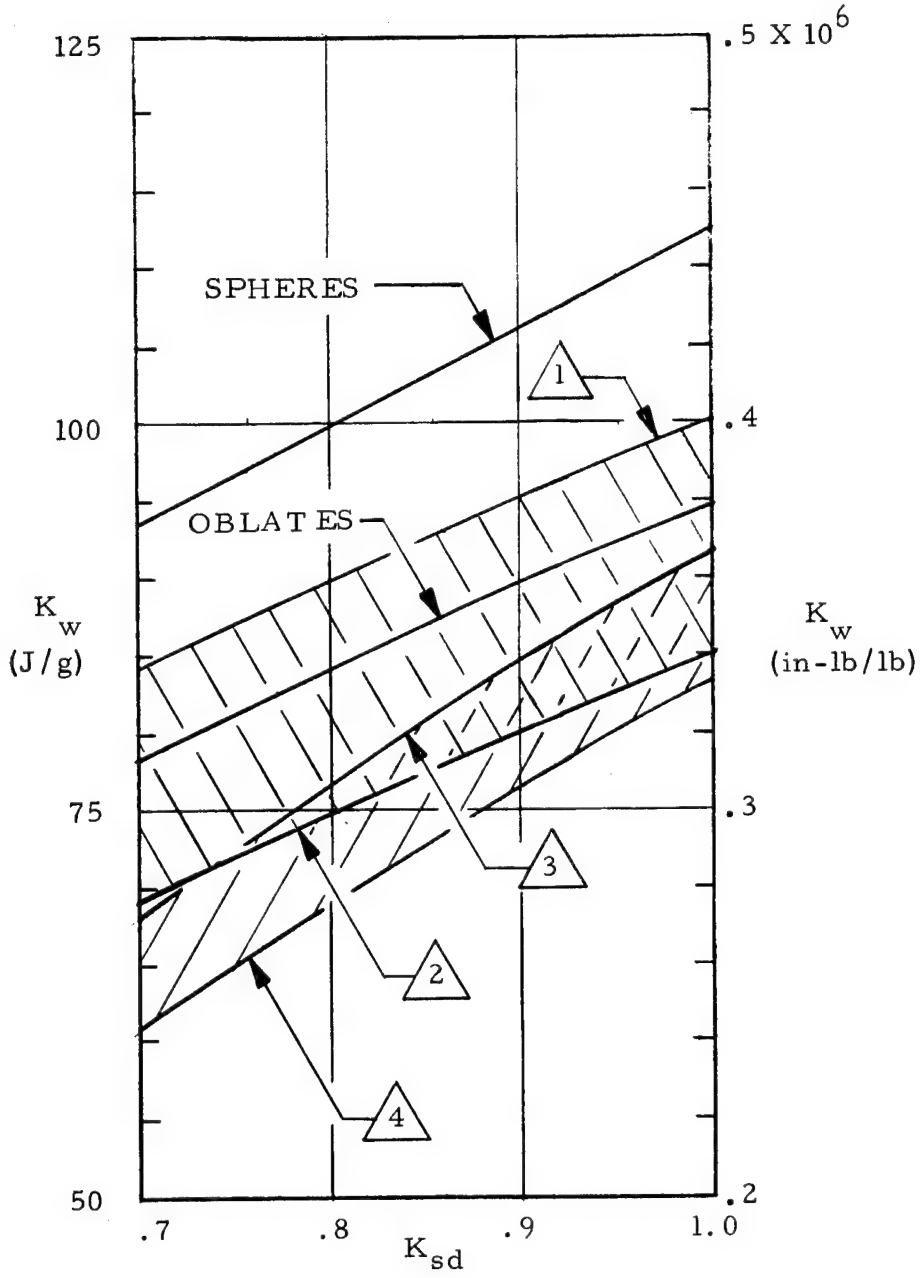

1 Completely Overwrapped Cylinders (L/D = ∞).
2 Completely Overwrapped Cylinders (L/D = 1).
3 Hoop Overwrapped Cylinders (L/D = ∞).
4 Hoop Overwrapped Cylinders (L/D= 2).

FIGURE 33: PERFORMANCE FACTORS FOR GFR INCONEL X-750 VESSELS OPERATED AT 77°K (-320°F)

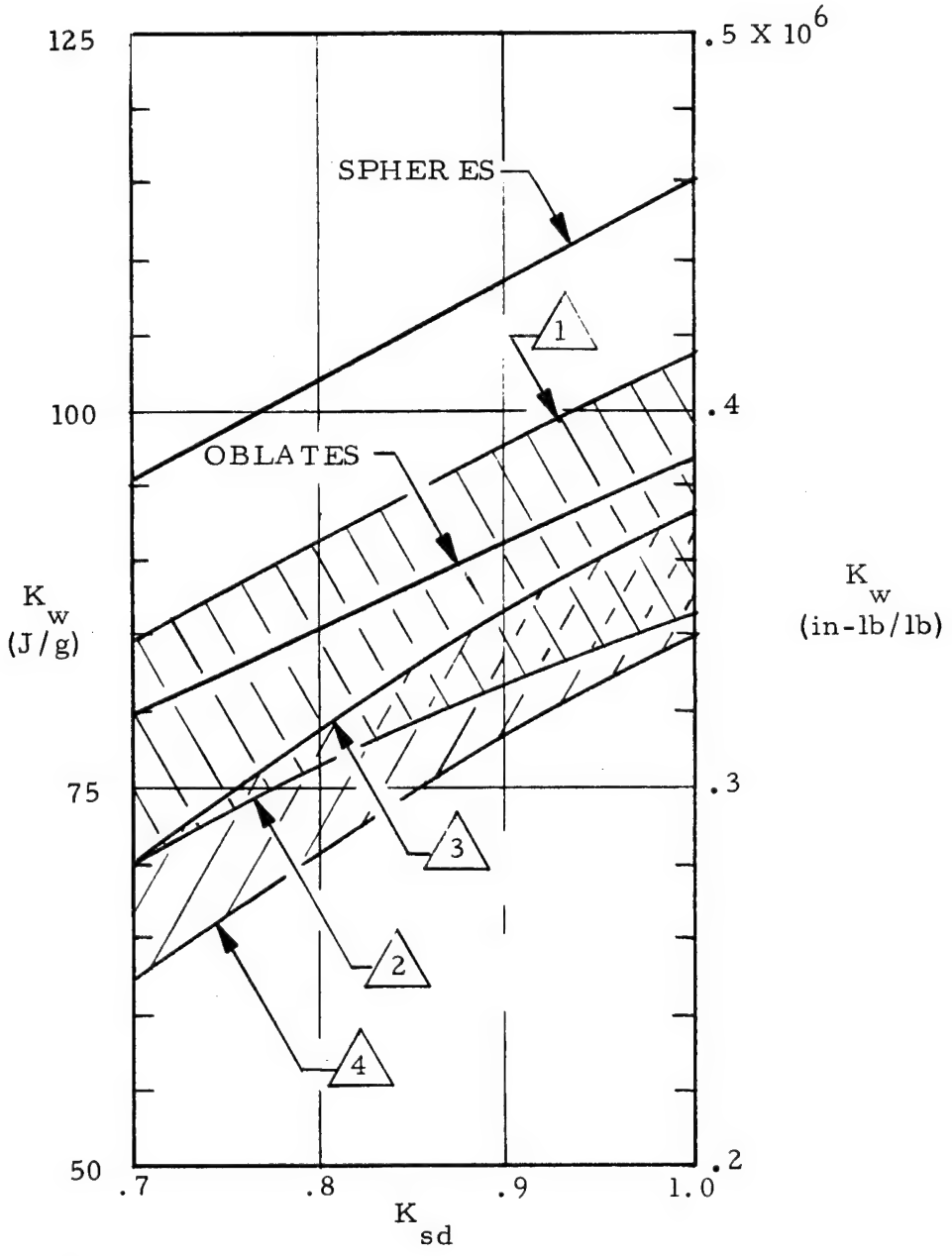

FIGURE 34: PERFORMANCE FACTORS FOR GFR INCONEL X-750 VESSELS OPERATED AT 20°K (-423° F)

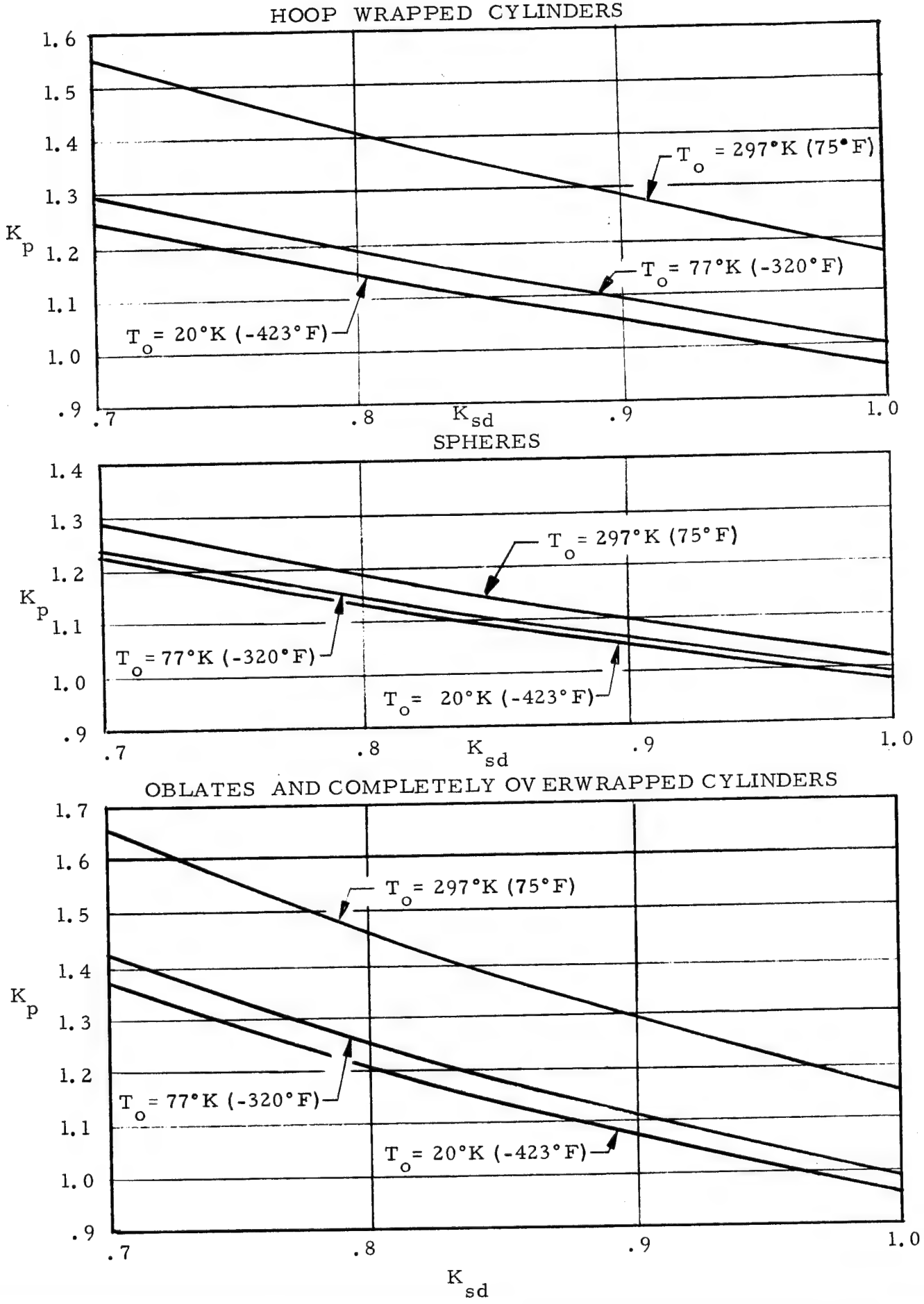

FIGURE 35: SIZING PRESSURE REQUIREMENTS FOR AMBIENT AND CRYOGENIC OPERATED GFR 301 STAINLESS STEEL PRESSURE VESSELS

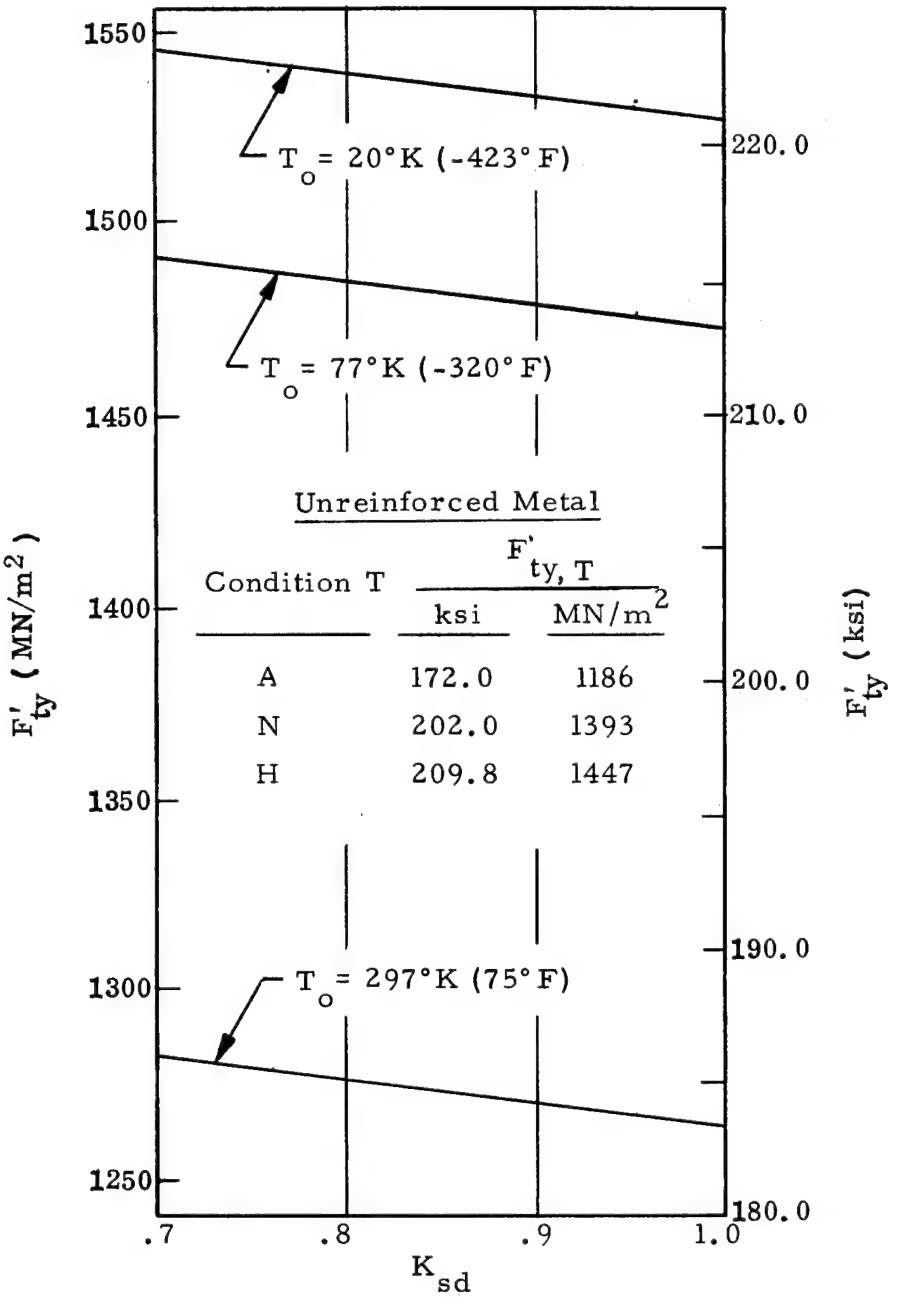

FIGURE 36: METAL SHELL OFFSET YIELD STRENGTH AT AMBIENT AND CRYOGENIC TEMPERATURE FOR SIZED GFR 301 STAINLESS STEEL SPHERES

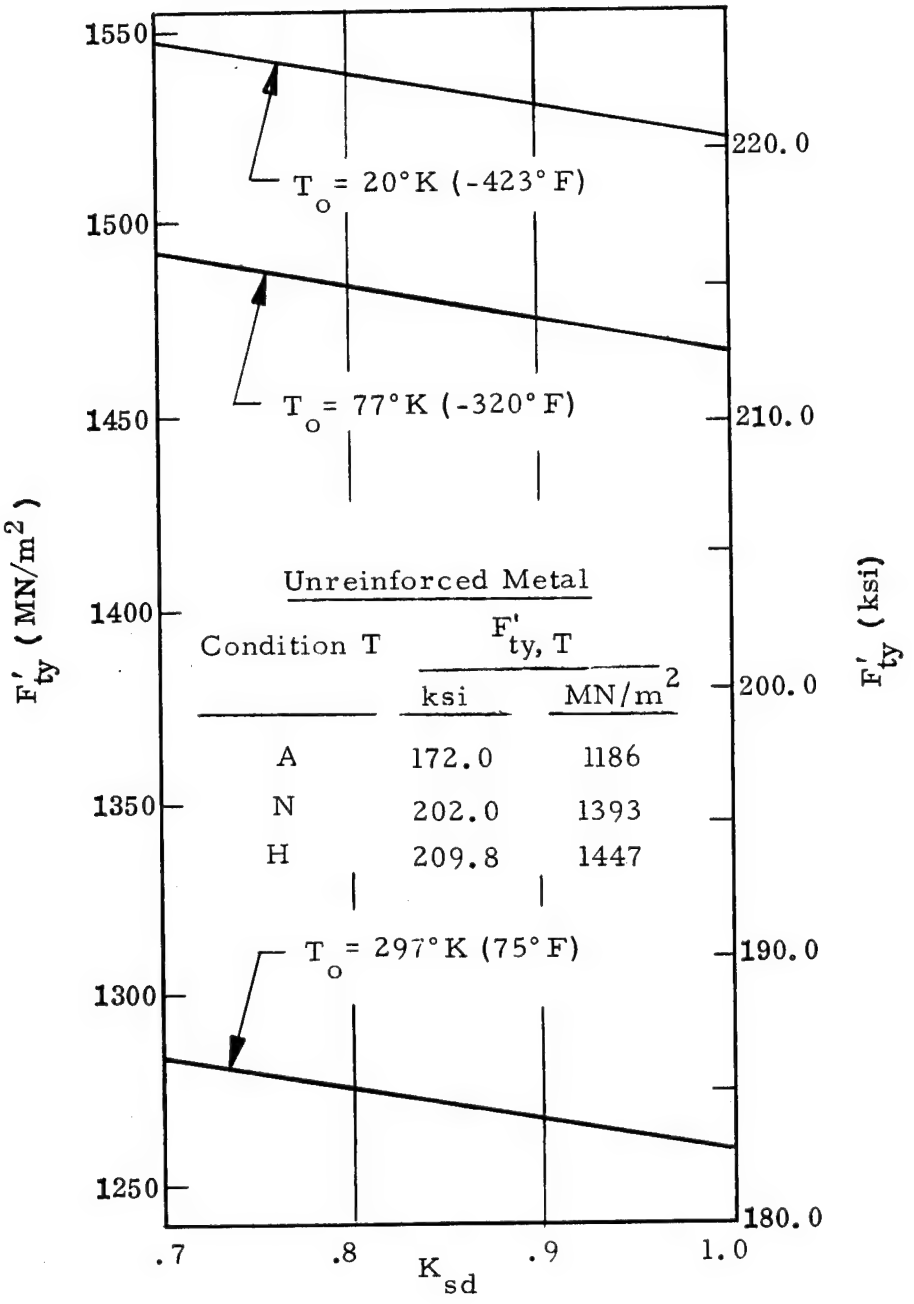

FIGURE 37: METAL SHELL OFFSET YIELD STRENGTH AT AMBIENT AND CRYOGENIC TEMPERATURE FOR SIZED COMPLETELY GFR 301 STAINLESS STEEL OBLATE SPHEROIDS AND CYLINDRICAL VESSELS

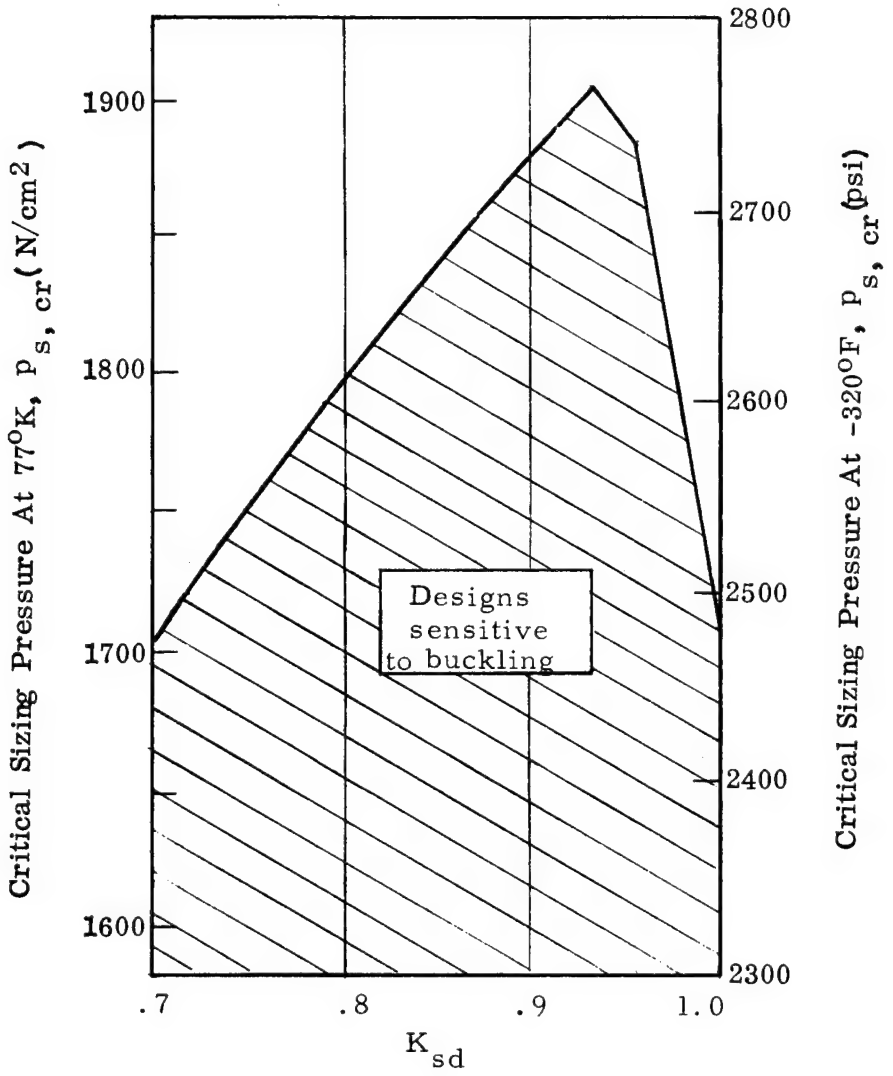

FIGURE 38: BUCKLING SENSITIVITY INDICATOR FOR HOOP GFR 301 STAINLESS STEEL PRESSURE VESSELS

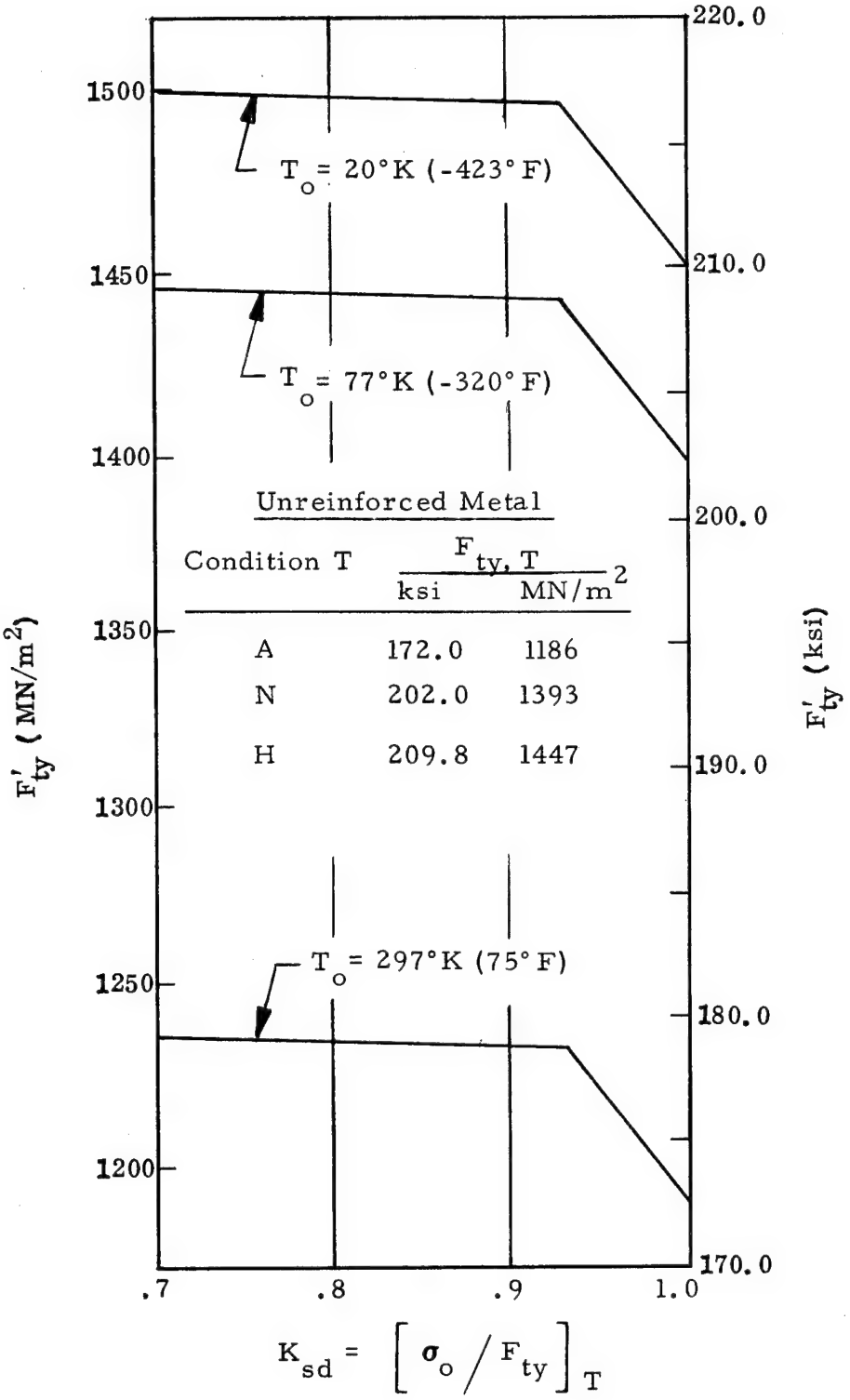

FIGURE 39: METAL SHELL OFFSET YIELD STRENGTH AT AMBIENT AND CRYOGENIC TEMPERATURE FOR SIZED HOOP GFR 301 STAINLESS STEEL CYLINDERS

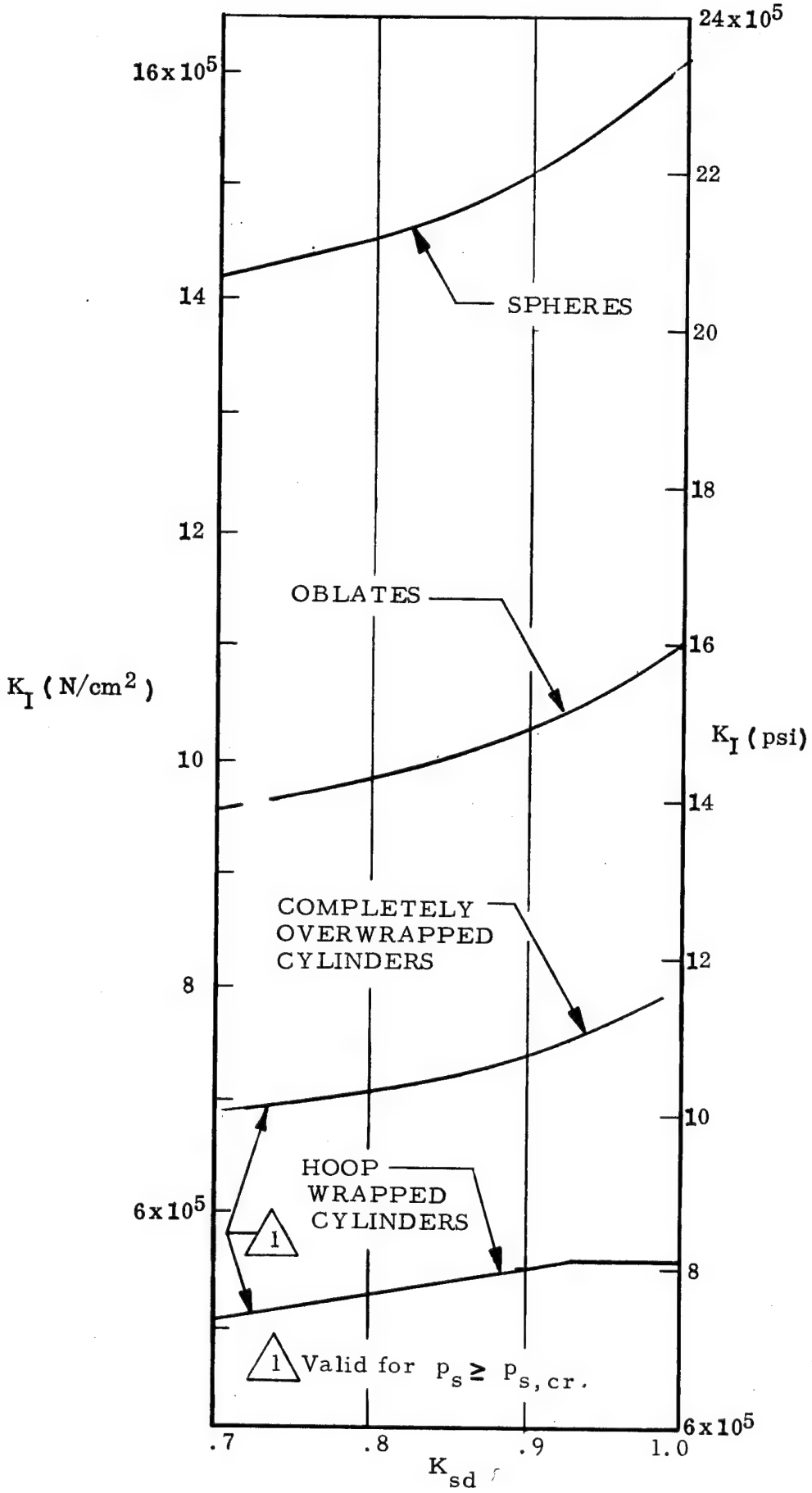

FIGURE 40: METAL SHELL THICKNESS PARAMETER FOR GFR 301 STAINLESS STEEL PRESSURE VESSELS

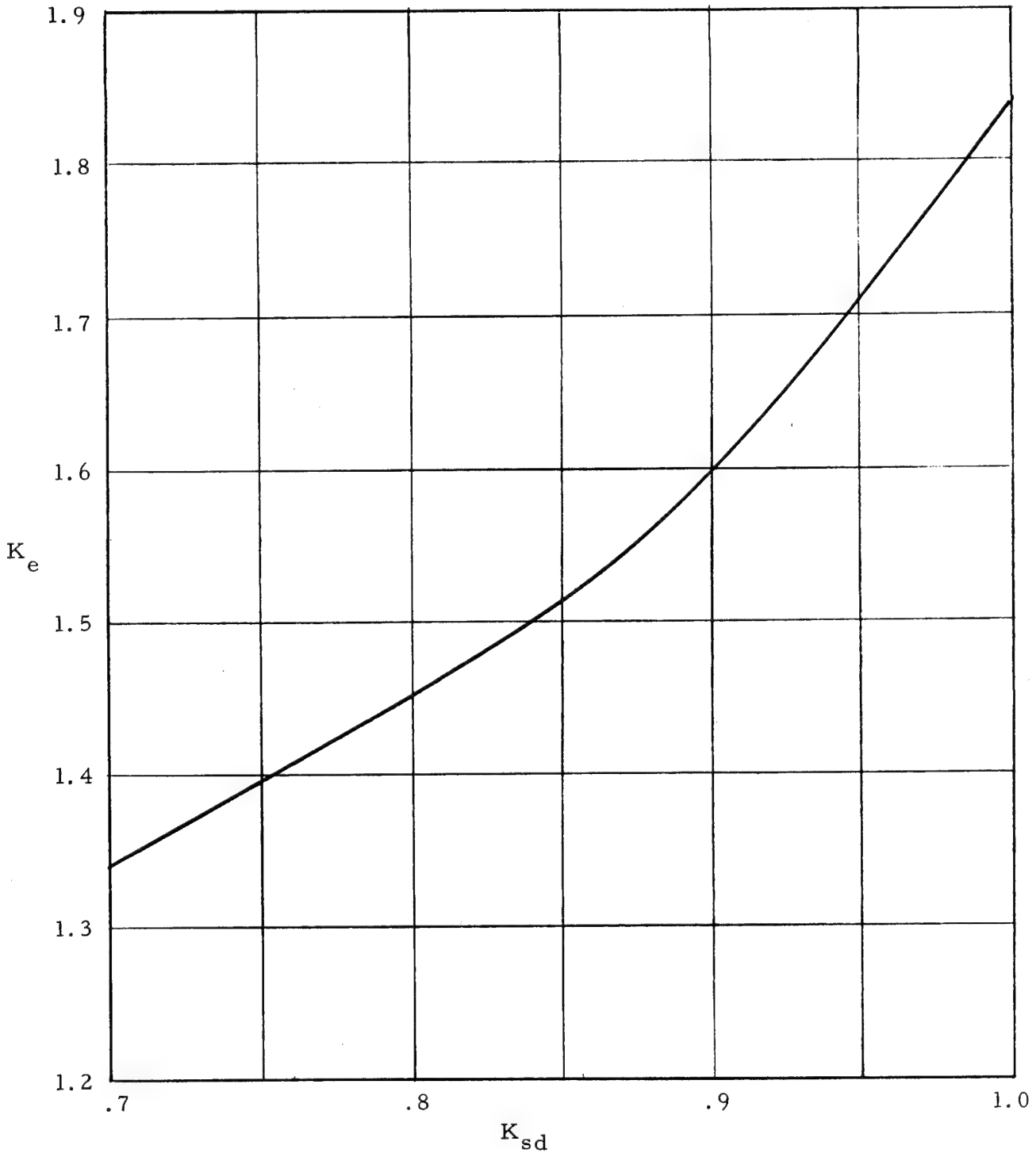

FIGURE 41: LONGITUDINAL FILAMENT THICKNESS PARAMETER FOR COMPLETELY GFR 301 STAINLESS STEEL SPHERES

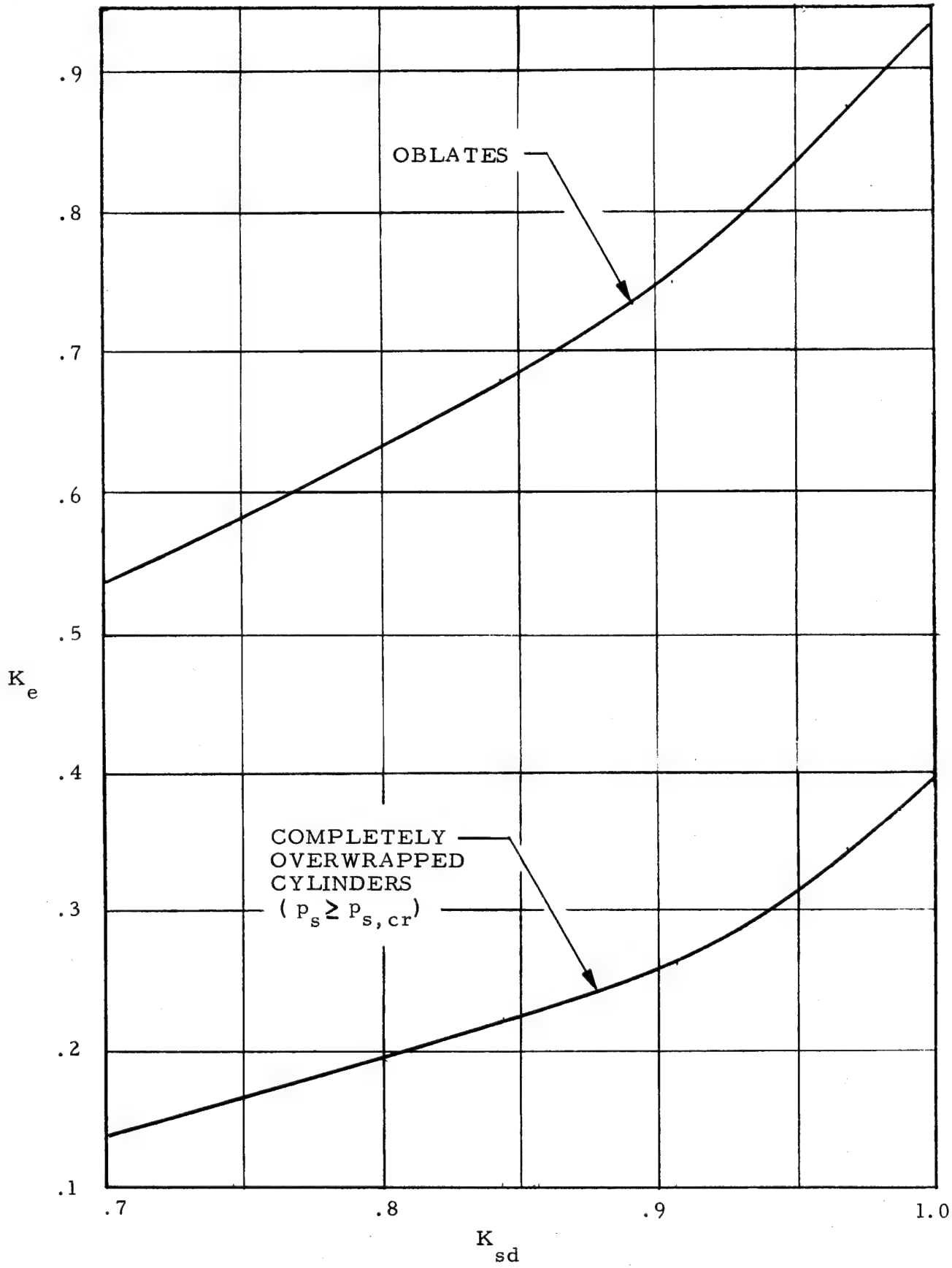

FIGURE 42: LONGITUDINAL FILAMENT THICKNESS PARAMETER FOR COMPLETELY GFR 301 STAINLESS STEEL OBLATE SPHEROIDS AND CYLINDRICAL VESSELS

Notes:

1. Curves valid for all $p_s \geq p_{s,cr}$.

2 Completely overwrapped cylindrical vessels.

3 Hoop wrapped cylinders.

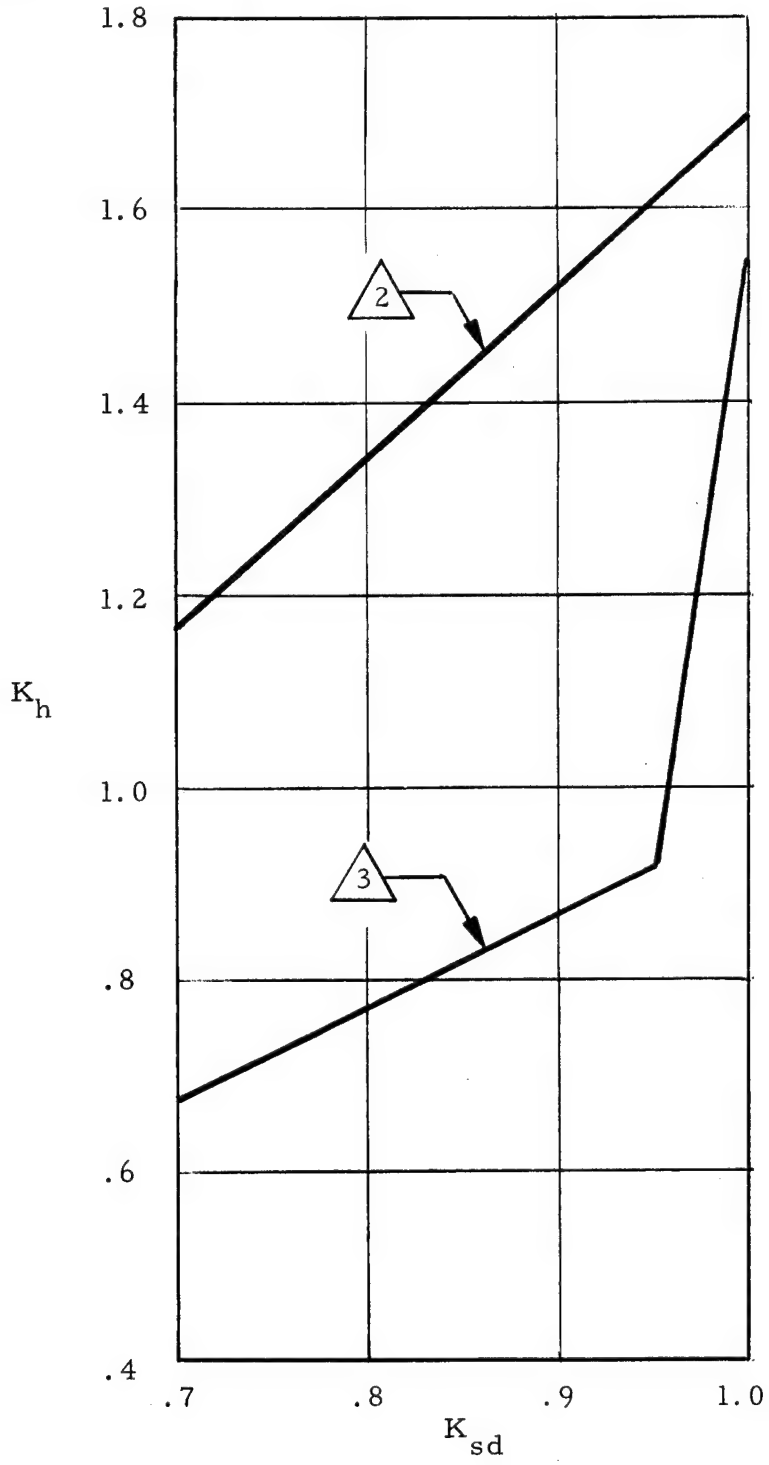

FIGURE 43: HOOP FILAMENT THICKNESS PARAMETER FOR GFR 301 STAINLESS STEEL CYLINDRICAL VESSELS

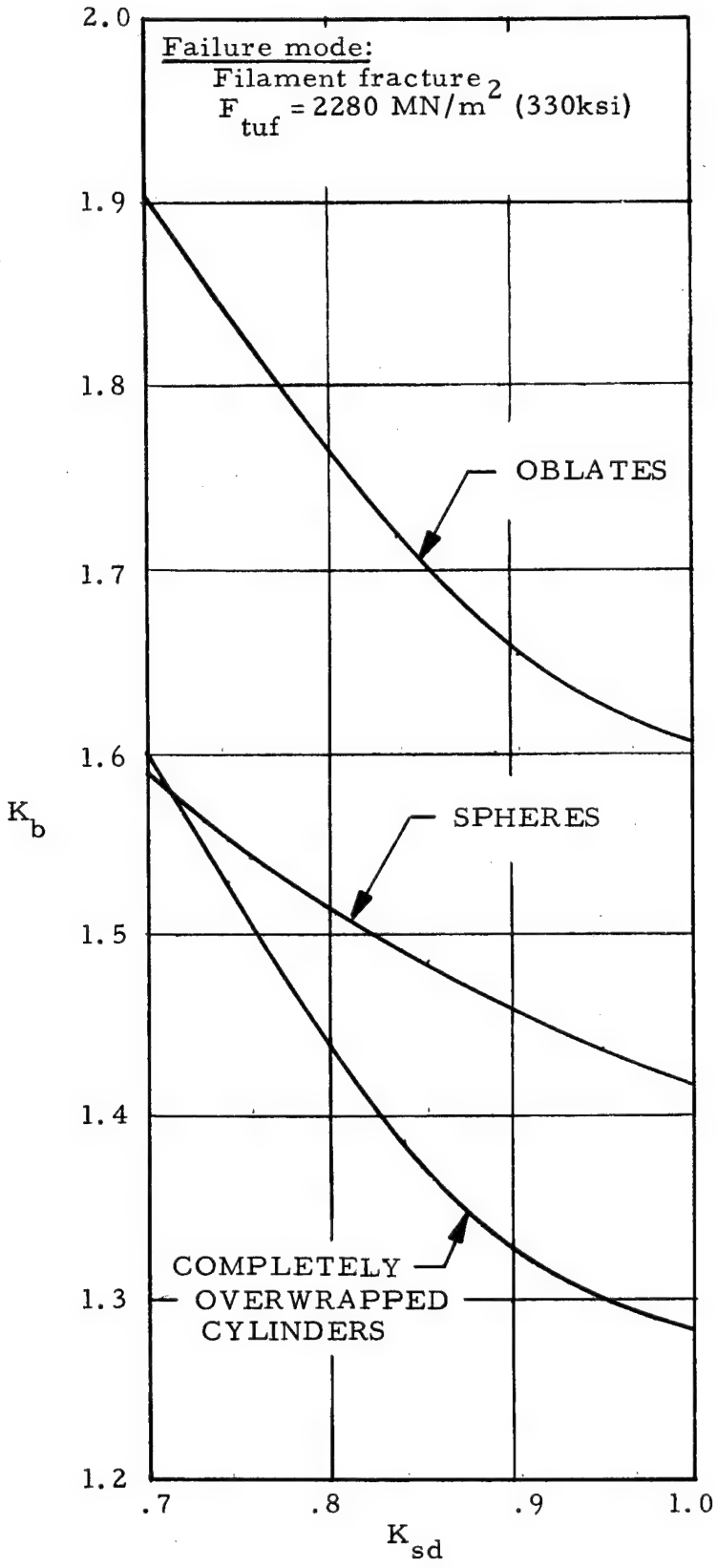

FIGURE 44: AMBIENT BURST PRESSURE FACTORS FOR COMPLETELY GFR 301 STAINLESS STEEL PRESSURE VESSELS

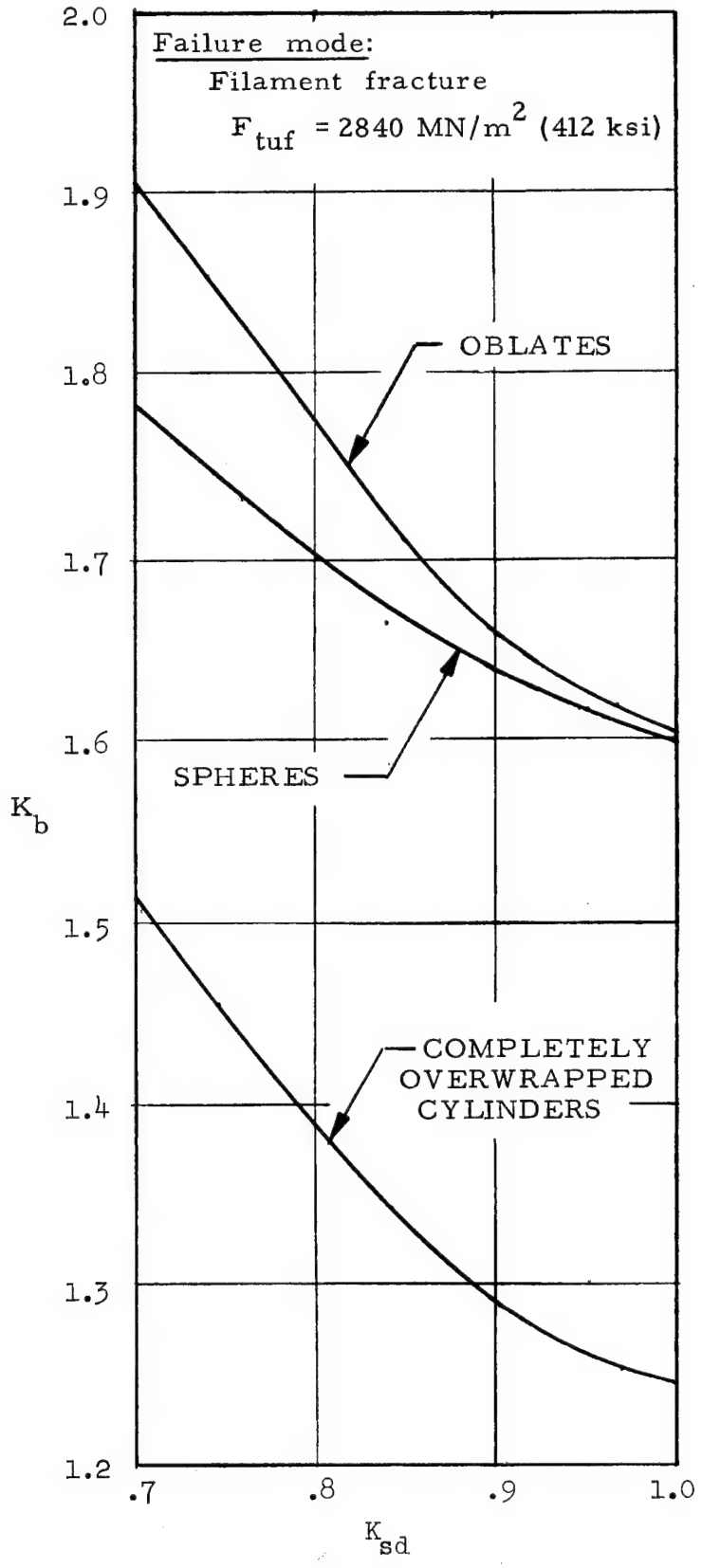

FIGURE 45: BURST PRESSURE FACTORS AT 77°K (-320°F) FOR COMPLETELY GFR 301 STAINLESS STEEL PRESSURE VESSELS

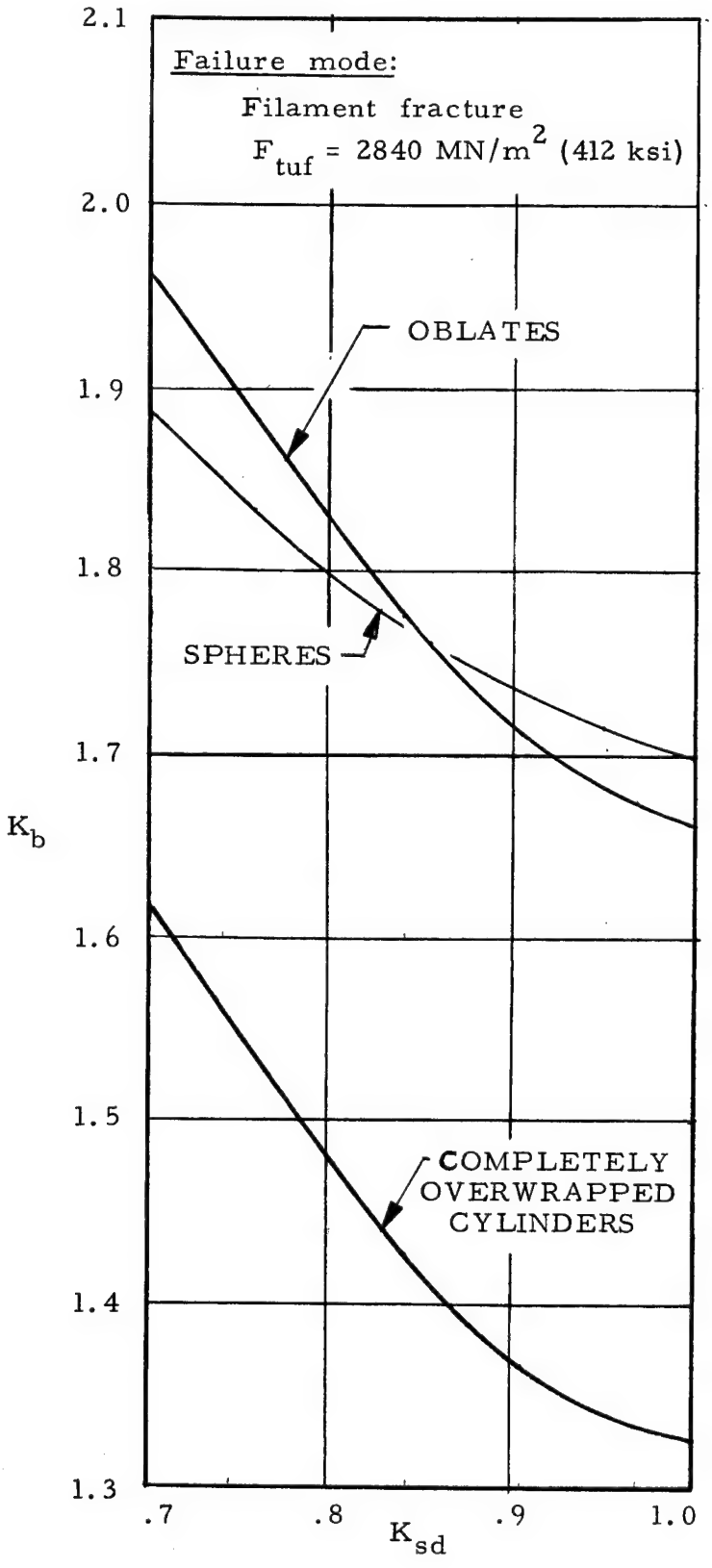

FIGURE 46: BURST PRESSURE FACTORS AT 20°K (-423° F) FOR COMPLETELY GFR 301 STAINLESS STEEL PRESSURE VESSELS

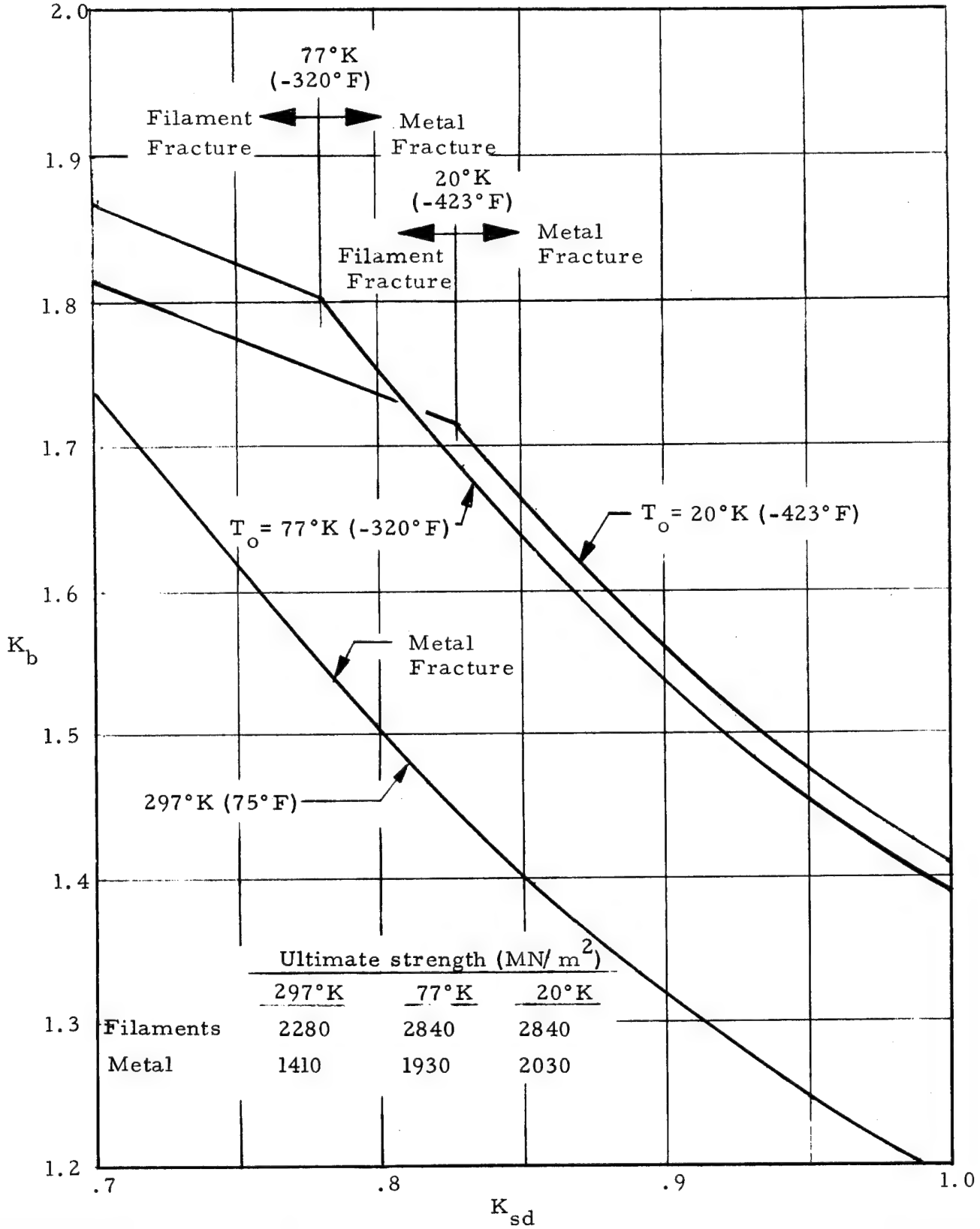

FIGURE 47: AMBIENT AND CRYOGENIC BURST PRESSURE FACTORS FOR HOOP GFR 301 STAINLESS STEEL PRESSURE VESSELS

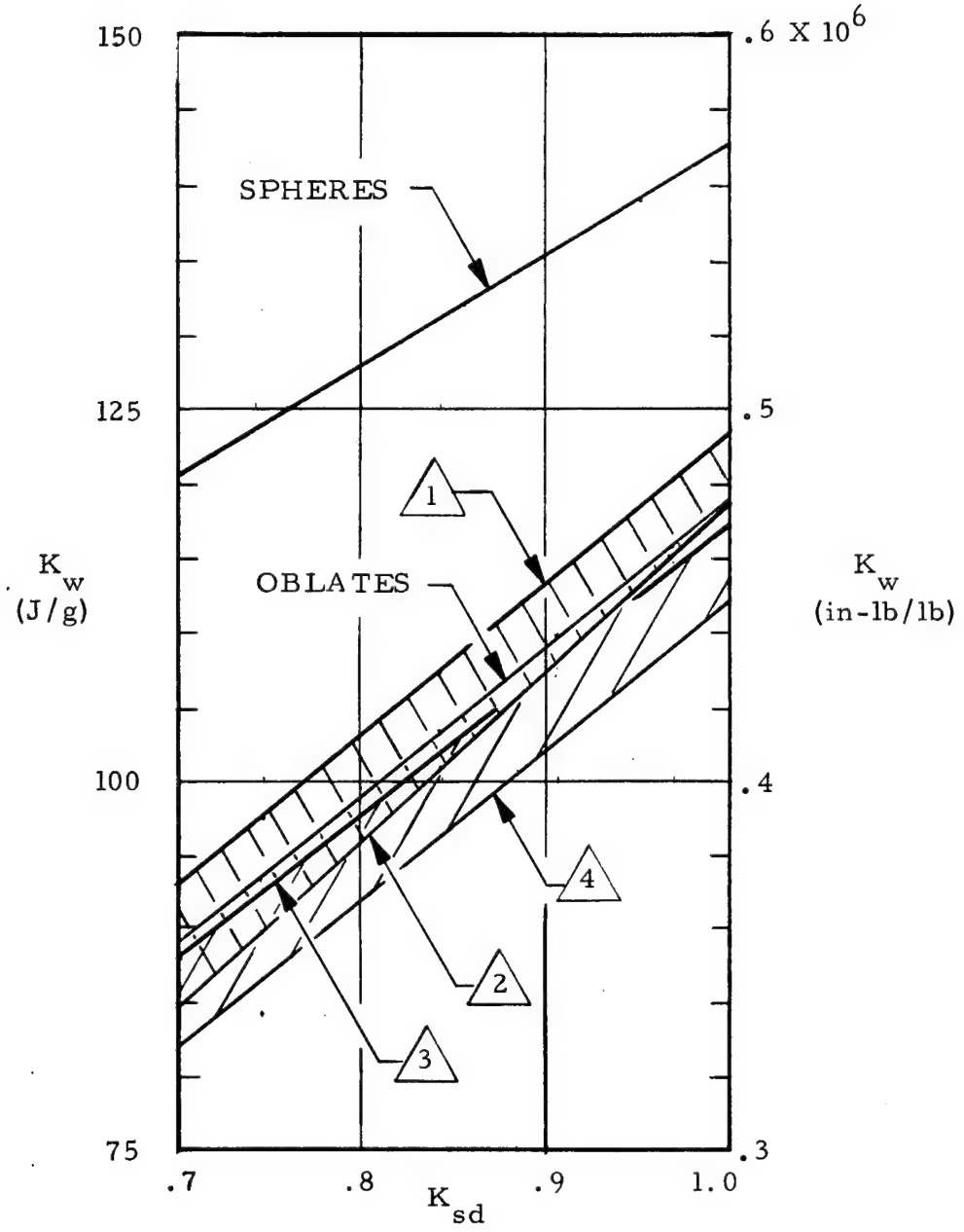

1 Completely Overwrapped Cylinders (L/D=).
2 Completely Overwrapped Cylinders (L/D= 1).
3 Hoop Wrapped Cylinders (L/D=).
4 Hoop Wrapped Cylinders (L/D = 2).

FIGURE 48: PERFORMANCE FACTORS FOR AMBIENT OPERATED GFR 301 STAINLESS STEEL PRESSURE VESSELS

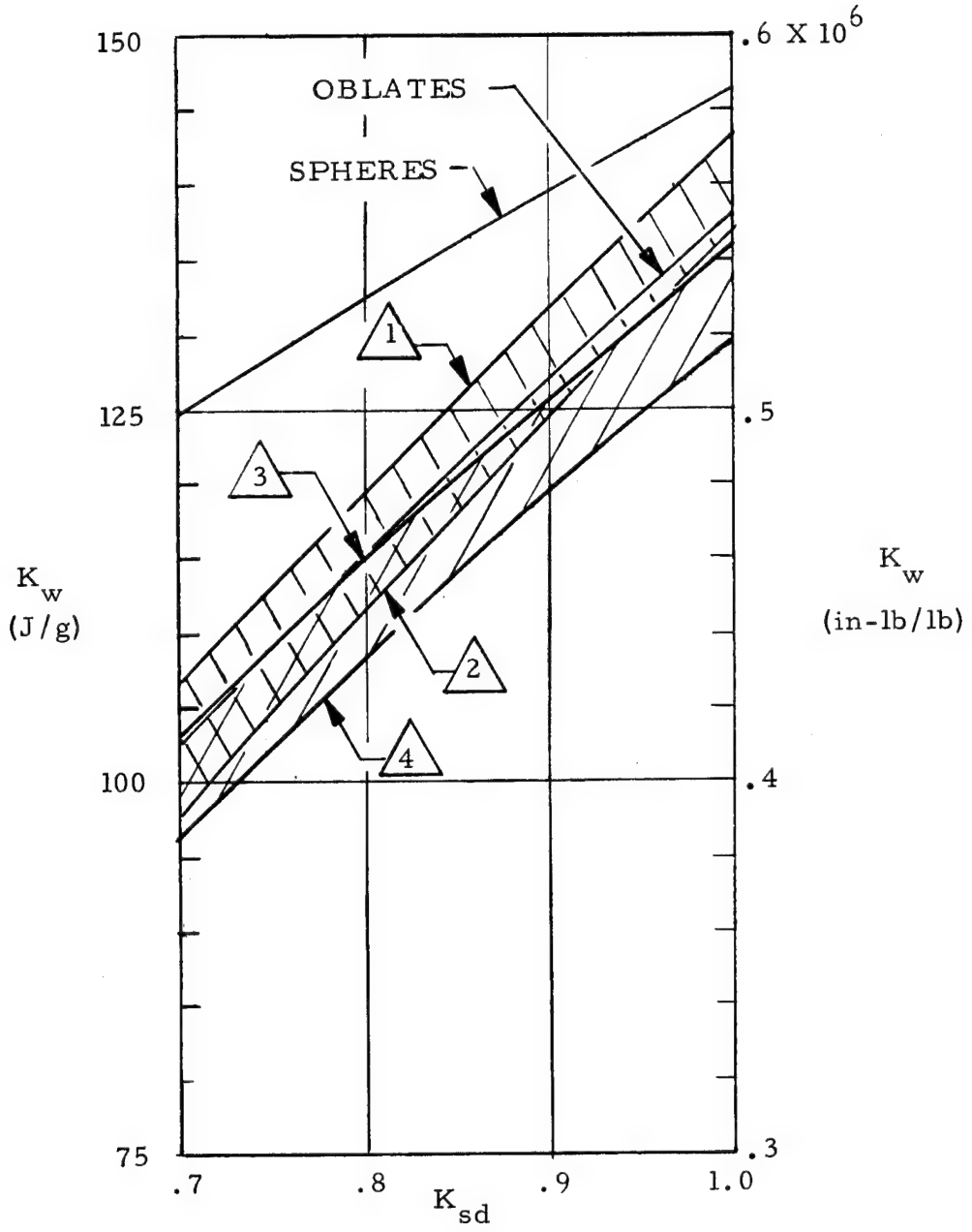

1 Completely Overwrapped Cylinders (L/D=∞).
2 Completely Overwrapped Cylinders (L/D= 1).
3 Hoop Wrapped Cylinders (L/D=∞).
4 Hoop Wrapped Cylinders (L/D= 2).

FIGURE 49: PERFORMANCE FACTORS FOR GFR 301 STAINLESS STEEL VESSELS OPERATED AT 77°K (-320° F)

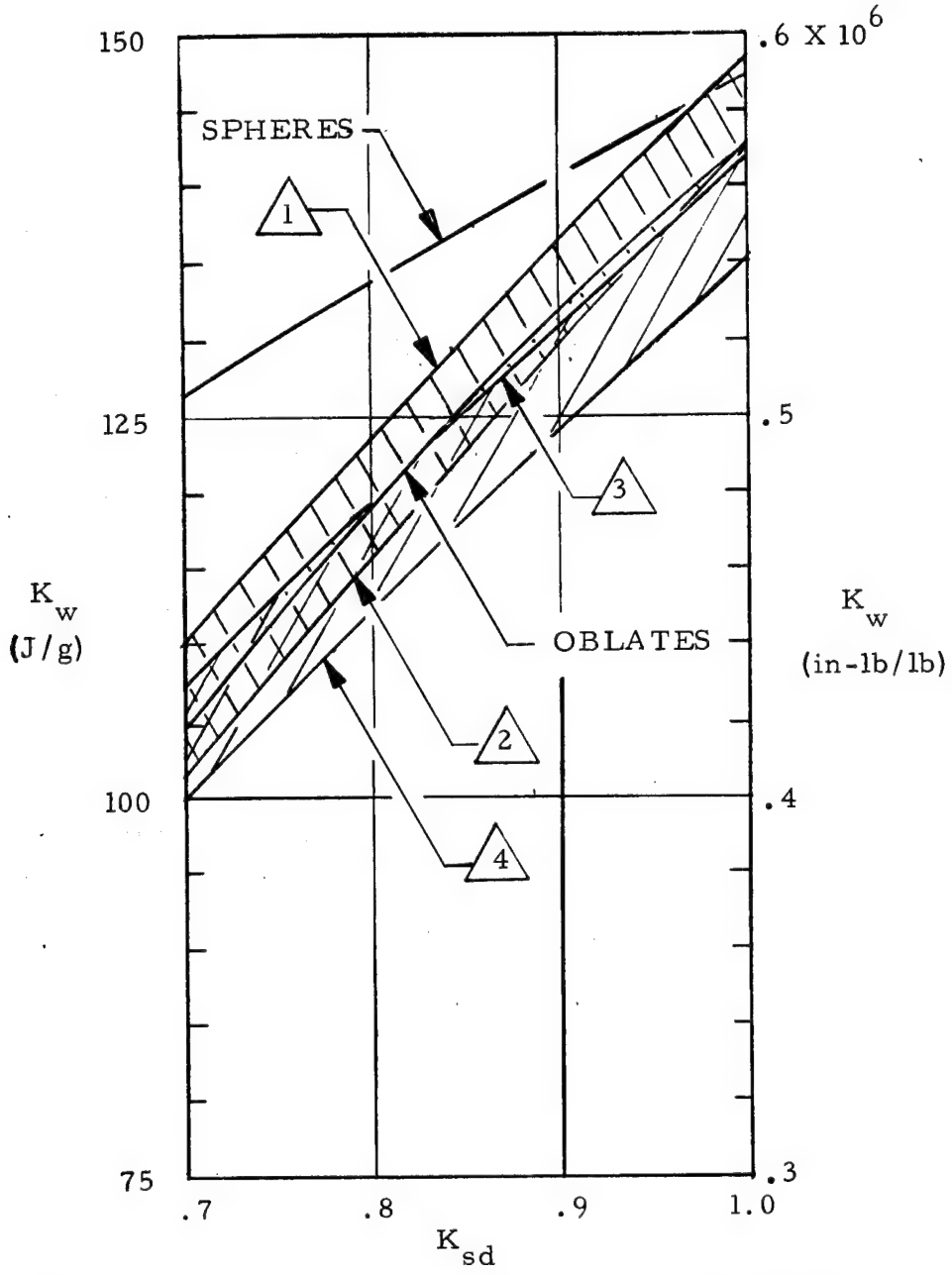

FIGURE 50: PERFORMANCE FACTORS FOR GFR 301 STAINLESS STEEL VESSELS OPERATED AT 20°K (-423°F)

REFERENCES

1. NASA RFP No. 9-BC421-67-2-40P, Space Shuttle Program, 17 March 1972.

2. Darms, F. J. and Landes, R. E.: "Computer Program for the Analysis of Filament-Reinforced Metal-Shell Pressure Vessels", NASA CR-72124, Aerojet-General Corporation, Rev. May 1972.

3. Morris, E. E., Darms, F. J., Landes, R. E. and Campbell, J. W.; "Parametric Study of Glass-Filament-Reinforced Metal Pressure Vessels", NASA CR 54-855, Aerojet-General Corporation, April 1966.

4. Morris, E. E.; "Glass-Fiber-Reinforced Metallic Tanks for Cryogenic Service", NASA CR-72224, Aerojet-General Corporation, June 1967.

5. Tiffany, C. F.,; "Fracture Control of Metallic Pressure Vessels", NASA Design Monograph SP-8040.

6. Buckling of Thin-Walled Doubly Curved Shells, NASA Space Vehicle Design Criteria, NASA SP-8032, August 1969.

7. Gleich, D.; "Development of a Filament-Overwrapped Cryoformed Metal Pressure Vessel", NASA CR-72753, January 1971, Arde, Inc.

8. Bixler, W. D.; "Development of a Fracture Control Method for Composite Tanks with Load Sharing Liners", (Interim Report), NASA CR-120918, Boeing Aerospace Company, March 1973.

DISTRIBUTION LIST FOR TOPICAL REPORT NASA CR-120917
CONTRACT NAS3-14380

GLASS FIBER REINFORCED METAL PRESSURE
VESSEL DESIGN GUIDE

STRUCTURAL COMPOSITES INDUSTRIES
AZUSA, CALIFORNIA

BOEING AEROSPACE COMPANY
SEATTLE, WASHINGTON

NASA-Lewis Research Center
21000 Brookpark Rd.
Cleveland, OH 44135

Attn:	E. J. Kolman, MS500-313	1
	J. R. Faddoul, MS 49-3	6
	R. H. Kemp, MS 49-3	1
	G. T. Smith, MS 49-3	1
	T. Gulko, MS 49-3	1
	H. W. Douglas, MS 500-205	1
	Library, MS 60-3	1
	AFSC Liaison Office, MS 501-3	3
	Technical Utilization, MS 3-19	1
	R. H. Johns, MS 49-3	1
	R. F. Lark, MS 49-3	1
	W. F. Brown, MS 105-1	1
	G. M. Ault, MS 3-13	1

National Aeronautics and Space Administration
Washington, D.C. 20546

Attn:	MTG/J. G. Malament	1
	MHE/N. G. Peil	1
	KT/Technology Utilization Office	1
	RWM/J. J. Gangler	1
	RWS/D. A. Gilstead	1
	RW/G. C. Deutsch	1
	Library	1

NASA-Ames Research Center
Moffett Field, CA 94035

Attn:	Library	1

NASA-George C. Marshall Space Flight Center
Marshall Space Flight Center, AL 35812

Attn:	S&E-ASTN-AA/C. Lifer	1
	S&E-ASTN-ES/E. Engler	1
	S&E-ASTN-MX/E. Cataldo	1
	S&E-PE-M/W. A. Wilson	1
	Library	1

NASA-Goddard Space Flight Center
Greenbelt, MD 20771

Attn:	Library	1

NASA-John F. Kennedy Space Center
Kennedy Space Center, FL 32899

Attn:	Library	1

NASA-Langley Research Center
Hampton, VA 23365

Attn:	R. W. Leonard, MS 188	1
	R. A. Pride, MS 188A	1
	Library	1

NASA-Manned Spacecraft Center
Houston, TX 77058

Attn:	ES-5/R. E. Johnson	1
	SMD/R. E. Vale	1
	Library	1

Jet Propulsion Laboratory
4800 Oak Grove Dr.
Pasadena, CA 91103

Attn:	W. Jensen	1
	W. M. Rowe	1
	Library	1

Scientific and Technical Information Facility 2
NASA Representative
Box 33
College Park, MD 20740

Aeronautical Systems Division
Air Force Systems Command
Wright-Patterson Air Force Base
Dayton, OH

Attn:	C. F. Tiffany/ASD/ENF	1
	Library	1

Air Force Aero Propulsion Laboratory
Research & Technology Division
Air Force Systems Command
United States Air Force
Wright-Patterson AFB, OH 45433

Attn:	ARRP (Library)	1

Air Force Material Laboratory
Wright-Patterson Air Force Base
Dayton, OH 45433

Attn:	J. D. Ray (MANC)	1
	H. S. Swartz (MAN)	1
	W. H. Gloor (MANF)	1
	G. P. Peterson (MAC)	1
	E. Jaffe (MAC)	1
	S. Litvak (MATC)	1

Air Force Missile Test Center
Patrick Air Force Base, FL

Attn:	Library	1

Air Force Office of Scientific Research
Washington, D.C. 20333

Attn:	Library	1

Air Force Rocket Propulsion Laboratory (RPM)
Edwards, CA 93523

Attn:	Library	1

Air Force Systems Command
Andrews Air Force Base
Washington, D.C. 20332

Attn:	Library	1

Arnold Engineering Development Center
Air Force Systems Command
Tullahoma, TN 37389

Attn: Library 1

Bureau of Naval Weapons
Department of the Navy
Washington, D.C.

Attn: Library 1

Commander
U.S. Naval Missile Center
Point Mugu, CA 93041

Attn: Technical Library 1

Commander
U.S. Naval Weapons Center
China Lake, CA 93557

Attn: Library 1

Commanding Officer
Naval Research Branch Office
1030 E. Green Street
Pasadena, CA 91101

Attn: Library 1

U.S. Army Missile Command
Redstone Scientific Information Center
Redstone Arsenal, AL 35808

Attn: Document Section 1

Commanding Officer
U.S. Army Research Office (Durham)
Box CM, Duke Station
Durham, NC 27706

Attn: Library 1

Director (Code 6T80)
U.S. Naval Research Laboratory
Washington, D.C. 20390

Attn: Library 1

Office of Research Analyses (OAR)
Holloman Air Force Base, NM 88330

Attn: Library RRRD 1

Picatinny Arsenal
Dover, N J 07801

Attn: Library 1

Plastics Technical Evaluation Center
Picatinny Arsenal
Dover, NJ 07801 1

Space & Missile Systems Organization
Air Force Unit Post Office
Los Angeles, CA 90045

Attn: Technical Data Center 1

U.S. Air Force
Washington, D.C.

Attn: Library 1

U.S. Air Force
Wright-Patterson AFB, OH 45433

Attn: AFFDL/W. H. Goesch 1
AFML/T. J. Reinhart, Jr. 1
AFML/J. Whitney 1

U.S. Naval Ordnance Laboratory
White Oak
Silver Spring, MD 20910

Attn: R. Simon, Nonmetallic Mat'ls. Div. 1
Library 1

Aerojet Nuclear Systems Company
P.O. Box 13070
Sacramento, CA 95813

Attn: Library 1

Ordnance Division
Aerojet-General Corporation
11711 South Woodruff Avenue
Downey, CA 90241

Attn: Library 1

Propulsion Division
Aerojet-General Corporation
P.O. Box 15847
Sacramento, CA 95803

Attn: Technical Library 2484-2015A 1

Space Division
Aerojet-General Corporation
9200 East Flair Drive
El Monte, CA 91734

Attn: Library 1

Aeronautronic Division of Philco Ford Corp.
Ford Road
Newport Beach, CA 92663

Attn: Technical Information Department 1

Aerospace Corporation
P.O. Box 95085
Los Angeles, CA 90045

Attn: Library-Documents 1

Air Products and Chemicals Company
Allentown, PA 18105

Attn: P. J. DeRea 1

Allegheny Ballistics Laboratory
Hercules, Inc.
P.O. Box 210
Cumberland, MD 21052

Attn: W. T. Freeman 1
Library 1

Atlantic Research Corporation
Shirley Highway & Edsall Road
Alexandria, VA 22314

Attn: Security Office for Library 1

Arde, Inc.
19 Industrial Ave.
Mahwah, NJ 07430 1

ARO, Incorporated
Arnold Engineering Development Center
Arnold Air Force Station, TN 37389 — 1

Battelle Memorial Institute
505 King Avenue
Columbus, OH 43201

Attn: Defense Metals Information Center — 1
Report Library, Room 6A — 1
L. E. Hulbert — 1

Beech Aircraft Corp.
Wichita, KS 67201

Attn: Library — 1

Bell Aerosystems
Box 1, Buffalo, NY 14205

Attn: T. Reinhardt — 1
Library — 1

B. F. Goodrich Company
Aerospace & Defense Products
500 South Main Street
Akron, OH 44311

Attn: Library — 1

Brunswick Corporation
Defense Products Division
P.O. Box 4594
43000 Industrial Avenue
Lincoln, NE 68504

Attn: J. Carter — 1
W. Morse — 1

General Dynamics/Convair
P.O. Box 1128
San Diego, CA 92112

Attn: H. F. Rodgers, MS 549-00 — 1
Library — 1

Goodyear Aerospace Corporation
1210 Massilon Road
Akron, OH 44306

Attn: Library 1

Grumman Aircraft Engineering Corp.
Bethpage, Long Island, NY 11714

Attn: W. Ludwig, Bldg. 25, Dept. 589 1
L. Mead, Bldg. 25 1
Library 1

Hamilton Standard Corporation
Windsor Locks, CT 06096

Attn: H. P. Borie 1
Library 1

IIT Research Institute
Technology Center
Chicago, IL 60616

Attn: R. H. Cornish, Mech. & Materials Div. 1

Lawrence Livermore Laboratory
Box 808
Livermore, CA 94550

Attn: T. T. Chiako 1

Lockheed-California Co.
Burbank, CA 91503

Attn: R. H. Stone/Dept 74-52, Bldg. 243, Plant 2 1

Lockheed-Georgia Company
Advanced Composites Information Center
Dept. 72-14, Zone 402
Marietta, GA 30060 1

Lockheed Missiles and Space Co.
P.O. Box 504
Sunnyvale ,CA 95087

Attn: J. F. Milton, Dept. 66-01, Bldg. 562 1
R. E. Lewis 1
Library 1

LTV Corporation
P.O. Box 5003
Dallas, TX 75222

Attn: Library 1

Marine Engineering Laboratory
NSRDC ANNADIV
Annapolis, MD 21402

Attn: Karl H. Keller, Code 560 1

Martin Marietta Corp.
P.O. Box 179
Denver, CO 80201

Attn: W. F. Barrett, Mail No. 1631 1
F. Swartzberg, Mail No. 1633 1
C. A. Hall 1
Dr. A. Feldman 1
Library 1

McDonnell-Douglas Corp.
5301 Bolsa Ave.
Huntington Beach CA 92647

Attn: R. F. Zemer, Dept. A3-250 1
H. Babel 1
R. Rawe 1
Library 1

McDonnell-Douglas Corp.
P.O. Box 516
St. Louis, MO 63166

Attn: R. Hepper, Dept. E400 1
Library 1

North American-Rockwell
12214 Lakewood Blvd.
Downey, CA 90241

Attn: R. Field, Mail Code AD75 1
L. J. Koob, Mail Code AD-88 1
J. Colipriest 1
Library 1

Rocketdyne Division
North American Rockwell
6633 Canoga Ave.
Canoga Park, CA 91304

Attn:	E. L. Hawkinson D/956 AC10	1
	R. P. Frohmberg BA-19	1
	Library	1

Oak Ridge National Laboratory
Oak Ridge, TN 37830

Attn:	T. W. Pickel	1

Owens-Corning Fiberglas
Technical Center
Granville, OH 43023

Attn:	A. B. Isham	1

Rohr Corporation
Department 145
Chula Vista, CA 91312 1

Sandia Laboratories
Albuquerque, NM 87115

Attn:	H. M. Stoller, Dept. 5310	1

Thiokol Chemical Corporation
Wasatch Division
P.O. Box 524
Brigham City, UT 84302

Attn:	Library Section	1

TRW Systems
1 Space Park
Redondo Beach, CA. 90200

Attn:	Tech. Lib. Doc. Acquisitions	1

United Aircraft Corporation
400 Main Street
East Hartford, CT 06108 1

United Aircraft Corporation
United Technology Center
P.O. Box 358
Sunnyvale, CA 94088

Attn: Librarian 1

U.S. Rubber Company
Mishawaka, IN 46544 1

Whittaker Corporation
3640 Aero Court
San Diego, CA 92123

Attn: V. Chase 1

University of Nebraska
Dept. of Engineering Mechanics
Lincoln, NE 68503

Attn: R. Foral 1

University of Oklahoma
School of Aerospace, Mechanical
and Nuclear Engineering
865 Asp Avenue, Room 200
Norman, OK 73069

Attn: C. W. Bert 1

National Technical Information Service
Springfield, VA 22151 20